DISSERTATION

ELUCIDATING THE ROLE OF IRON IN THE PATHOGENESIS OF IDIOPATHIC OSTEOARTHRITIS IN THE DUNKIN-HARTLEY ANIMAL MODEL

Submitted by

Lindsey Hammond Burton

Department of Environmental and Radiological Health Sciences

In partial fulfillment of the requirements

For the Degree of Doctor of Philosophy

Colorado State University

Fort Collins, Colorado

Spring 2021

Doctoral Committee:

Advisor: Ronald Tjalkens
Co-Advisor: Kelly Santangelo

Marie Legare
Laurie Goodrich
Lucas Argueso

ABSTRACT

ELUCIDATING THE ROLE OF IRON IN THE PATHOGENESIS OF IDIOPATHIC OSTEOARTHRITIS IN THE DUNKIN-HARTLEY ANIMAL MODEL

Osteoarthritis (OA) is the most prevalent musculoskeletal disorder, affecting millions of individuals worldwide. While OA is characterized by the progressive loss of articular cartilage, it is now widely accepted to be a whole joint disorder, with changes such as synovial hyperplasia, subchondral bone remodeling, and osteophyte formation accompanying cartilage degeneration. The knee is one of the joints most affected by OA. Patients with knee OA exhibit painful and/or limited mobility as a consequence of the disorder, resulting in an increased risk of comorbidities such as heart disease, obesity, diabetes, and depression. Unfortunately, the mechanisms driving OA pathogenesis remain poorly understood, and there are no effective therapies available for treating the disorder. Therefore, there is a need to understand factors contributing to OA to identify potential targets for combating the condition.

Iron is the most abundant mineral in the human body and is essential for conducting numerous physiologic processes. However, unbound or partially-liganded iron can participate in redox reactions that produce reactive oxygen species and free radicals capable of inciting tissue damage. As such, iron needs to be tightly managed within the body. Mammals do not possess a regulated mechanism for excreting iron, and iron progressively accumulates within tissues throughout the aging process. Primary/idiopathic OA does not have any known, identifiable cause for disease development, but the largest risk factor associated with the disorder is advancing age.

To address this gap in knowledge, we designed a series of experiments to elucidate the contributions of iron to the pathogenesis of idiopathic OA. The main animal model used for this work is the Dunkin-Hartley guinea pig, which spontaneously develops age-related OA with a histopathology similar to that observed in humans. In the first study, we quantified tissue iron levels at different ages in OA-prone Dunkin-Hartley guinea pigs relative to an outbred, control strain not used in OA research. While the control strain accumulated iron in the liver with age, but not within cartilage, the Hartleys demonstrated a significant increase in cartilage iron concentration at 7-8 months-of-age. This increase in cartilage iron concentration was more significant in males, though it was also observed in females. As this timepoint corresponds to a moderate stage of disease progression, this finding suggests that iron may play a role in OA development and/or progression in Hartley guinea pigs. This concept was supported by gene expression analysis of iron-related genes. Notably, both male and female Dunkin-Hartley guinea pigs had decreased transcript expression of ferritin heavy chain and ferroportin at 7-8 months, which may contribute to cartilage iron accumulation at this age by inappropriately storing iron in chondrocytes.

Because of this intriguing association, we wanted to investigate the gene expression changes occurring with systemic iron manipulation in knee joint tissues. Exogenous iron overload resulted in worsening of OA pathology in the disease-resistant Strain 13 guinea pig. The systemic administration of iron dextran caused iron to accumulate within articular cartilage from a diarthrodial joint environment and was accompanied by gene expression changes within knee tissues. Notably, systemic iron overload altered the expression of several iron-related genes in this control strain, indicating that both the cartilage and a large adipose depot, the infrapatellar fat pad, were able to detect and respond to changes in tissue iron levels in the presence of joint

pathology. Conversely, systemic iron deficiency, achieved by supplying an iron deficient diet, decreased cartilage lesions within OA-prone male Hartley guinea pigs. In this proof-of-principle study, the reduction in cartilage iron concentration was accompanied by the altered expression of two iron transport genes, the importer transferrin receptor 1 and the cellular iron exporter ferroportin.

As iron deficiency is not a recommended pursuit, we investigated the effects of systemic iron *reduction*, without clinical iron deficiency or anemia, on OA pathogenesis. The commercially available pharmacologic iron chelator deferoxamine (DFO) was used to reduce total iron levels in the body of male and female Dunkin-Hartley guinea pigs. In males, administration of DFO was successful at reducing tissue iron levels both systemically and in a diarthrodial joint environment, and this was accompanied by a significant decrease in the severity of cartilage lesions. The reduction in joint pathology observed with treatment was largely attributed to a decrease in chondrocyte cell death; this finding was supported by the decreased expression of several proapoptotic genes within knee articular cartilage. Conversely, tissue iron levels were not altered by administration of the same dose of DFO in females, suggesting the presence of sex differences in systemic iron homeostasis. There was a relative reduction in histologic OA score in treated female animals, which may be due to the beneficial mobilization of iron by DFO that was also noted in males. The modest reduction in female joint pathology with treatment was largely driven by decreased tidemark advancement. Tidemark replication is associated with articular cartilage mineralization and was almost completely absent in all males evaluated, implying there may also be differences in OA pathogenesis between male and female Dunkin-Hartley guinea pigs.

ACKNOWLEDGEMENTS

There are many people that I must thank, as without them this work would not have been possible. First, it is my pleasure to express sincere gratitude to my co-advisor, Kelly Santangelo, not only for adopting me into her lab and allowing me to work on such a unique subject but also for serving as an excellent mentor and friend throughout this process. I appreciate you always being available to talk, whether it be about science or life, and your insight has always provided me with confidence to take the next steps forward. It is through your unwavering support that I have been able to achieve this degree, and I am endlessly thankful. I would also like to thank Dr. Marie Legare for initially providing me with this opportunity and believing in my abilities since the first day I walked into her classroom 10 years ago. I would like to acknowledge Dr. Ron Tjalkens for serving as my co- advisor and, along with my committee members Dr. Laurie Goodrich and Dr. Lucas Argueso, helping make this degree possible by providing invaluable insight. I feel honored to have a committee of professors that represent the researcher I hope to become in my career, and I thank you for listening to my many presentations over the last 5 years. I am so grateful that I have been able to work with Dr. Mary Afzali throughout the last decade—thank you for serving as a wonderful mentor, friend, and collaborator all of these years, both in the lab and outside of it. I am so appreciative to all members of the Santangelo lab for creating such a fun and positive work environment. Thank you to my support system of friends, who have always been there to cheer me on through every triumph and defeat. Finally, and perhaps most importantly, I want to extend my deepest gratitude to my parents—thank you for always believing in me and encouraging me to follow my dreams. Without you both, I would not be where I am today.

TABLE OF CONTENTS

LIST OF FIGURES

CHAPTER 1

LITERATURE REVIEW

1.1 Importance of Iron.

Iron is essential for sustaining life in living organisms and is the most abundant trace element within mammalian bodies (1). The ability of iron to readily cycle between ferric (Fe^{3+}) and ferrous (Fe^{2+}) states makes it well suited for participating in numerous physiologic processes, including oxygen transport, energy production, nucleic acid replication, and cellular metabolism and signaling. However, excess or improperly managed iron encourages the presence of free, unliganded iron in the body, which can be toxic. Due to its electron structure, unbound iron participates in oxidation-reduction (redox) reactions that generate harmful reactive oxygen species (ROS) and free radicals capable of inciting tissue damage. Among these iron-mediated redox reactions is the Fenton reaction, which produces the highly reactive hydroxyl radical from the interaction of ferrous iron with the hydrogen peroxide abundant in cells (2-3). The resulting hydroxyl radical can then go on to produce additional free radical species via additional redox reactions or directly react with biological molecules such as lipids, proteins, and nucleic acids (4). Thus, the presence of hydroxyl radicals in cells has the potential to be cytotoxic, and iron present in the body must be tightly regulated to limit its formation.

1.2 Iron Metabolism and Homeostasis.

1.2.1 Dietary Forms of Iron and Iron Absorption.

Mammals have evolved an intricate system for regulating the presence and availability of iron. Dietary iron can be present in either the form of heme, from animal-derived foods, or non-

heme iron. The non-heme iron present in unmodified foods is largely insoluble and thus, has low bioavailability. Conversely, heme iron is readily absorbed through the intestine, but the regular availability of these foods is a recent development within human history and remains limited in certain locations, such as developing areas, as well as within some societies. In an attempt to correct nutritional iron deficiencies, the United States and other industrialized countries began the widespread fortification of foods with iron in the 1940's. The production of these iron-enriched foods has drastically increased the bioavailability of dietary iron, as evidenced by a significantly reduced risk of iron deficiency and anemia in individuals consuming these foods (5).

Mammals do not possess a dedicated mechanism for excretion, reflecting the limited availability of this element throughout the majority of evolution. As such, iron levels are managed by modulating the amount of iron absorbed through the gastrointestinal (GI) tract. Iron present in the ferric form, such as non-heme iron, needs to be converted to ferrous iron by the membrane-bound reductase duodenal cytochrome B prior to absorption. Ferrous iron is then transported across the apical membrane of enterocytes by divalent metal transporter 1 (DMT1), a protein capable of transporting several divalent cations in addition to iron. Inside the cell, the fate of iron is determined by the total iron status of the body. If iron stores are replete, the iron will be sequestered in the storage protein ferritin to prevent participation in redox reactions and eventually expelled from normal sloughing of the epithelium. When levels are depleted, iron will be transported across the basolateral membrane of the cell into systemic circulation by the only known iron export protein, ferroportin (FPN). The release of ferrous iron from cells is accompanied by oxidation to the ferric form by the ferroxidase enzyme hephaestin, allowing the newly released iron to bind to the plasma protein transferrin (TF) for systemic circulation in the

blood (6). Though iron chaperoned by TF is preferred to prevent redox cycling, circulating iron can also be present in the unliganded form as non-transferrin bound iron (NTBI).

1.2.2 Systemic Iron Circulation and Import into Cells.

Transferrin-bound iron (TBI) is primarily delivered to cells by binding to the ubiquitously expressed membrane transporter transferrin receptor 1 (TFR1). The transferrin-receptor complex is taken into the cell by clathrin-mediated endocytosis (7). Within the cell, the acidic environment of the endosome facilitates the release of iron from transferrin and iron is reduced to the ferrous form, while the apotransferrin and TFR1 are then recycled back to the cell surface. Historically, export of iron from the endosome was proposed to be primarily mediated by DMT1. However, recent studies have detected the presence of the metal ion transporter ZRT/IRT-like protein 14 (ZIP14) in the endosomes of cells, suggesting that this protein also facilitates iron export from these organelles in conjunction with DMT1 (8-9). Iron is released from the endosomes into the labile iron pool (LIP) present within the cytosol of cells.

Once reduced by ferroreductases at the cell surface, NTBI is imported into cells by DMT1 and ZIP-family proteins (such as ZIP8 and ZIP14) (10). The relative abundance of these transporters appears to vary by cell/tissue type (11-13). The uptake of NTBI does not involve endocytosis, and the iron is directly deposited within the LIP. Similar to the process of intestinal iron absorption, the fate of imported iron depends on the requirements of the cell. The mechanisms for sensing and responding to cellular iron levels are outlined in section 1.2.4.

1.2.3 Cellular Iron Storage and Utilization.

The LIP is a transitory reservoir of bioavailable, redox-active iron that, under normal conditions, the cell tries to maintain at a low concentration. If there are not immediate demands for iron to be utilized or integrated into proteins, it will be stored in ferritin. Systemically, the

liver serves as the major iron repository, but all nucleated cells are able to stow iron for future metabolic needs (or supply, if faced with iron deficiency). Binding iron to ferritin keeps it in an inert state and, therefore, helps to protect the cell by preventing the unmitigated formation of reactive species. The ferritin protein consists of two subunits: the first being the heavy chain (FTH) molecule and second, a light chain (FTL). Collectively, a single ferritin protein can hold 4500 atoms of ferric iron (14), and the expression of this protein increases with cellular iron loading as well as oxidative stress (15). Cytosolic labile iron (Fe^{2+}) is incorporated into ferritin through the ferroxidase activity of FTH, oxidizing iron to the ferric state for storage.

When the cell requires iron, it is released from ferritin primarily through lysosomal digestion (16-19), though a proteasomal pathway of iron release may also exist (20-21). The lysosomal compartment is essential for normal cell maintenance and plays a critical role in the degradation of cellular components, such as aged or damaged organelles and proteins, as well as endocytosed macromolecules (22). Iron liberated from ferritin in the lysosomes is returned to the cytosolic LIP, likely through involvement of DMT1 (17), for incorporation into proteins or utilization in the mitochondria. The cell may also export superfluous iron back into systemic circulation via ferroportin (23).

1.2.4 Regulation of Iron Metabolism and Homeostasis.

As previously stated, mammals possess highly evolved systems for maintaining appropriate iron levels. The regulation of iron metabolism occurs at both the organism level as well as within individual cells.

Systemic iron homeostasis is essential to maintaining appropriate iron levels both within tissues as well as in circulation. Systemic iron levels are controlled at the site of absorption, as iron present within the body is continuously recycled by macrophages rather than excreted.

When a mammal requires iron, it is mobilized out of body iron stores and the GI absorption of iron will be increased. Conversely, when iron stores are replete, the body will limit dietary absorption and increase the amount of iron stored. This process is mediated by the liver-derived hormone hepcidin. Hepcidin production stimulates the degradation of the iron export protein ferroportin, thereby limiting the amount of iron released from cells, such as GI enterocytes, into circulation. Accordingly, hepcidin expression is upregulated when total iron stores are high. Hepcidin production can also be increased during inflammation (from pathologic infections or other sources), hypoxia, and/or oxidative stress to limit the availability of iron (24).

Iron is also tightly controlled within the cell. Though cellular iron homeostasis can be maintained through several mechanisms, a major method of iron regulation is through the interaction of iron regulatory proteins (IRPs) with iron-responsive elements (IREs) located within the mRNA of certain proteins such as TFR1, DMT1, ferritin, and ferroportin (25). The gene transcripts for TFR1 (gene symbol TFRC) and DMT1 (SLC11A2) contain IRE(s) within the 3' untranslated region (UTR) of the mRNA, while the IRE for ferritin heavy chain (FTH), ferritin light chain (FTL), and ferroportin (SLC40A1) is located within the 5' UTR (25-26). The inclusion of IREs within gene transcripts allows for the expression to be modulated relative to cellular iron levels through interactions with cytosolic proteins IRP1 and IRP2. When iron levels are low, the conformation of the IRPs allows for binding to the IREs in mRNA. For genes with IREs in the 3' UTR (TFRC and SLC11A2), IRP-binding stabilizes the mRNA, thereby preventing its degradation and increasing the amount of iron imported into cells (27). Conversely, transcripts with IREs within the 5' UTR are regulated at the post-transcriptional level and IRP-IRE interaction prevents the translation of genes to proteins (26-27). Thus, in addition to increasing cellular iron import, IRP-binding traps iron in cells by preventing export

via ferroportin while increasing the amount of available iron by decreasing storage in ferritin. When the cell does not immediately require iron, the conformation if the IRPs changes to prevent interaction with IREs. In the absence of IRP binding, cellular iron import via TFR1 and DMT1 is decreased, and the protein expression of ferritin and ferroportin is maintained to allow for cellular iron storage and export, respectively. Notably, despite having a high-affinity for transporting NTBI, gene transcripts for ZIP-family proteins do not contain an identifiable IRE and therefore are not regulated by this iron-dependent mechanism (28-29).

1.3 Osteoarthritis.

1.3.1 Significance of Osteoarthritis and Epidemiology.

Osteoarthritis (OA) is considered the most prevalent musculoskeletal disorder globally (30) and is currently the fifth leading cause for disability worldwide (31). OA is a degenerative disorder characterized by the degeneration of articular cartilage within an affected diarthrodial joint, accompanied by changes such as the thickening of subchondral bone, osteophyte formation, and synovial hyperplasia that collectively contribute to the progression of the disease (32). Thus, OA is now recognized as a whole organ disease involving all tissues of the joint. The result is painful and/or reduced mobility, which contributes to decreased quality of life and an increased susceptibility to comorbidities including obesity, heart disease, type II diabetes, depression (33-35). The knee and hip appear to be the most significant joints contributing to the total burden of OA-associated pain and disability (36), with the majority of end-stage knee OA cases needing prosthetic joint replacement to remedy/mediate the degenerative effects of the disease (37-38). The economic burden OA is also considerable, with the cost of treating knee OA contributing more than $27 billion dollars to annual health care expenses by 2013 (39). In

addition to the clinical costs associated with the disorder, a study conducted in 2012 revealed that the work loss from OA cost the United States economy over 100 billion dollars annually (40).

OA can be further characterized into 2 subcategories. Primary OA, the main focus of this dissertation, has no known etiology for the onset and/or progression of the disorder and is therefore considered idiopathic. However, similar to other degenerative disorders, advancing age has been highlighted as the most significant risk factor for developing primary OA (41-42). Indeed, primary or idiopathic OA is estimated to affect approximately 10% of the total global population aged over 60 (30) and, as the worlds aging population continues to grow, it is anticipated that more than 130 million people across the globe will be affected with OA by 2050 (43). Other risk factors for developing idiopathic OA include genetics, obesity, gender, bone density, joint malalignment, and reduced physical activity (44-45). Conversely, post-traumatic OA (PTOA) arises after a joint has sustained an injury and initiates the degenerative changes characteristic of OA. As PTOA is injury-related, it tends to affect a younger demographic than idiopathic OA (41,46). Though the factors driving OA differ between the 2 subcategories, the resulting joint pathology can broadly share similarities and, therefore, face the similar obstacles for preventing and/or treating the disorder.

OA is a progressive disorder, and unfortunately, the mechanisms driving disease pathogenesis remain largely unknown. As a result, there are currently no known treatments that can halt, slow, and/or reverse the effects of OA (43), and therapies are directed towards minimizing the pain associated with the disorder. In fact, it is estimated that patients will spend an average of 13 years exhausting pain-relieving medications prior to pursuing total knee replacement for OA (39). The undesirable effects occurring with chronic use these pharmaceutics (47) makes this an ineffective, long-term solution, particularly as these

interventions fail to address the underlying causes of pain. Thus, there is a clear need for better understanding OA pathogenesis such that effective treatment strategies can be identified for combating the disorder.

1.3.2 Overview of the Current Understanding of Osteoarthritis Pathogenesis.

Articular cartilage is an avascular tissue sparsely populated by the only cell type present, the chondrocyte. As post-mitotic cells, chondrocytes have low levels of replication and as a result, articular cartilage has very limited regenerative capabilities (48). Chondrocytes are metabolically active cells that secrete macromolecules, such as collagens, proteoglycans, and glycoproteins, that comprise the extracellular matrix (ECM) and collectively maintain the structure and integrity of the tissue through a delicate balance of catabolic and anabolic events (49). Chondrocyte activity is influenced by mechanical forces as well as numerous molecular factors, such as proinflammatory mediators and reactive oxygen species (ROS), that are released into the synovial fluid by neighboring joint tissues in addition to being produced by chondrocytes themselves. In OA, the production and relative abundance of these factors becomes dysregulated and can inappropriately upregulate catabolic events, contributing to progressive cartilage degeneration. Furthermore, the presence of degraded ECM components itself also stimulates the production of these signaling molecules and proinflammatory mediators, further propagating this dyshomeostasis and tissue loss.

Besides mechanical stress, it is currently unknown what initiates cartilage degeneration in OA. In early stages of disease, this breakdown occurs at the microscopic level at the articular cartilage surface, releasing fragments into the synovial fluid. The presence of degraded extracellular matrix (ECM) components stimulates the production of matrix degrading enzymes and inflammatory cytokines by both synoviocytes and chondrocytes, further propagating tissue

degradation (32,50). Additionally, cells present within the synovium phagocytose the ECM fragments present in the synovial fluid, causing synovial hyperplasia and the infiltration of inflammatory cells (51). The aberrant production of these mediators causes chondrocytes to produce elevated levels of ROS and reactive nitrogen species (RNS) (52). While normally present at low levels to function in numerous physiologic processes, the increased production of ROS/RNS by chondrocytes contributes to altered cell signaling and cartilage tissue damage, and further stimulates the inflammatory response by the synovium (52-53). The presence of peroxidation products in OA-affected cartilage supports the involvement of these molecules in the disease process (52-53).

Chondrocytes initially attempt to offset the breakdown of matrix constituents by increasing the production of ECM macromolecules and growth factors than can contribute to the formation of osteophytes and tissue vascularization, particularly within the synovium (54-56). This “boost” in anabolic activity is accompanied by increased chondrocyte proliferation, giving rise to the aggregates of chondrocytes commonly observed in this stage of disease (54). However, this attempt is futile, as chondrocytes eventually reach a point of exhausting their synthesizing capabilities (57). At this point, the rate of matrix degradation overthrows that of synthesis, and cartilage degradation becomes severe. Chondrocyte cell loss becomes diffuse within the ECM, likely in part from the elevated production of inflammatory cytokines and ROS/RNS, as well as the overall disrupted ECM structure (58). At the same time, the proliferative chondrocytes from earlier stages express a hypertrophic phenotype and seem to re-establish the process of endochondral ossification normally occurring during growth plate fusion (59-61). This phenotypic shift causes cartilage mineralization, eventually decreasing the

thickness of the tissue and altering the architecture of the subchondral bone that's observed in late stages of disease (62).

1.3.3 Laboratory Rodent Models of Idiopathic Osteoarthritis.

As the natural development of idiopathic OA spans across decades in humans, the need for laboratory models with accelerated, but accurate pathogenesis is necessary to increase understanding of disease. Furthermore, patients do not tend to seek clinical care until the negative symptoms of OA become pronounced, usually occurring at later stages of disease. Thus, use of laboratory models also allows for researchers to investigate initial changes within the joint to better understand early stages of the disorder and factors contributing to the disease.

Both large and small animals have been used to investigate OA, and the selection of the correct animal model is dependent on several factors such as the type of experiment, length of study, husbandry costs, and desired outcome measurements. Overall, rodent models are commonly used in laboratory settings due to their small size, relatively low associated costs, ease of implementation, and short lifespan (63). Mice are an obvious option due to their widespread use in research; however, most mouse strains do not naturally develop OA and require a stimulating event (chemical, mechanical, surgical) or genetic/genomic manipulation to incite OA pathology. Human idiopathic OA is widely considered to be multifactorial in nature and cannot be attributed to a single cause or gene mutation (32). As such, the use of a genetically altered animal likely oversimplifies the disease process. Additionally, as presented in section 1.3.1, the development of OA following a traumatic joint event is classified as an entirely separate type of OA (PTOA) and therefore should not be used to evaluate the processes occurring in idiopathic OA. By requiring an exogenous influence, mouse models of OA are not truly spontaneous, and the resulting pathophysiology may not accurately reflect what is observed in humans (64). Thus,

mice are best suited for OA studies related to secondary OA or PTOA. Like mice, rats do not tend to spontaneously develop OA (65).

Guinea pigs have been widely used as models for biomedical research. Despite current classification in the order Rodentia, the taxonomic classification of guinea pigs has been continuously up for debate, and guinea pigs may be more closely related to humans than other rodents (66). Indeed, the sequences of several guinea pig proteins are largely homologous to those in humans (67). Several physiologic and anatomic features of guinea pigs also make them well-suited for certain studies of human disorders, including those related to reproduction and pregnancy, allergic disorders and hypersensitivity reactions, respiratory diseases, hearing, and lipid metabolism (68-69). With respect to other rodents, guinea pigs have the unique dietary requirement of vitamin C, a naturally occurring antioxidant compound that is also essential in humans (69). Therefore, the presence of dietary vitamin C may be useful in studying redox reactions and oxidative stress as they occur in humans.

The Dunkin-Hartley guinea pig is an outbred, non-genetically manipulated strain with widespread use in immunological research (70). Notably, this strain of guinea pig naturally and spontaneously develops knee OA with advancing age, and the resulting histopathology closely resembles that observed in humans (71-72). Within this model, articular cartilage lesions are first observed in the medial compartment of the knee and become more severe with disease progression; this is characteristic of the disorder in humans (73). Though the progression of OA is relatively slow in Hartley guinea pigs than other animal models, this allows for researchers to investigate stages in disease pathogenesis and is therefore an additional benefit of the model. The availability of control guinea pig strains with decreased propensity for OA allows for the factors contributing to disease to be further investigated, representing a final benefit to the use of guinea

pigs in OA research. Collectively, the Dunkin Hartley guinea pig is a well-characterized model of OA (71-74) may provide the most accurate representation of the disorder as it occurs in humans and was the primary animal model used for the studies presented in this dissertation. Limitations for the use of guinea pigs include the limited availability of species-compatible reagents, relatively higher cost, and an incompletely sequenced genome.

1.3.4 Relevant Methods for the Laboratory Evaluation of Knee Osteoarthritis.

Clinically, there is no single test for the determination of OA. The use of appropriate methods allows for structural, biomechanical, pain, and/or movement-related changes to be evaluated in the context of the disorder.

The most common outcome used for laboratory OA assessment remains histopathology (75). The use of select histologic stains allows for the severity of tissue degradation to be evaluated spatially within the joint tissue. Numerous grading schemes have been published in an attempt to standardize the histologic assessment of knee joints between studies, such that findings could be compared between works. Initial scoring systems were based on observations made in human pathology (76) and consequently had inherent limitations for use in animal models. This gap led to the Osteoarthritis Research Society International (OARSI) Histopathology Initiative, publishing separate grading schemes for histologic evaluation in common OA animal models. The guinea pig OARSI recommendations include 3 core assessment categories relating to the structure of articular cartilage, proteoglycan content, and chondrocyte cellularity within the ECM (74). Optional categories for evaluation include tidemark evaluation and the presence of osteophytes (74). The limitations for histopathology include the invasiveness of the procedure, which prevents longitudinal assessments being made at different timepoints throughout the study. Additionally, histologic evaluations are conducted on one

region/tissue section and therefore does not provide a comprehensive evaluation of the entire joint structure.

There are several non-invasive imaging techniques used to complement the structural assessment of joints with histopathology. Radiographic imaging remains the principal method for diagnosing and monitoring OA in humans and therefore holds translational value within animal models (77). X-ray imaging allows for the visualization of OA-related bony changes including osteophyte formation, joint space narrowing, and subchondral bone sclerosis in a single tissue plane (77). Computed tomography (CT) scans construct 3D composites from serial 2D radiographic images and thus allow for comprehensive evaluation of the whole joint structure. Use of this technology on a scale better suited for smaller laboratory animals is called microCT and is a commonly used for laboratory evaluation of osteophytes as well as subchondral bone cysts and sclerosis (78). Notably, a scoring system for microCT has been developed for use in assessing OA in the guinea pig (78). Unfortunately, radiographic technology is not sensitive enough to detect subtle changes in joint pathology and prevents evaluation of the articular cartilage, menisci, or other soft tissue components of the joint (79). Magnetic resonance imaging (MRI) is an alternative imaging method that addresses the pitfalls encountered with radiology, allowing for the soft tissue and bone-related joint tissues to be evaluated simultaneously (79). Unfortunately, use of this technology is quite expensive, limiting its use in animal research.

As a main consequence of OA is decreased and/or painful mobility, the laboratory evaluation of animal movement seems important. Gait analysis systems involve a camera or other sensor usually fixed below a clear platform for experimental animals to walk across. These apparatuses can either be treadmill-based, which includes a belt moving at a standard speed to propel the animal forward, or a catwalk concept that allows for animals to move by their own

volition. In either scenario, the recording of animal's paw placement while walking allows for researchers to analyze locomotion as it may relate to joint pathology (80). Conversely, the use of overhead enclosure monitoring allows for the activity of animals to be recorded while freely moving within an apparatus. Benefits of overhead enclosure monitoring include capturing inherent animal movement without direct influence from the researcher.

1.4 The Potential Role of Iron in Osteoarthritis.

As previously stated in section 1.1, unbound or partially-liganded iron can participate in redox-chemistry (1-2). These reactions generate harmful ROS and free radicals that can elicit and/or perpetuate inflammatory responses, injure cellular components, and promote cell death, which collectively fosters tissue damage. Thus, the risk for iron-mediated toxicity is not limited to overt excess and can also arise from conditions where intracellular iron becomes delocalized and/or inappropriately stored (81-83).

Iron has been demonstrated to progressively accumulate throughout the aging process (84-85). Increased tissue iron has been connected to several aging-associated chronic disorders, including atherosclerosis (86), neurodegenerative disorders (87-88), type II diabetes (89), certain forms of cancer (90), ocular disorders such as retinal degeneration and age-related macular degeneration (91-92), and sarcopenia (93). Excess and/or improperly managed iron has also been implicated in disorders with associated arthropathies, including hereditary hemochromatosis (94), hemophilic arthropathy (95), traumatic arthropathy, and rheumatoid arthritis (RA) (96). Pertaining to the joint environment, iron has been demonstrated to have a direct effect on articular cartilage by mediating the production of the hydroxyl radical capable of inducing chondrocyte apoptosis and contributing to the breakdown of matrix constituents (97-99). Additionally, iron-loaded synoviocytes produce proinflammatory cytokines such as interleukin

(IL)-6, IL-1ß, and tumor necrosis factor, that further stimulate the catabolic activity of chondrocytes, further promoting joint tissue degradation (97).

Though the role of iron has been explored in the aforementioned conditions, it has yet to be widely explored within the context of idiopathic OA. One human study reported that synovial fluid iron concentration was significantly higher in OA-affected patients relative to both healthy controls and individuals with RA (100). Another study found that serum ferritin levels were positively correlated with the severity of cartilage damage in people affected by OA; this finding was independent of age, sex, and BMI (101). Finally, enhanced iron deposition in the synovium has been reported in patients with OA (102). These studies suggest that iron may be a contributing factor in knee OA and may provide mechanistic insight to the development of the disorder.

1.5 Global Hypothesis.

The work presented in this dissertation was designed to elucidate the potential role that iron contributes to the onset, progression, and/or severity of idiopathic OA. The global hypothesis for this research is that iron homeostasis becomes dysregulated during the aging process, eventually leading to accumulation within knee joints and contributing to OA pathology and tissue damage.

1.6 References.

1. Linder MC. Mobilization of stored iron in mammals: a review. Nutrients. 2013; 5(10): 4022-4050. doi: 10.3390/nu5104022.
2. Winterbourn CC. Toxicity of iron and hydrogen peroxide: the Fenton reaction. *Toxicol Lett*. 1995; 82-83:969-74. doi: 10.1016/0378-4274(95)03532-x.
3. Koppenol WH, Hider RH. Iron and redox cycling. Do's and don'ts. *Free Radic Biol Med*. 2019; 133: 3-10. doi: 10.1016/j.freeradbiomed.2018.09.022.
4. Maurya PK. Animal biotechnology as a tool to understand and fight aging. In: Verma AS, Singh A, eds. Animal biotechnology. Amsterdam: Academic Press; 2014. p. 177-91. doi: 10.1016/B978-0-12-416002-6.00010-9.
5. Gera T, Sachdev HS, Boy E. Effect of iron-fortified foods on hematologic and biological outcomes: systematic review of randomized controlled trials. *Am J Clin Nutr*. 2012; 96(2): 309-24. doi: 10.3945/ajcn.111.031500.
6. Camaschella C, Nai A, Silvestri L. Iron metabolism and iron disorders revisited in the hepcidin era. Haematologica. 2020; 105(2): 260-72. doi: 10.3324/haematol.2019.232124.
7. Frazer DM, Anderson CJ. The regulation of iron transport. *Biofactors*. 2014; 40(2): 206-14. doi: 10.1002/biof.1148.
8. Zhao N, Gao J, Enns CA, Knutson MD. ZRT/IRT-like protein 14 (ZIP14) promotes the cellular assimilation of iron from transferrin. *J Biol Chem*. 2010; 285(42): 32141-50. doi: 10.1074/jbc.M110.143248.
9. Van Raaij SEG, Srai SKS, Swinkels DW, van Swelm RPL. Iron uptake by ZIP8 and ZIP14 in human proximal tubular epithelial cells. *Biometals*. 2019; 32(2): 211-226. doi: 10.1007/s10534-019-00183-7.
10. Knutson MD. Non-transferrin-bound iron transporters. Free Radic Biol Med. 2019; 133: 101-11. doi: 10.1016/j.freeradbiomed.2018.10.413.
11. Liuzzi JP, Aydemir F, Nam H, Knutson MD, Cousins RJ. ZIP14 (slc39a14) mediates non-transferrin-bound iron uptake into cells. *Proc Natl Acad Sci USA*. 2006; 103(37): 13612-7. doi: 10.1073/pnas.0606424103.
12. Nam H, Wang CY, Zhang L, Zhang W, Hojyo S, Fukada T, et al. ZIP14 and DMT1 in the liver, pancreas, and heart are differentially regulated by iron deficiency and overload: implications for tissue iron uptake in iron-related disorders. *Haematologica*. 2013; 98(7): 1049-57. doi: 10.3324/haematol.2012.072314.
13. Koch RO, Zoller H, Theuri I, Obrist P, Egg G, Strohmayer W, et al. Distribution of DMT1 within the human glandular system. *Histol Histopathol*. 2003; 18(4): 1095-101. doi: 10.14670/HH-18.1095.
14. Harrison PM, Banyard SH, Hoare RJ, Russell SM, Treffry A. The structure and function of ferritin. Ciba Found Symp. 1976; (51): 19-40. doi: 10.1002/9780470720325.ch2.
15. Arosio P, Elia L, Poli M. Ferritin, cellular iron storage and regulation. *IUBMB Life*. 2017; 69(6): 414-22. doi: 10.1002/iub.1621.
16. Zhang Y, Mikhael M, Xu D, Li Y, Soe-Lin S, Ning B, et al. Lysosomal proteolysis is the primary degradation pathway for cytosolic ferritin and cytosolic ferritin degradation is necessary for iron exit. *Antioxid Redox Signal*. 2010; 13(7): 999-1009. doi: 10.1089/ars.2010.3129.
17. Kurz T, Eaton JW, Brunk UT. The role of lysosomes in iron metabolism and recycling. *Int J Biochem Cell Biol*. 2011; 43(12): 1686-97. doi: 10.1016/j.biocel.2011.08.016.

18. Yu Z, Persson LH, Eaton JW, Brunk UT. Intralysosomal iron: a major determinant of oxidant-induced cell death. *Free Radic Biol Med*. 2003; 34(10): 1243-52. doi: 10.1016/s0891-5849(03)00109-6.
19. Garner B, Roberg K, Brunk UT. Endogenous ferritin protects cells with iron-laden lysosomes against oxidative stress. *Free Radic Res*. 1998; 29(2): 103-14. doi: 10.1080/10715769800300121.
20. Silva B, Faustino P. An overview of the molecular basis of iron metabolism regulation and the associated pathologies. *Biochim Biophys Acta*. 2015; 1852(7): 1347-59. doi: 10.1016/j.bbadis.2015.03.011.
21. De Domenico I, Vaughn MB, Li L, Bagley D, Musci G, Ward DM, et al. Ferroportin-mediated mobilization of ferritin iron precedes ferritin degradation by the proteasome. *EMBO J*. 2006; 25(22): 5396-404. doi: 10.1038/sj.emboj.7601409.
22. Luzio JP, Pryor PR, Bright NA. Lysosomes: fusion and function. *Nat Rev Mol Cell Biol*. 2007; 8(8): 622-32. doi: 10.1038/nrm2217.
23. Anderson GJ, Frazer DM. Current understanding of iron homeostasis. *Am J Clin Nutr*. 2017; 106(Suppl 6): 1559S-66S. doi: 10.3945/ajcn.117.155804.
24. Anderson ER, Shah YM. Iron homeostasis in the liver. *Compr Physiol*. 2013; 3(1): 315-30. doi: 10.1002/cphy.c120016.
25. Zhou ZD, Tan EK. Iron regulatory protein (IRP)-iron responsive element (IRE) signaling pathway in human neurodegenerative diseases. *Mol Neurodegener*. 2017; 12(1): 75. doi: 10.1186/s13024-017-0218-4.
26. Cairo G, Recalcati S. Iron-regulatory proteins: molecular biology and pathophysiological implications. *Expert Rev Mol Med*. 2007; 9(33): 1-13. doi: 10.1017/S1462399407000531.
27. Wilkinson N, Pantopoulos K. The IRP/IRE system in vivo: insights from mouse models. *Front Pharmacol*. 2014;5:176. doi: 10.3389/fphar.2014.00176.
28. Bogdan AR, Miyazawa M, Hashimoto K, Tsuji Y. Regulators of iron homeostasis: new players in metabolism, cell death, and disease. *Trends Biochem Sci*. 2016; 41(3): 274-286. doi: 10.1016/j.tibs.2015.11.012.
29. Zhao N, Zhang AS, Worthen C, Knutson MD, Enns CA. An iron-regulated and glycosylation-dependent proteasomal degradation pathway for the plasma membrane metal transporter ZIP14. *Proc Natl Acad Sci USA*. 2014; 111(25): 9175-80. doi: 10.1073/pnas.1405355111.
30. Pereira D, Peleteiro B, Araujo J, Branco J, Santos RA, Ramos E. The effect of osteoarthritis definition on prevalence and incidence estimates: a systematic review. *Osteoarthritis Cartilage*. 2011;19(11): 1270-85. doi: 10.1016/j.joca.2011.08.009.
31. Murray L, Helmick CG. The impact of osteoarthritis in the United States: a population-health perspective: a population-based review of the fourth most common cause of hospitalization in U.S. adults. *Orthop Nurs*. 2012; 31(2): 85-91. doi: 10.1097/NOR.0b013e31824fcd42.
32. Man GS, Mologhianu G. Osteoarthritis pathogenesis—a complex process that involves the entire joint. *J Med Life*. 2014; 7(1): 37-41. https://pubmed.ncbi.nlm.nih.gov/24653755/.
33. Suri P, Morgenroth DC, Hunter DJ. Epidemiology of osteoarthritis and associated comorbidities. *PM R*. 2012; 4(5 Suppl): S10-9. doi: 10.1016/j.pmrj.2012.01.007.
34. Hunter DJ, Neogi T, Hochberg MC. Quality of osteoarthritis management and the need for reform in the US. *Arthritis Care Res*. 2011; 63(1): 31-8. doi: 10.1002/acr.20278.

35. Gore M, Tai KS, Sadosky A, Leslie D, Stacey BR. Clinical comorbidities, treatment patterns, and direct medical costs of patients with osteoarthritis in usual care: a retrospective claims database analysis. *J Med Econ*. 2011;14(4): 497-507. doi: 10.3111/13696998.2011.594347.
36. Litwic A, Edwards MH, Dennison EM, Cooper C. Epidemiology and burden of osteoarthritis. *Br Med Bull*. 2013; 105: 185-99. doi: 10.1093/bmb/lds038.
37. Losina E, Thornhill TS, Rome BN, Wright J, Katz JN. The dramatic increase in total knee replacement utilization rates in the United States cannot be fully explained by growth in population size and the obesity epidemic. *J Bone Joint Surg Am*. 2012; 94(3): 201-7. doi: 10.2106/JBJS.J.01958.
38. Hochberg MC, Altman RD, April KT, Benkhalti M, Guyatt G, McGowan J, et al. American college of rheumatology 2012 recommendations for the use of nonpharmacologic and pharmacologic therapies in osteoarthritis of the hand, hip, and knee. *Arthritis Care Res (Hoboken)*. 2012; 64(4): 465-74. doi: 10.1002/acr.21596.
39. Losina E, Paltiel AD, Weinstein AM, Yelin E, Hunter DJ, Chen SP, et al. Lifetime medical costs of knee osteoarthritis management in the United States: impact of extending indications for total knee arthroplasty. *Arthritis Care Res (Hoboken)*. 2015; 67(2): 203-15. doi: 10.1002/acr.22412.
40. Sandell LJ. Etiology of osteoarthritis: genetics and synovial joint development. *Nat Rev Rheumatol*. 2012; 8(2): 77-89. doi: 10.1038/nrrheum.2011.199.
41. Johnson VL, Hunter DJ. The epidemiology of osteoarthritis. *Best Pract Res Clin Rheumatol*. 2014; 28(1): 5-15. doi: 10.1016/j.berh.2014.01.004.
42. Felson DT. The epidemiology of knee osteoarthritis: Results from the Framingham osteoarthritis study. *Semin Arthritis Rheum*. 1990;20(3):42-50. doi:10.1016/0049-0172(90)90046-I.
43. Maiese K. Picking a bone with WISP1 (CCN4): new strategies against degenerative joint disease. *J Transl Sci*. 2016; 1(3): 83-85. https://pubmed.ncbi.nlm.nih.gov/26893943/.
44. Gabay O, Clouse KA. Epigenetics of cartilage diseases. *Joint Bone Spine*. 2016; 83(5): 491-4. doi: 10.1016/j.jbspin.2015.10.004.
45. Hunter DJ, Bierma-Zeinstra S. Osteoarthritis. *Lancet*. 2019; 393(10182): 1745-59. doi: 10.1016/S0140-6736(19)30417-9.
46. Brown TD, Johnston RC, Saltzman CL, Marsh JL, Buckwalter JA. Posttraumatic osteoarthritis: a first estimate of incidence, prevalence, and burden of disease. *J Orthop Trauma*. 2006; 20(10): 739-44. doi: 10.1097/01.bot.0000246468.80635.ef.
47. Crofford LJ. Use of NSAIDs in treating patients with arthritis. *Arthritis Res Ther*. 2013; 15 Suppl 3(Suppl 3): S2. doi: 10.1186/ar4174.
48. Aigner T, Kim HA, Roach HI. Apoptosis in osteoarthritis. *Rheum Dis Clin North Am*. 2004; 30(3): 639-53. doi: 10.1016/j.rdc.2004.04.002.
49. Sophia Fox AJ, Bedi A, Rodeo SA. The basic science of articular cartilage: structure, composition, and function. *Sports Health*. 2009;1(6):461-468. doi:10.1177/1941738109350438.
50. Glyn-Jones S, Palmer AJR, Agricola R, Price AJ, Vincent TL, Weinans H, et al. Osteoarthritis. *Lancet*. 2015; 386(9991): 376-87. doi: 10.1016/S0140-6736(14)60802-3.
51. Sellam J, Berenbaum F. The role of synovitis in pathophysiology and clinical symptoms of osteoarthritis. *Nat Rev Rheumatol*. 2010; 6(11): 625-35. doi: 10.1038/nrrheum.2010.159.

52. Henrotin YE, Bruckner P, Pukol JPL. The role of reactive oxygen species in the homeostasis and degradation of cartilage. *Osteoarthritis Cartilage*. 2003; 11(10): 747-55. doi: 10.1016/s1063-4584(03)00150-x.
53. Henrotin Y, Kurz B, Aigner T. Oxygen and reactive oxygen species in cartilage degradation: friends or foes? *Osteoarthritis Cartilage*. 2005; 13(8): 643-54. doi: 10.1016/j.joca.2005.04.002.
54. Buckwalter JA, Mankin HJ. Articular cartilage: degeneration and osteoarthritis, repair, regeneration, and transplantation. *Instr Course Lect*. 1998; 47: 487-504. https://pubmed.ncbi.nlm.nih.gov/9571450/.
55. Hashimoto S, Creighton-Achermann L, Takahashi K, Amiel D, Coutts RD, Lotz M. Development and regulation of osteophyte formation during experimental osteoarthritis. *Osteoarthritis Cartilage*. 2002; 10(3): 180-7. doi: 10.1053/joca.2001.0505.
56. Van denBerg WB. Osteophyte formation in osteoarthritis. *Osteoarthritis Cartilage*. 1999; 7(3): 333. doi: 10.1053/joca.1998.0186.
57. Lorenz H, Richter W. Osteoarthritis: cellular and molecular changes in degenerating cartilage. *Prog Histochem Cytochem*. 2006; 40(3): 135-63. doi: 10.1016/j.proghi.2006.02.003.
58. Charlier E, Relic B, Deroyer C, Malaise O, Neuville S, Collee J, et al. Insights on molecular mechanisms of chondrocytes death in osteoarthritis. *Int J Mol Sci*. 2016;17(12):2146. doi: 10.3390/ijms17122146.
59. Goldring SR. Role of bone in osteoarthritis pathogenesis. *Med Clin North Am*. 2009; 93(1): 25-35. doi: 10.1016/j.mcna.2008.09.006.
60. von der Mark K, Kirsch T, Nerlich A, Kuss A, Weseloh G, Gluckert K, et al. Type X collagen synthesis in human osteoarthritic cartilage. Indication of chondrocyte hypertrophy. *Arthritis Rheum*. 1992; 35(7): 806-11. doi: 10.1002/art.1780350715.
61. Hoyland JA, Thomas JT, Donn R, Marriott A, Ayad S, Boot-Handford RP. Distribution of type X collagen mRNA in normal and osteoarthritic human cartilage. *Bone Miner*. 1991; 15(2): 151-63. doi: 10.1016/0169-6009(91)90005-k.
62. Lane LB, Bullough PG. Age-related changes in the thickness of the calcified zone and the number of tidemarks in adult human articular cartilage. *J Bone Joint Surg Br*. 1980; 62(3): 372-5. doi: 10.1302/0301-620X.62B3.7410471.
63. Bryda EC. The mighty mouse: the impact of rodents on advances in biomedical research. *Mo Med*. 2013; 110(3): 207-211. https://pubmed.ncbi.nlm.nih.gov/23829104/.
64. Staines KA, Poulet B, Wentworth DN, Pitsillides AA. The STR/ort mouse model of spontaneous osteoarthritis—an update. *Osteoarthritis Cartilage*. 2017; 25(6): 802-808. doi: 10.1016/j.joca.2016.12.014.
65. McCoy AM. Animal models of osteoarthritis: comparisons and key considerations. Vet Pathol. 2015; 52(5): 803-18. doi: 10.1177/0300985815588611.
66. Graur D, Hide WA, Li WH. Is the guinea-pig a rodent?. *Nature*. 1991; 351(6328): 649-52. doi: 10.1038/351649a0.
67. Aoki I, Shindoh Y, Nakai S, Hong YM, Mio M, Saito T, et al. Comparison between the amino acid and nucleotide sequences between human and two guinea pig major basic proteins. *FEBS Lett*. 1991; 282(1): 56-60. doi: 10.1016/0014-5793(91)80443-7.
68. Bahr A, Wolf E. Domestic animal models for biomedical research. *Reprod Domest Anim*. 2012; 47 Suppl 4: 59-71. doi: 10.1111/j.1439-0531.2012.02056.x.

69. Taylor DK, Lee VK. Guinea pigs as experimental models. In: Suckow MA, Stevens KA, Wilson RP, eds. The laboratory rabbit, guinea pig, hamster, and other rodents. Amsterdam: Academic Press; 2012. p. 705-44. doi: 10.1016/B978-0-12-380920-9.00025-0.
70. Clark S, Hall Y, Williams A. Animal models of tuberculosis: guinea pigs. *Cold Spring Harb Perspect Med*. 2014; 5(5): a018572. doi: 10.1101/cshperspect.a018572.
71. Jimenez PA, Glasson SS< Trubetskoy OV, Haimes HB. Spontaneous osteoarthritis in Dunkin Hartley guinea pigs: histologic, radiologic, and biochemical changes. *Lab Anim Sci*. 1997; 47(6): 598-601. https://pubmed.ncbi.nlm.nih.gov/9433695/.
72. Tessier JJ, Bowyer J, Brownrigg NJ, Peers IS, Westwood FR, Waterton JC, et al. Characterisation of the guinea pig model of osteoarthritis by in vivo three-dimensional magnetic resonance imaging. *Osteoarthritis Cartilage*. 2003; 11(12): 845-53. doi: 10.1016/s1063-4584(03)00162-6.
73. Bendele AM, Hulman JF. Spontaneous cartilage degeneration in guinea pigs. *Arthritis Rheum*. 1988; 31(4): 561-5. doi: 10.1002/art.1780310416.
74. Kraus VB, Huebner JL, DeGroot J, Bendele A. The OARSI histopathology initiative—recommendations for histological assessments of osteoarthritis in the guinea pig. *Osteoarthritis Cartilage*. 2010; 18 Suppl 3(Suppl 3): S35-52. doi: 10.1016/j.joca.2010.04.015.
75. Rutgers M, van Pelt MJP, Dhert WJA, Creemes LB, Saris DBF. Evaluation of histological scoring systems for tissue-engineered, repaired and osteoarthritic cartilage. *Osteoarthritis Cartilage*. 2010; 18(1): 12-23. doi: 10.1016/j.joca.2009.08.009.
76. Mankin HJ, Dorfman H, Lippiello L, Zarins A. Biochemical and metabolic abnormalities in articular cartilage from osteo-arthritic human hips. II. Correlation of morphology with biochemical and metabolic data. *J Bone Joint Surg Am*. 1971; 53(3): 523-37. https://pubmed.ncbi.nlm.nih.gov/5580011/.
77. Braun HJ, Gold GE. Diagnosis of osteoarthritis: imaging. *Bone*. 2012; 51(2): 278-88. doi: 10.1016/j.bone.2011.11.019.
78. Radakovich LB, Marolf AJ, Shannon JP, Pannone SC, Sherk VD, Santangelo KS. Development of a microcomputed tomography scoring system to characterize disease progression in the Hartley guinea pig model of spontaneous osteoarthritis. *Connect Tissue Res*. December 2017:1-11. doi:10.1080/03008207.2017.1409218.
79. Roemer FW, Eckstein F, Hayashi D, Guermazi A. The role of imaging in osteoarthritis. *Best Pract Res Clin Rheumatol*. 2014; 28(1): 31-60. doi: 10.1016/j.berh.2014.02.002.
80. Vandeputte C, Taymans JM, Casteels C, Coun F, Ni Y, Van Laere K, et al. Automated quantitative gait analysis in animal models of movement disorders. *BMC Neurosci*. 2010; 11: 92. doi: 10.1186/1471-2202-11-92.
81. Xu J, Marzetti E, Seo AY, Kim JS, Prolla TA, Leeuwenburgh C. The emerging role of iron dyshomeostasis in the mitochondrial decay of aging. *Mech Ageing Dev*. 2010; 131(7-8): 487-93. doi: 10.1016/j.mad.2010.04.007.
82. Paesano R, Natalizi T, Berlutti F, Valenti P. Body iron delocalization: the serious drawback in iron disorders in both developing and developed countries. *Pathog Glob Health*. 2012; 106(4): 200-16. doi: 10.1179/2047773212Y.0000000043.
83. Wessling-Resnick M. Iron homeostasis and the inflammatory response. *Annu Rev Nutr*. 2010; 30: 105-22. doi: 10.1146/annurev.nutr.012809.104804.
84. Cook CI, Yu BP. Iron accumulation in aging: modulation by dietary restriction. *Mech Ageing Dev*. 1998; 102(1): 1-13. doi: 10.1016/s0047-6374(98)00005-0.

85. Zacharski LR, Ornstein DL, Woloshin S, Schwartz LM. Association of age, sex, and race with body iron stores in adults: analysis of NHANES III data. *Am Heart J*. 2000; 140(1): 98-104. doi: 10.1067/mhj.2000.106646.
86. Stadler N, Lindner RA, Davies MJ. Direct detection and quantification of transition metal ions in human atherosclerotic plaques: evidence for the presence of elevated levels of iron and copper. *Arterioscler Thromb Vasc Biol*. 2004; 24(5): 949-54. doi: 10.1161/01.ATV.0000124892.90999.cb.
87. Smith MA, Harris PL, Sayre LM, Perry G. Iron accumulation in Alzheimer disease is a source of redox-generated free radicals. *Proc Natl Acad Sci*. 1997; 94(18): 9866-8. doi: 10.1073/pnas.94.18.9866.
88. Ashraf A, Jeandriens J, Parkes HG, So PW. Iron dyshomeostasis, lipid peroxidation and perturbed expression of cystine/glutamate antiporter in Alzheimer's disease: Evidence of ferroptosis. *Redox Biol*. 2020; 32: 101494. doi: 10.1016/j.redox.2020.101494.
89. Ford ES, Cogswell ME. Diabetes and serum ferritin concentration among U.S. adults. *Diabetes Care*. 1999; 22(12): 1978-83. doi: 10.2337/diacare.22.12.1978.
90. Stevens RG, Graubard BI, Micozzi MS, Neriishi K, Blumberg BS. Moderate elevation of body iron level and increased risk of cancer occurrence and death. *Int J Cancer*. 1994; 56(3): 364-9. doi: 10.1002/ijc.2910560312.
91. He X, Hahn P, Lacovelli J, Wong R, King C, Bhisitkul R, et al. Iron homeostasis and toxicity in retinal degeneration. *Prog Retin Eye Res*. 2007; 26(6): 649-73. doi: 10.1016/j.preteyeres.2007.07.004.
92. Blasiak J, Sklodowska A, Ulinska M, Szaflik JP. Iron and age-related macular degeneration. *Klin Oczna*. 2009; 111(4-6): 174-7. https://pubmed.ncbi.nlm.nih.gov/19673453/.
93. Hung SH, DeRuisseau LR, Kavazis AN, DeRuisseau KC. Plantaris muscle of aged rats demonstrates iron accumulation and altered expression of iron regulated proteins. *Exp Physiol*. 2008; 93(3): 407-14. doi: 10.1113/expphysiol.2007.039453.
94. Richette P, Ottaviani S, Vicaut E, Bardin T. Musculoskeletal complications of hereditary hemochromatosis: a case-control study. *J Rheumatol*. 2010; 37(10): 2145-50. doi: 10.3899/jrheum.100234.
95. Roosendaal G, Vianen ME, Venting MJ, van Rinsum AC, van den Berg HM, Lafeber FP. Iron deposits and catabolic properties of synovial tissue from patients with haemophilia. *J Bone Joint Surg Br*. 1998; 80(3): 540-5. doi: 10.1302/0301-620x.80b3.7807.
96. Biemond P, Swaak AJ, van Eijk HG, Koster JF. Intraarticular ferritin-bound iron in rheumatoid arthritis. A factor that increases oxygen free radical-induced tissue destruction. *Arthritis Rheum*. 1986; 29(10): 1187-93. doi: 10.1002/art.1780291002.
97. Nieuwenhuizen L, Schutgens REG, van Asbeck BS, Wenting MJ, van Veghel K, Roosendaal G, et al. Identification and expression of iron regulators in human synovium: evidence for upregulation in haemophilic arthropathy compared to rheumatoid arthritis, osteoarthritis, and healthy controls. *Haemophilia*. 2013; 19(4): e218-27. doi: 10.1111/hae.12208.
98. Hooiveld MJ, Roosendaal G, van den Berg HM, Bijlsma JW, Lafeber FP. Haemoglobin-derived iron-dependent hydroxyl radical formation in blood-induced joint damage: an in vitro study. *Rheumatology (Oxford)*. 2003;42(6):784-790. doi:10.1093/rheumatology/keg220.
99. Carroll GJ, Sharma G, Upadhyay A, Jazayeri JA. Ferritin concentrations in synovial fluid are higher in osteoarthritis patients with HFE gene mutations (C282Y or H63D). *Scand J Rheumatol*. 2010;39(5):413-420. doi:10.3109/03009741003677449.

100. Yazer M, Sarban S, Kocyigit A, Isikan UE. Synovial fluid and plasma selenium, copper, zinc, and iron concentrations in patients with rheumatoid arthritis and osteoarthritis. *Biol Trace Elem Res*. 2005;106(2): 123-32. doi: 10.1385/BTER:106:2:123.
101. Nugzar O, Zandman-Goddard G, Oz H, Lakstein D, Feldbrin Z, Shargorodsky M. The role of ferritin and adiponectin as predictors of cartilage damage assessed by arthroscopy in patients with symptomatic knee osteoarthritis. *Best Pract Rest Clin Rheumatol*. 2018; 32(5): 662-8. doi: 10.1016/j.berh.2019.04.004.
102. Ogilvie-Harris DJ, Fornasier VL. Synovial iron deposition in osteoarthritis and rheumatoid arthritis. *J Rheumatol*. 1980; 7(1): 30-6. https://pubmed.ncbi.nlm.nih.gov/7354467/.

CHAPTER 2

AGE AND SEX COMPARISONS OF TISSUE IRON CONCENTRATION AND THE EXPRESSION OF IRON-RELATED GENES IN TWO GUINEA PIG STRAINS

2.1 Introduction.

Osteoarthritis (OA) is the most prevalent joint disorder and affects millions of individuals worldwide (1). Though the disorder is recognized to involve all tissues within an affected joint, it is clinically characterized by the progressive loss of articular cartilage. Articular cartilage is a unique, avascular tissue maintained by chondrocytes, which secrete extracellular matrix (ECM) molecules that provide structure to the tissue (2). As post-mitotic cells, chondrocytes have limited regenerative ability (3) and, once the native articular cartilage is lost, it largely cannot be replaced. Unfortunately, the current understanding of the mechanisms driving OA pathogenesis remain poorly understood, and there are currently no treatments or therapies available to regenerate or replace articular cartilage after it has been degraded.

Though little is known about the factors contributing to OA, advancing age has been identified as the leading risk factor for disease development (4). Several aging-associated disorders including atherosclerosis (5), type II diabetes (6), sarcopenia (7), cancers (8), and neurodegenerative disorders (9-11) have documented iron dyshomeostasis and/or excess in the pathogenesis of the disease. Iron is essential for conducting numerous physiologic processes but can also participate in redox reactions, such as the Fenton reaction, which generate harmful reactive oxygen species (ROS) and free radicals capable of damaging tissue (12-13). As such, iron needs to be properly managed to limit the unmitigated formation of free radical species.

Excess tissue iron has also been documented in several disorders with associated arthropathies, including hereditary hemochromatosis (14), transfusion-related iron overload (15-16), hemophilic arthropathy (17), and rheumatoid arthritis (RA) (18). Relevant to these conditions, the presence of excess iron has been demonstrated to induce hydroxyl radical-driven chondrocyte apoptosis and the breakdown of matrix components (19).

Within the context of OA, iron has only been explored in a handful of manuscripts. One such study found that serum ferritin levels positively correlated with the severity of cartilage degeneration in patients affected by OA (20). Notably, the reported association between serum ferritin and cartilage degeneration was maintained after correcting for age, sex, and BMI, suggesting that the involvement of iron in OA may be consistent between multiple risk factors (20). Another study conducted in humans found that iron concentration in the synovial fluid was significantly higher in OA-affected individuals relative to both unaffected controls and patients with RA (21). Finally, increased iron deposits have been documented in the synovium of persons with OA (22). Collectively, the results from these studies suggest that iron may contribute to the pathology of knee OA.

Despite the potential association between iron, aging, and joint pathology, the expression of iron-transporting genes has not been widely documented within articular cartilage, particularly without the presence of genetic abnormalities. Thus, the objective of this study was 2-fold: first, to establish differences in tissue iron concentrations between the OA-prone Hartley guinea pig and a control guinea pig strain at 2 ages. Secondly, to investigate the gene expression of several molecules involved in iron metabolism within knee cartilage tissue of Hartley guinea pigs at ages representing different stages of OA progression. We hypothesize that, relative to the control

strain, the concentration of iron is significantly higher within the articular cartilage from OA-prone guinea pigs due to dysregulated expression of genes related to iron homeostasis.

2.2 Materials and Methods.

2.2.1 Animals.

All procedures were approved by the Institutional Animal Care and Use Committee and performed in accordance with the NIH Guide for the Care and Use of Laboratory Animals. Sixteen 5 month-old (n = 4 males and n = 4 females) and 15 month-old (n = 4 males and n = 4 females) pigmented strain guinea pigs were purchased from Elm Hill Labs (Chelmsford, MA). Tissues from a total of 128 Dunkin-Hartley guinea pigs (n = 62 males and n = 66 females) at ages 5 months (n = 17 males and n = 15 females), 7 months (n = 8 males and n = 16 females), 8 months (n = 7 males and n = 8 females), 12 months (n = 16 males and n = 16 females), and 15 months (n = 14 males and n = 11 females) were analyzed for various outcomes included in this study. The Dunkin-Hartley animal tissues utilized in this study were previously purchased from Charles River Laboratories (Wilmington, MA) for use as control animals in independent, but related, work. Animals were housed individually in solid bottom cages and monitored daily by a veterinarian. Food and standard guinea pig chow were provided *ad libitium*.

2.2.2 Specimen Collection.

Animals were placed under isoflurane anesthesia, and blood was collected via direct cardiac puncture with a 20-gauge butterfly needle. Serum was separated from whole blood and submitted for iron quantification using the Roche Cobas 6000 (Basel, Switzerland). A portion of the liver was collected from each animal at the same anatomic location and placed into 10% neutral buffered formalin (NBF) for 48 hours for iron quantification by atomic absorption spectroscopy (AAS).

Hind limbs were removed at the coxofemoral joint. The right hind limb was dissected to expose the knee joint, and articular cartilage was collected from the weight bearing regions of the femoral condyles and tibial plateaus, as well as from the articular surface of the patella. Collected cartilage was placed into RNAlater (Qiagen, Hilden, Germany) and stored at -80ºC for RNA isolation and subsequent gene analysis. For Dunkin-Hartley animals euthanized at 5 and 15 months-of-age, the femoral head from the right limb was frozen at -80ºC at the time of harvest and was subsequently fixed in 10% NBF for 48 hours prior to analysis by AAS. The right femoral heads isolated from all remaining study animals were placed into 10% NBF for 48 hours immediately at the time of harvest and were subsequently submitted for evaluation by AAS. Of note, the authors have found no significant difference in the iron content of tissues preserved by freezing vs. formalin fixation (data not shown).

2.2.3 Tissue Iron Quantification by Atomic Absorption Spectroscopy (AAS).

Gene expression analysis of knee articular cartilage prevented use of this tissue for iron quantification. As such, iron quantification for diarthrodial joint cartilage was conducted on femoral head articular cartilage samples. Iron concentration of livers was determined for pigmented strain guinea pigs at 5 months (n = 8) and 15 months-of-age (n = 8). Iron content was also determined for sections of liver isolated from Dunkin-Hartley guinea pigs at 5 months (n = 23), 8 months (n = 15), and 15 months-of-age (n = 24). As previously described (23), dried samples were weighed, ashed, sonicated in nitric acid, and diluted 30-fold with deionized water (24). Diluted samples were analyzed using a Model 240 AA flame atomic absorption spectrometer and SpectraAA software (Agilent Technologies, Santa Clara, CA) (25). Iron levels were reported as parts per million (ppm) dry weight (26).

2.2.4 Gene Expression Analysis of Knee Articular Cartilage.

Total RNA was isolated from knee articular cartilage using the RNeasy Lipid Tissue Mini Kit (Qiagen) and was sent to the University of Arizona Genetics Core (University of Arizona, Tucson, AZ) for analysis, as previously described (23). A custom set of guinea pig-specific probes were designed and manufactured by NanoString Technologies (Seattle, WA) and included the following genes: Ferritin heavy chain (FTH), transferrin receptor 1 (TFR1), divalent metal transporter 1 (SLC11A2/DMT1), ZRT/IRT-like protein 14 (SLC39A14/ZIP14), and ferroportin (SLC40A1/FPN). Based on initial RNA quantification (Invitrogen Qubit 2.0 Fluorometer and RNA High Sensitivity Assay Kit, Thermo Fisher Scientific, Waltham, MA) and fragment analysis quality control subsets (Fragment Analyzer Automated CE System and High Sensitivity RNA Assay Kit, Agilent Technologies), the optimal amount of total RNA (150-400 ng) was hybridized with the custom codeset in an overnight incubation at 65ºC, followed by processing on the NanoString nCounter® FLEX Analysis System (NanoString Technologies). Results are reported as absolute transcript counts normalized to two housekeeping genes, β-actin (ACTB) and eukaryotic elongation factor 1α1 (EEF1A1). Any potential sample input variance was normalized by use of housekeeping genes and application of a sample-specific correction factor to all target probes. Data analysis was conducted using nSolver™ software (NanoString Technologies).

2.2.5 Statistical Analyses.

Statistical analyses were performed with GraphPad Prism 8.4.2 (La Jolla, CA). Strain comparisons data between pigmented controls and Hartley guinea pigs were compared by two-way analysis of variance (ANOVA) with Sidak multiple comparisons test. Data within each strain was compared by either t-test (for 2 groups) or one-way ANOVA (for 3+ groups). The

distribution and variance of data sets analyzed by t-test were determined with the Shapiro-Wilk and F-Test, respectively. For one-way ANOVA, the distribution and variance of data sets was determined with the Shapiro-Wilk and Brown-Forsythe test, respectively. Lines on graph represent mean values. Statistical significance was set at $p \leq 0.05$, and trends were highlighted for p-values ≤ 0.09.

2.3 Results.

2.3.1 Liver Iron Concentration.

Between 5 months and 15 months-of-age, pigmented control animals exhibited a significant increase in liver iron concentration ($p = 0.002$; Figure 2.1). This trend was maintained when each sex was analyzed separately, but the difference in liver iron concentration with age was greater within females. Within male pigmented control animals, mean liver iron concentration increased from 802.30 ppm at 5 months-of-age to 1873.00 ppm at 15 months-of-age ($p = 0.002$). The mean liver iron concentration in 5 month-old female pigmented animals was 842.50 ppm and increased to 2140.00 ppm at 15 months-of-age ($p < 0.0001$). There was no significant sex difference in liver iron concentration for pigmented control animals at either 5-months ($p = 0.5$) or 15-months ($p = 0.2$).

Conversely, OA-prone Hartley guinea pigs did not have a significant difference in liver concentration between 5 months-of-age and 15 months-of-age ($p = 0.5$; Figure 2.1). When an additional timepoint was added to represent 8 months-of-age, the lack of statistical differences between Hartley liver iron concentration was consistent (Figure 2.1). There were no significant differences present when each sex was analyzed separately. For male Hartley guinea pigs, mean liver iron concentration was 435.80 ppm at 5-months and was 397.80 at 15 months-of-age ($p = 0.7$). Five-month-old female Hartley animals had a mean liver iron concentration of 417.90 ppm,

while at 15 months-of-age the mean liver iron concentration was 579.40 ($p = 0.2$). There was no significant difference between sexes for liver iron concentration at 5-months ($p = 0.8$) or 15 months-of-age ($p = 0.2$).

2.3.2 Iron Concentration of Femoral Head Articular Cartilage.

Pigmented control guinea pigs did not have a significant difference in the iron concentration of femoral head articular cartilage between 5 months and 15 months-of-age ($p = 0.3$; Figure 2.2). Male pigmented animals had a relatively higher articular cartilage iron concentration at 15 months-of-age (30.45 ppm) than at 5 months-of-age (26.60 ppm), although this difference was not significant ($p = 0.11$). Female pigmented controls did not have a significant difference in cartilage iron concentration between 5 months (35.93 ppm) and 15 months-of-age (31.68 ppm) ($p = 0.6$). There was no notable difference between sexes for cartilage iron concentration at 5 months-of-age ($p = 0.2$) and 15 months-of-age ($p = 0.7$).

Hartley guinea pigs had a significant decrease in the iron concentration of femoral head articular cartilage between 5 and 15-months of age ($p = 0.02$; Figure 2.2). However, when additional ages (representing various stages in OA progression) were investigated, there was a significant increase in cartilage iron concentration between 5 months and 7-8 months of age ($p < 0.0001$), which then progressively decreased at 12 and 15 months (Figure 2.2). This observation was maintained when each sex was analyzed separately, with males having more significant fluctuations in cartilage iron concentration than females at the ages investigated (Figure 2.3 A-B). Analysis revealed that males had significantly higher cartilage iron concentration than females at 7-8 months of age ($p < 0.001$), but cartilage iron concentrations were comparable between sexes at all other ages investigated. Overall, Hartley guinea pigs had higher cartilage

iron concentrations than pigmented control animals at 5 months ($p = 0.03$) and, to a lesser degree, at 15 months-of-age ($p = 0.1$).

2.3.3 Gene Expression of Knee Articular Cartilage: Strain Comparisons.

2.3.3.1 Transferrin Receptor 1 (TFR1).

Both pigmented control animals and Hartley guinea pigs exhibited similar trends in expression of TFR1 within knee articular cartilage, which decreased between 5 and 15 months-of-age (Figure 2.4 A). Transcript counts of TFR1 were comparable between strains at 5 months-of-age ($p > 0.9999$), though at 15 months-of age pigmented animals had slightly higher expression of TFR than Hartley guinea pigs ($p = 0.08$; Figure 2.4 A). The decrease in gene expression of TFR1 was not significant in pigmented control animals between 5 and 15 months-of-age ($p = 0.1$) but was significant in Hartley guinea pigs at the same ages ($p < 0.0001$; Figure 2.4 A).

2.3.3.2 Divalent Metal Transporter 1 (DMT1).

Relative to pigmented controls, Hartley guinea pigs had higher transcript counts for DMT1 at either age investigated (Figure 2.4 B). DMT1 gene expression decreased significantly between 5 months and 15 months-of-age in pigmented animals ($p = 0.05$; Figure 2.4 B). Conversely, DMT1 mRNA expression remained high and was not significantly different between 5 months and 15 months-of-age for Hartley guinea pigs ($p = 0.95$; Figure 2.4 B).

2.3.3.3 ZRT/IRT-Like Protein 14 (ZIP14).

Transcript counts for ZIP14 were similar between animal strains at either age investigated (Figure 2.4 C). Likewise, ZIP14 gene expression was not significantly different between 5 months and 15 months-of-age for either pigmented guinea pigs ($p = 0.3$) or OA-prone Hartleys ($p = 0.2$; Figure 2.4 C).

2.3.3.4 Ferritin Heavy Chain (FTH).

Overall, pigmented animals had significantly lower transcript counts than Hartley guinea pigs at either age investigated (Figure 2.4 D). Gene expression of FTH was not significantly different between ages for either pigmented controls ($p = 0.97$) or Hartley guinea pigs ($p = 0.99$; Figure 2.4 D).

2.3.3.5 Ferroportin (FPN).

As observed with DMT1 and FTH, Hartley guinea pigs had significantly higher transcript counts of FPN within articular cartilage than pigmented controls at either age investigated (Figure 2.4 E). There was no difference in mRNA counts between 5 months and 15 months-of-age within knee articular cartilage from control animals ($p = 0.99$) or Hartley guinea pigs ($p = 0.6$; Figure 2.4 E).

2.3.4 Gene Expression of Knee Articular Cartilage: Hartley Sex Comparisons.

2.3.4.1 Transferrin Receptor 1 (TFR1).

Male and female Hartleys exhibited similar trends for TFR1 gene expression at 5 months, 8 months, and 15 months-of-age (Figure 2.5 A). The mean abundance of TFR1 transcripts significantly decreased between 5 months and 8 months in both sexes, though this pattern was more pronounced in females ($p = 0.03$ in males and $p < 0.0001$ in females; Figure 2.5 A). Between 8 months and 15 months-of-age, mRNA counts for TFR1 remained relatively consistent in both sexes.

2.3.4.2 Divalent Metal Transporter 1 (DMT1).

Transcript counts for DMT1 did not significantly change among ages in the knee articular cartilage from male Hartley guinea pigs (Figure 2.5 B). In contrast, within cartilage from female animals, DMT1 expression was comparable between 5 and 15 months-of-age ($p = 0.99$), with a

significant decrease in DMT1 mRNA at the 8-month timepoint ($p < 0.0001$; Figure 2.5 B). Notably, transcript counts of DMT1 at 8 months-of-age were significantly lower in females than in males ($p < 0.0001$; Figure 2.5 B).

2.3.4.3 ZRT/IRT-Like Protein 14 (ZIP14).

Gene expression of ZIP14 did not significantly change within male cartilage between 5 months, 8 months, and 15 months-of-age ($p = 0.99$ and $p = 0.4$, respectively; Figure 2.5 C). In female Hartley animals, mRNA levels of ZIP14 were not statistically different between 5 and 8 months-of age ($p = 0.6$; Figure 2.5 C). Transcript counts of ZIP14 increased significantly in female knee articular cartilage between 8 and 15 months-of-age ($p = 0.001$; Figure 2.5 C). Similar to what was observed for DMT1, gene expression levels of ZIP14 were significantly lower in females than in males at 8 months-of-age ($p = 0.0002$; Figure 2.5 C).

2.3.4.4 Ferritin Heavy Chain (FTH).

Transcript counts of FTH significantly decreased between 5 months and 8 months-of-age in the knee articular cartilage from both male and female Hartley guinea pigs ($p = 0.003$ for males and $p < 0.0001$ in females; Figure 2.5 D). Within males, mRNA expression of FTH did not significantly change between 8 months and 15 months-of age ($p = 0.3$; Figure 2.5 D). Conversely, gene expression of FTH significantly increased in female knee cartilage between 8 months and 15 months-of-age ($p < 0.0001$; Figure 2.5 D).

2.3.4.5 Ferroportin (FPN).

Gene expression of FPN displayed a similar pattern in males and females at the ages investigated (Figure 2.5 E). Within male Hartley guinea pigs, mRNA levels of FPN decreased between 5 and 8 months-of-age ($p < 0.0001$) and then increased between 8 and 15-months of age ($p < 0.0001$; Figure 2.5 E).

Akin to that observed in males, gene expression of FPN was also decreased between 5 and 8 months-of-age in female cartilage. However, expression of FPN between 8 and 15 months-of-age did not increase as significantly in female Hartleys as it did in males ($p = 0.0003$; Figure 2.5 E). As such, the normalized counts of FPN were significantly lower in females at 15 months-of-age than observed at 5 months-of-age ($p = 0.0002$; Figure 2.5 E). Finally, the abundance of FPN mRNA was lower in males at 5 months-of-age than in females ($p = 0.01$; Figure 2.5 E).

2.4 Discussion.

The results from this work suggest that Hartley guinea pigs may have altered systemic iron homeostasis when compared to an outbred control strain not used to model OA. These perturbations in iron status appear to affect tissue iron levels, particularly cartilage iron concentration, which may contribute to accelerated aging and OA development in the Hartley guinea pig.

Analysis of liver iron concentration revealed that, overall, Hartley guinea pigs are storing less iron in the liver than pigmented control animals. Though the liver iron concentration of pigmented animals increased with age between 5 and 15 months, the levels of iron within the livers of Hartley guinea pigs remained similar throughout the ages investigated. The lower concentrations of liver iron, coupled with the lack of liver iron accumulation with age, may contribute to the higher tissue iron levels observed within the cartilage of Hartley guinea pigs. This theory was supported by evaluation of serum iron values, which reflected the overall higher tissue iron concentration observed in the cartilage of OA-prone Hartley guinea pigs (Figure 2.6). Similar to cartilage iron content, pigmented animals had lower levels of serum iron than Hartley guinea pigs at all ages investigated. Unfortunately, serum iron measurements were not available for 15-month Hartley guinea pigs.

Though direct comparison of cartilage iron concentration revealed a decrease between 5 and 15 months-of-age in Hartleys, we hypothesize this may be consequence of extracellular matrix (ECM) degradation occurring in OA pathogenesis. Indeed, a common feature of OA-associated cartilage degeneration is the loss of chondrocyte cell density within the ECM (27-28) and has been documented between 5 and 15-month-old Hartleys within our laboratory (data not shown). As such, the decrease in cartilage iron concentration may be a reflection of decreased cell density within the articular cartilage rather than a true decrease in tissue iron levels at these specific ages. In this scenario, it is possible that the remaining chondrocytes in the ECM have relatively high cellular iron levels. However, even enhanced histologic staining methods have not been sensitive enough to detect cellular iron changes within articular cartilage tissue (data not shown); this relationship should be further explored as new techniques for cellular iron detection are developed in the future.

The addition of intermediate ages for cartilage iron measurement in Hartley guinea pigs revealed a drastic increase in articular cartilage iron concentration at 7-8 months of age. To our knowledge, this is the first report of cartilage iron levels varying with age in animals predisposed to OA development without known genetic abnormalities. Within this animal model, knee OA is in early stages of development at 5 months-of-age, reaches moderate severity at 7-8 months of age, progresses to severe degeneration at 12 months-of-age, and reaches end-stage for the disease around 15 months-of-age (29). The drastic increase in cartilage iron concentration observed at 7-8 months in Hartley guinea pigs aligns with moderate OA development in this strain and suggests that iron dysregulation may be a contributing factor in earlier stages of OA pathogenesis.

Gene expression analysis revealed that transcript numbers of TFR1 reflected the consistent cartilage iron concentration in pigmented animals between 5 and 15 months-of-age. Similarly, TFR1 expression mirrored the cartilage iron accumulation occurring in Hartleys between 5- and 8-month-old months of age; this trend was maintained when males and females were investigated separately. Expression of DMT1, ZIP14, FTH, and FPN were not significantly altered between 5 and 15 months-of-age in either strain investigated. TFR1, FTH, FPN, and 2 of the 4 known transcript variants of DMT1 all contain at least one iron regulatory element (IRE) region within the mRNA, which allow for protein expression to be modulated relative to cellular iron levels. TFR1 contains 5 iron regulatory elements (IREs) in the 3' untranslated region of its mRNA, while the +IRE transcripts for FTH, DMT1, and FPN only contain 1 region (30-31). The unique presence of multiple IRE regions may allow TFR1 to better sense and respond to iron levels in the cartilage, with higher levels of cellular iron prompting rapid degradation of TFR1 mRNA. As such, the maintained levels of TFR1 mRNA between 8- and 15-month-old Hartleys may further support the theory that chondrocytes remaining in the OA-degraded ECM may be iron loaded. As cartilage iron concentration did not significantly alter between ages of pigmented animals, the maintained abundance of the investigated IRE-containing genes is logical within this strain. The availability of additional, intermediate ages for the Hartley guinea pig allowed the relationship between cartilage iron levels and gene expression to be further investigated in the context of knee OA.

Evaluation of additional timepoints for Hartley guinea pigs revealed changes in gene expression that were unable to be captured by directly comparing 5 months-of-age to 15 months. Notably, the mRNA levels of FTH and FPN decreased significantly at 8 months-of-age in both male and female Hartley guinea pigs. The increase in tissue iron at 7-8 months implies that iron

was being transported into chondrocytes. To prevent iron from participating in deleterious redox reactions, cells utilize the protein ferritin to bind iron in a catalytically inactive state. As the FTH transcript codes for a portion of ferritin protein, a decrease in expression would not be expected under iron loaded conditions. Thus, this decrease in FTH gene expression appears highly inappropriate. The reason for this unexpected expression of FTH is unknown and may contribute to the susceptibility for Hartley guinea pigs to OA development. If maintained at the protein level, the decrease in FTH expression occurring with increased cartilage iron concentration may augment the labile iron present in chondrocytes (32) and potentially contribute to iron dyshomeostasis and eventual tissue damage.

Similar to FTH, gene expression of FPN was reduced at the 8-month timepoint in Hartley guinea pigs. FPN is the only known protein capable of removing iron from cells into systemic blood circulation and is differentially regulated in tissues by complex interactions at the transcriptional, translational, and post-translational levels (33-34). Though classic models of IRE regulation primarily include translational modulation of FPN, several studies have demonstrated that expression of FPN mRNA increases with tissue iron levels, suggesting that iron-mediated regulation can also occur at the transcriptional level (34-38). In the present study, the opposite trend was observed in chondrocytes from Hartley guinea pigs, with FPN mRNA decreasing with higher tissue iron levels. If this pattern is conserved for the protein expression of FPN, it may contribute to increased tissue iron concentrations at this age by trapping iron within cells. As regulation of FPN seems to be cell specific (34), future work should focus on characterizing FPN gene and protein regulation within chondrocytes to determine relative contributions to cartilage iron accumulation and implications to OA pathogenesis.

Finally, there were some noteworthy sex differences present in Hartley guinea pigs for the genes investigated. The gene expression of both DMT1 and ZIP14 did not significantly change between the ages investigated for male guinea pigs. In female Hartley animals, transcript expression of DMT1 decreased significantly at 8 months-of-age, while ZIP14 mRNA increased at 15 months-of-age. Both DMT1 and ZIP14 transport divalent, non-transferrin bound iron (NTBI) across cellular membranes. The presence of NTBI may play a key role in the toxicity of iron, even in the absence of overt iron overload, by damaging the cellular environment (39-40). The ability for iron to regulate DMT1 expression has been demonstrated to vary substantially between cell types (31,41), and a study in mice revealed that DMT mRNA levels positively correlated with cardiac iron levels in male mice (35). The sustained expression of DMT1 across all ages investigated may have contributed to the drastic increase in cartilage iron at 7-8 months of age in male Hartley guinea pigs.

Despite having a high affinity for iron transport, ZIP14 mRNA does not contain an IRE, and like DMT1, expression of ZIP14 has been demonstrated to widely vary between tissues (42). Of note, levels of ZIP14 protein have been shown to increase with rising cellular iron levels in some tissue types (43). However, total cartilage iron concentrations were demonstrated to be comparable in males and females at 15 months-of-age, though this measurement would be influenced by differences in chondrocyte cellularity and/or cellular iron status. Whether the sex differences observed for ZIP14 expression are due to differences in chondrocyte density and/or iron status at 15 months-of-age, or due to another regulatory interaction, should be studied in the future.

Collectively, the results from this work demonstrate that OA-prone Hartley guinea pigs manage tissue iron levels differently than an outbred control strain, and these differences may

influence the propensity for OA development. Specifically, Hartley guinea pigs appear to inappropriately express FTH and FPN relative to tissue iron concentration, which may cause an increase in redox-active iron within the cell by preventing storage of liganded iron and cellular export. Additionally, the expression of two divalent iron transporters (DMT1 and ZIP14) were varied between male and female Hartley guinea pigs and may further contribute to iron loading of chondrocytes, particularly in the form of NTBI. NTBI contributing to pathology has been documented in non-iron overload disorders, including diabetes (44) and renal disease (45), and may similarly be involved in OA pathogenesis. Future work should focus on examining the expression of these iron-related proteins within normal articular cartilage to continue characterizing tissue differences in expression, particularly for FPN, DMT1, ZIP14. Additionally, investigation of these molecules within OA-prone articular cartilage will serve to further elucidate their respective contributions to tissue iron status in animals predisposed to OA. Finally, future work should continue to establish the relationship between both systemic and local iron status and OA pathogenesis.

2.5 Figures.

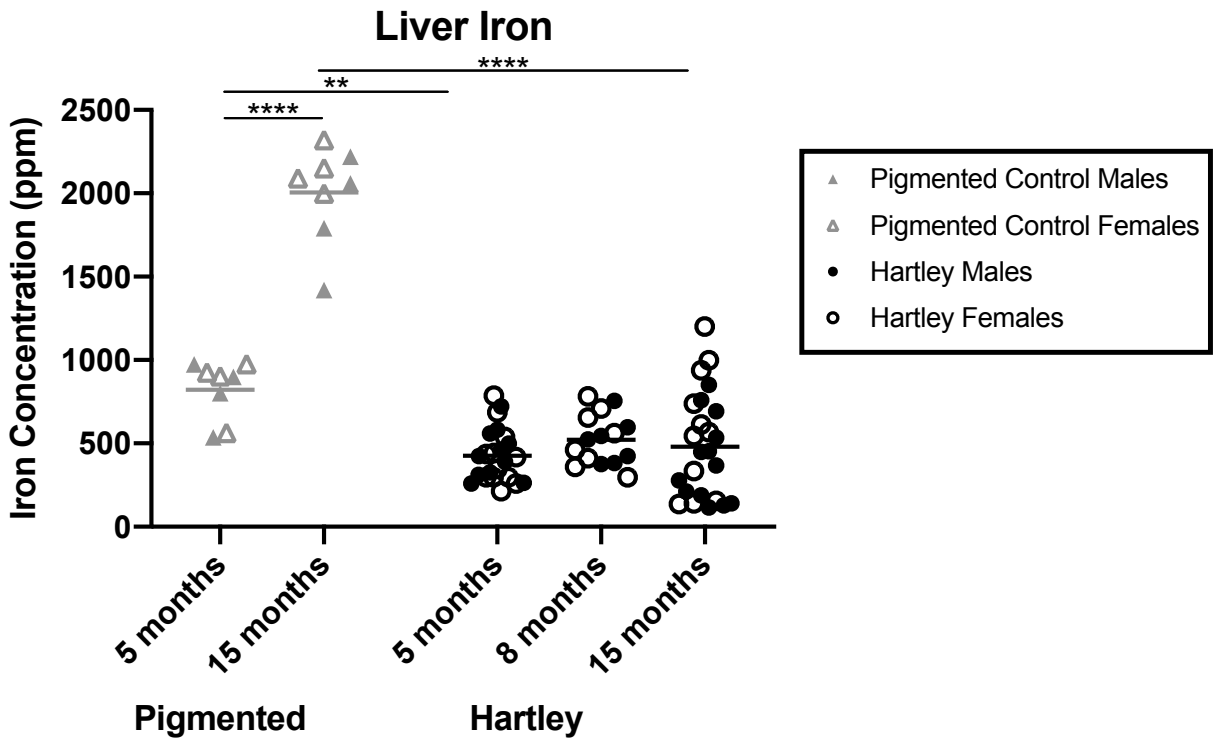

Figure 2.1. Strain comparison of liver iron quantification. Mean liver iron concentration was 822.40 ppm in 5-month-old pigmented control animals and was 2006.00 ppm in 15-month-old pigmented control animals. Mean liver iron concentration was 426.50 ppm in 5-month-old Hartley guinea pigs, 522.60 ppm in 7-month-old Hartley guinea pigs, and 481.10 ppm in 15-month-old Hartley guinea pigs.

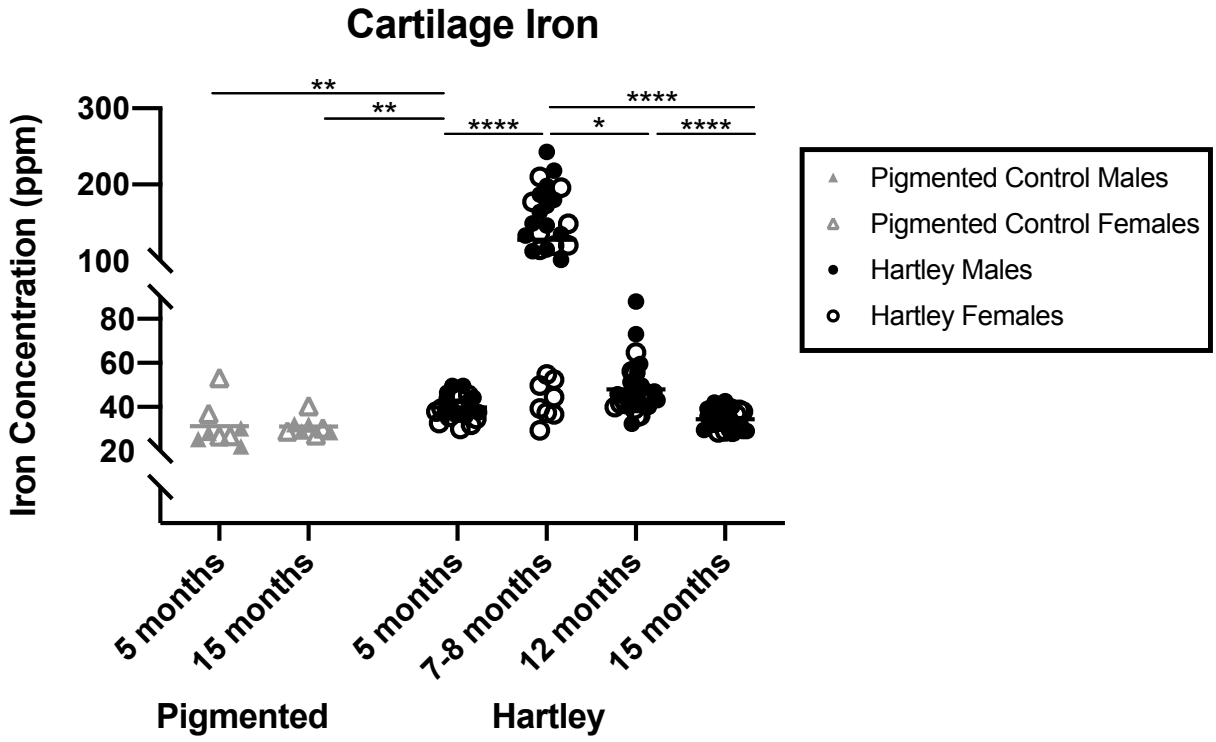

Figure 2.2. Strain comparison of cartilage iron quantification. Mean cartilage iron concentration was 31.26 ppm in 5-month-old pigmented control animals and was 31.06 ppm in 15-month-old pigmented control animals. Mean cartilage iron concentration was 39.72 ppm in 5-month-old Hartley guinea pigs, 127.40 ppm in 7-8-month-old Hartley guinea pigs, 48.04 ppm in 12-month-old Hartley guinea pigs, and 34.51 ppm in 15-month-old Hartley guinea pigs.

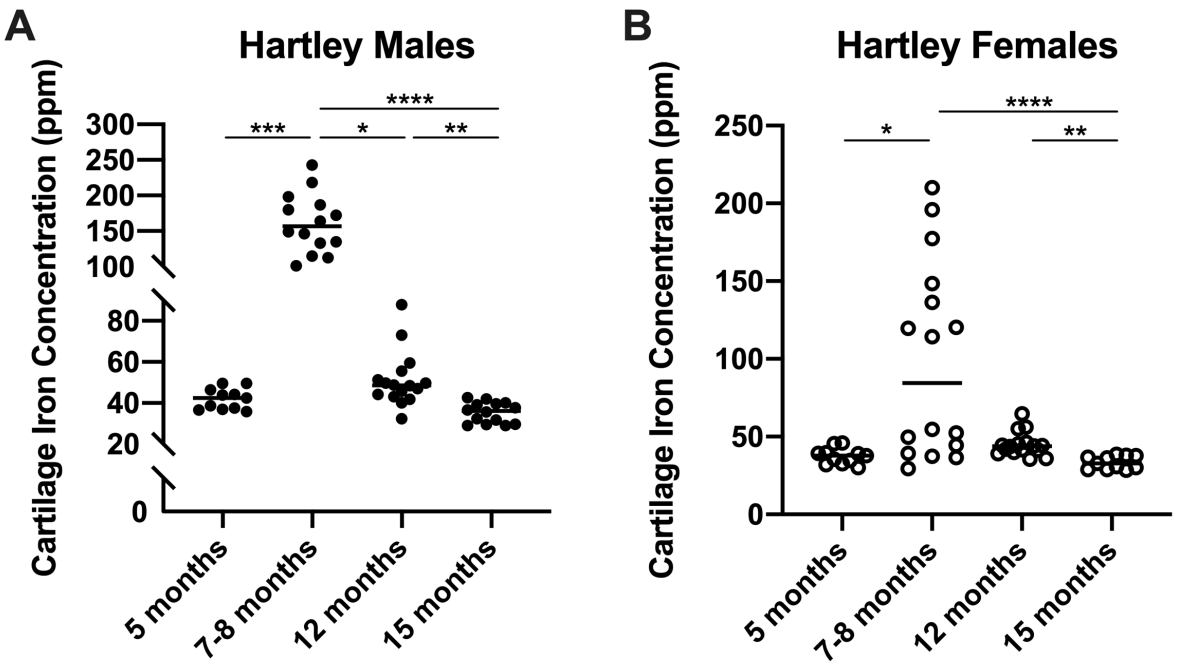

Figure 2.3. Cartilage iron quantification in male and female Dunkin-Hartley guinea pigs. (A) Mean cartilage iron concentration was 41.96 ppm in 5-month-old male Hartley guinea pigs, 161.00 ppm in 7-8-month-old male Hartley guinea pigs, 51.13 ppm in 12-month-old male Hartley guinea pigs, and 35.36 ppm in 15-month-old male Hartley guinea pigs. (B) Mean cartilage iron concentration was 37.47 ppm in 5-month-old female Hartley guinea pigs, 97.89 ppm in 7-8-month-old female Hartley guinea pigs, 44.96 ppm in 12-month-old female Hartley guinea pigs, and 33.43 ppm in 15-month-old female Hartley guinea pigs.

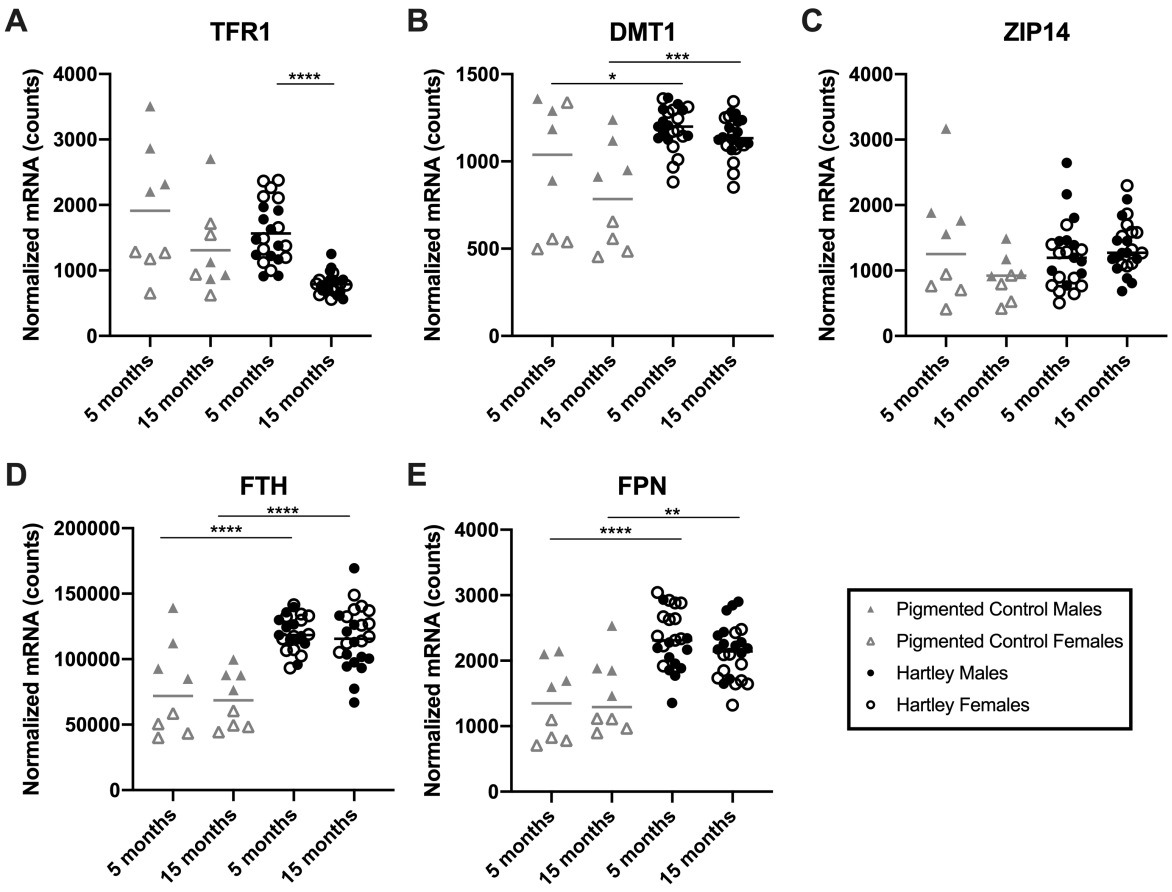

Figure 2.4. Strain comparison for genes related to iron metabolism. Mean transcript counts for iron-related genes in pigmented control animals and Dunkin-Hartley guinea pigs at 5 months-of-age and 15 months-of-age. (A) TFR1. (B) DMT1. (C) ZIP14. (D) FTH. (E) FPN.

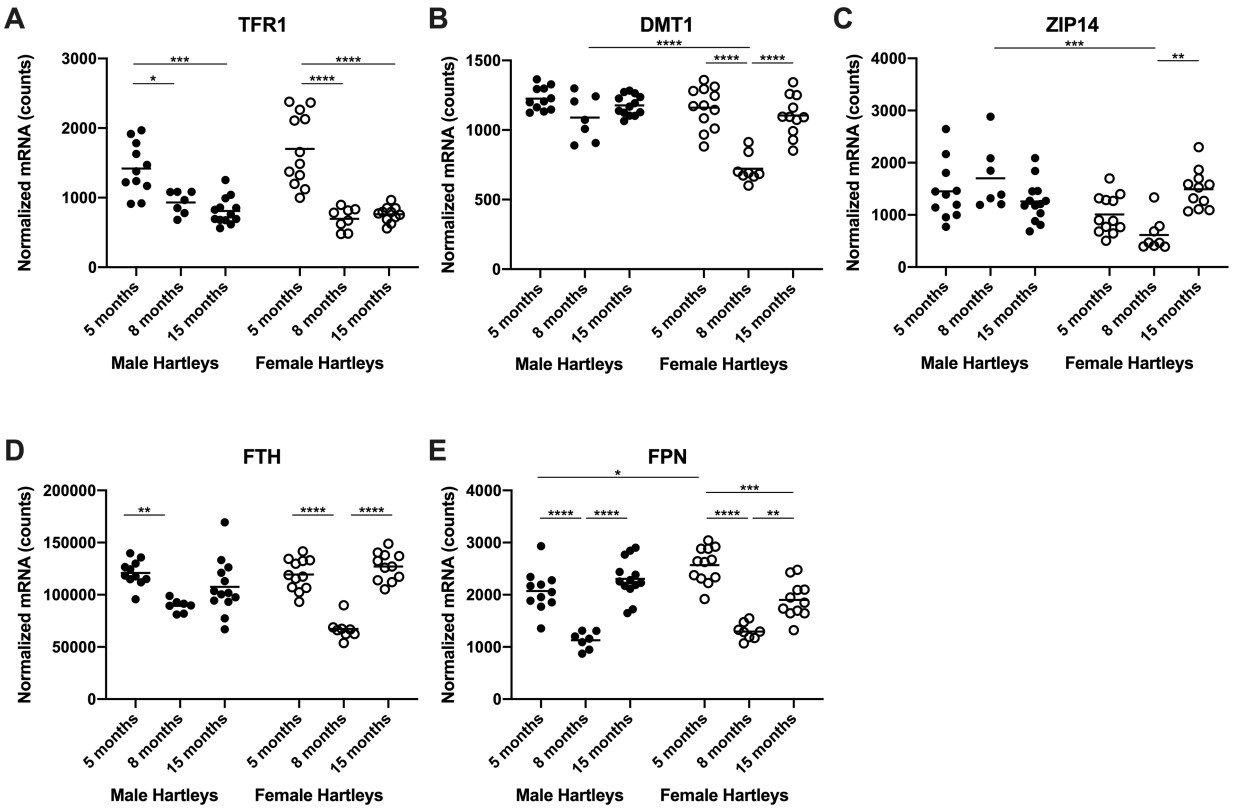

Figure 2.5. Sex comparison for genes related to iron metabolism in Dunkin-Hartley guinea pigs. Mean transcript counts for iron-related genes in male and female Dunkin-Hartley guinea pigs at 5 months-of-age, 8 months-of-age, and 15 months-of-age. (A) TFR1. (B) DMT1. (C) ZIP14. (D) FTH. (E) FPN.

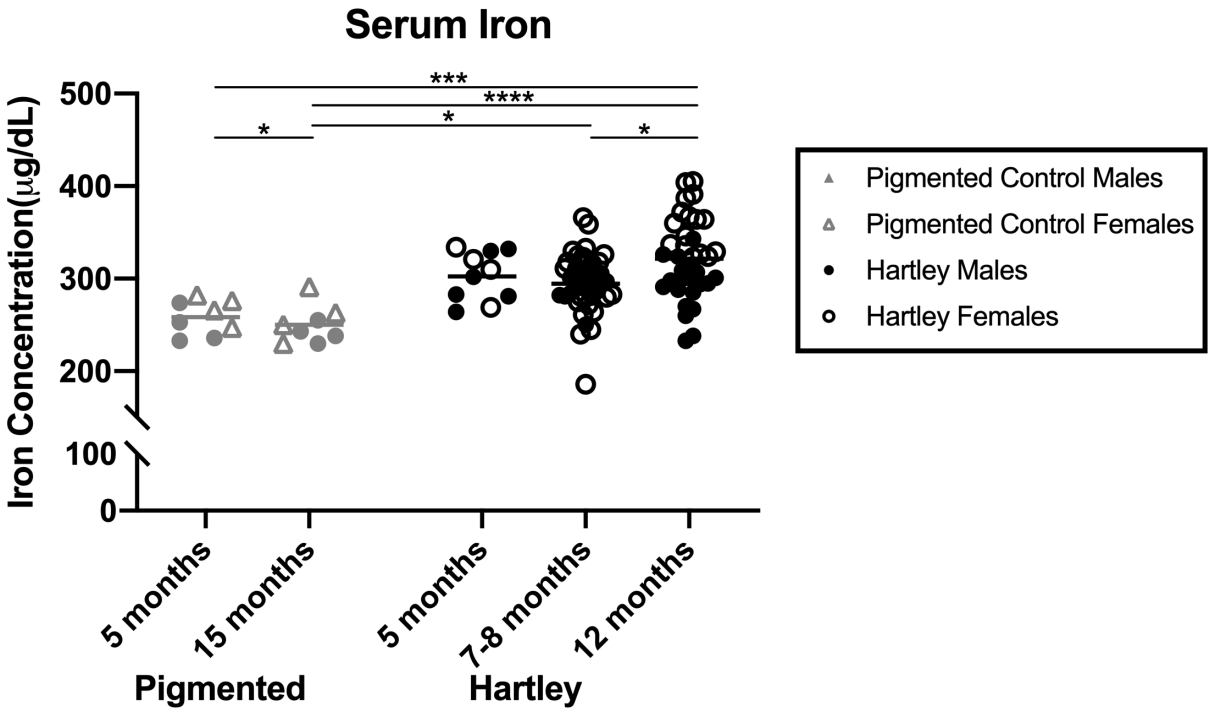

Figure 2.6. Strain comparison of serum iron quantification (supplemental). Mean serum iron concentration was 258.40 micrograms/deciliter (µg/dL) in 5-month-old pigmented control animals and was 250.00 µg/dL in 15-month-old pigmented control animals. Mean serum iron concentration was 302.60 µg/dL in 5-month-old Hartley guinea pigs, 294.70 µg/dL in 7-8-month-old Hartley guinea pigs, and 321.70 µg/dL in 12-month-old Hartley guinea pigs.

2.6 References.

1. Pereira D, Peleteiro B, Araujo J, Branco J, Santos RA, Ramos E. The effect of osteoarthritis definition on prevalence and incidence estimates: a systematic review. *Osteoarthritis Cartilage*. 2011;19(11): 1270-85. doi: 10.1016/j.joca.2011.08.009.
2. Sophia Fox AJ, Bedi A, Rodeo SA. The basic science of articular cartilage: structure, composition, and function. *Sports Health*. 2009;1(6):461-468. doi:10.1177/1941738109350438.
3. Kapoor M. Pathogenesis of Osteoarthritis. In: Kapoor M, Mahomed N, eds. Osteoarthritis. Auckland: Adis; 2015. p. 1-28. https://doi.org/10.1007/978-3-319-19560-5_1.
4. Felson DT. The epidemiology of knee osteoarthritis: Results from the Framingham osteoarthritis study. *Semin Arthritis Rheum*. 1990;20(3):42-50. doi:10.1016/0049-0172(90)90046-I.
5. Stadler N, Lindner RA, Davies MJ. Direct detection and quantification of transition metal ions in human atherosclerotic plaques: evidence for the presence of elevated levels of iron and copper. *Arterioscler Thromb Vasc Biol*. 2004; 24(5): 949-54. doi: 10.1161/01.ATV.0000124892.90999.cb.
6. Ford ES, Cogswell ME. Diabetes and serum ferritin concentration among U.S. adults. *Diabetes Care*. 1999; 22(12): 1978-83. doi: 10.2337/diacare.22.12.1978.
7. Hung SH, DeRuisseau LR, Kavazis AN, DeRuisseau KC. Plantaris muscle of aged rats demonstrates iron accumulation and altered expression of iron regulated proteins. *Exp Physiol*. 2008; 93(3): 407-14. doi: 10.1113/expphysiol.2007.039453.
8. Stevens RG, Graubard BI, Micozzi MS, Neriishi K, Blumberg BS. Moderate elevation of body iron level and increased risk of cancer occurrence and death. *Int J Cancer*. 1994; 56(3): 364-9. doi: 10.1002/ijc.2910560312.
9. Smith MA, Harris PL, Sayre LM, Perry G. Iron accumulation in Alzheimer disease is a source of redox-generated free radicals. *Proc Natl Acad Sci*. 1997; 94(18): 9866-8. doi: 10.1073/pnas.94.18.9866.
10. Myhre O, Ultkilen H, Duale N, Brunborg G, Hofer T. Metal dyshomeostasis and inflammation in Alzheimer's and Parkinson's diseases: possible impact of environmental exposures. *Oxid Med Cell Longev*. 2013; 2013: 726954. doi: 10.1155/2013/726954.
11. Ashraf A, Jeandriens J, Parkes HG, So PW. Iron dyshomeostasis, lipid peroxidation and perturbed expression of cystine/glutamate antiporter in Alzheimer's disease: Evidence of ferroptosis. *Redox Biol*. 2020; 32: 101494. doi: 10.1016/j.redox.2020.101494.
12. Winterbourn CC. Toxicity of iron and hydrogen peroxide: the Fenton reaction. *Toxicol Lett*. 1995; 82-83:969-74. doi: 10.1016/0378-4274(95)03532-x.
13. Koppenol WH, Hider RH. Iron and redox cycling. Do's and don'ts. *Free Radic Biol Med*. 2019; 133: 3-10. doi: 10.1016/j.freeradbiomed.2018.09.022.
14. Richette P, Ottaviani S, Vicaut E, Bardin T. Musculoskeletal complications of hereditary hemochromatosis: a case-control study. *J Rheumatol*. 2010; 37(10): 2145-50. doi: 10.3899/jrheum.100234.
15. Shander A, Cappellini MD, Goodnough LT. Iron overload and toxicity: the hidden risk of multiple blood transfusions. *Vox Sang*. 2009;97(3):185-97. doi: 10.1111/j.1423-0410.2009.01207.x.

16. Noureldine MHA, Taher AT, Haydar AA, Berjawi A, Khamashta MA, Uthman I. Rheumatological complications of beta-thalassaemia: an overview. *Rheumatology*. 2018;57(1):19-27. doi: 10.1093/rheumatology/kex058.
17. Roosendaal G, Vianen ME, Venting MJ, van Rinsum AC, van den Berg HM, Lafeber FP. Iron deposits and catabolic properties of synovial tissue from patients with haemophilia. *J Bone Joint Surg Br*. 1998; 80(3): 540-5. doi: 10.1302/0301-620x.80b3.7807.
18. Biemond P, Swaak AJ, van Eijk HG, Koster JF. Intraarticular ferritin-bound iron in rheumatoid arthritis. A factor that increases oxygen free radical-induced tissue destruction. *Arthritis Rheum*. 1986; 29(10): 1187-93. doi: 10.1002/art.1780291002.
19. Nieuwenhuizen L, Schutgens REG, van Asbeck BS, Wenting MJ, van Veghel K, Roosendaal G, et al. Identification and expression of iron regulators in human synovium: evidence for upregulation in haemophilic arthropathy compared to rheumatoid arthritis, osteoarthritis, and healthy controls. *Haemophilia*. 2013; 19(4): e218-27. doi: 10.1111/hae.12208.
20. Nugzar O, Zandman-Goddard G, Oz H, Lakstein D, Feldbrin Z, Shargorodsky M. The role of ferritin and adiponectin as predictors of cartilage damage assessed by arthroscopy in patients with symptomatic knee osteoarthritis. *Best Pract Rest Clin Rheumatol*. 2018; 32(5): 662-8. doi: 10.1016/j.berh.2019.04.004.
21. Yazer M, Sarban S, Kocyigit A, Isikan UE. Synovial fluid and plasma selenium, copper, zinc, and iron concentrations in patients with rheumatoid arthritis and osteoarthritis. *Biol Trace Elem Res*. 2005;106(2): 123-32. doi: 10.1385/BTER:106:2:123.
22. Ogilvie-Harris DJ, Fornasier VL. Synovial iron deposition in osteoarthritis and rheumatoid arthritis. *J Rheumatol*. 1980; 7(1): 30-6. PMID: 7354467.
23. Burton LH, Radakovich LB, Marolf AJ, Santangelo KS. Systemic iron overload exacerbates osteoarthritis in the strain 13 guinea pig. *Osteoarthritis Cartilage*. 2020; 28(9): 1265-75. doi: 10.1016/j.joca.2020.06.005.
24. Helrich, K, eds; Association of Official Analytical Chemists. *Official Methods of Analysis of AOAC International*. 15th ed. Gaithersburg, MD, USA; AOAC International; 1990. Official method 968.08D.
25. Helrich, K, eds; Association of Official Analytical Chemists. *Official Methods of Analysis of AOAC International*. 15th ed. Gaithersburg, MD, USA; AOAC International; 1990. Official method 974.27A, B, E and F.
26. Helrich, K, eds; Association of Official Analytical Chemists. *Official Methods of Analysis of AOAC International*. 15th ed. Gaithersburg, MD, USA; AOAC International; 1990. Official method 985.40D.
27. Hwang HS, Kim HA. Chondrocyte apoptosis in the pathogenesis of osteoarthritis. *Int J Mol Sci*. 2015;16(11):26035-54. doi: 10.3390/ijms161125943.
28. Charlier E, Relic B, Deroyer C, Malaise O, Neuville S, Collee J, et al. Insights on molecular mechanisms of chondrocytes death in osteoarthritis. *Int J Mol Sci*. 2016;17(12):2146. doi: 10.3390/ijms17122146.
29. Radakovich LB, Marolf AJ, Shannon JP, Pannone SC, Sherk VD, Santangelo KS. Development of a microcomputed tomography scoring system to characterize disease progression in the Hartley guinea pig model of spontaneous osteoarthritis. *Connect Tissue Res*. 2018;59(6): 523-533.
30. Wilkinson N, Pantopoulos K. The IRP/IRE system in vivo: insights from mouse models. Front Pharmacol. 2014;5:176. doi: 10.3389/fphar.2014.00176.

31. Hubert N, Hentze MW. Previously uncharacterized isoforms of divalent metal transporter (DMT)-1: implications for regulation and cellular function. *Proc Natl Acad Sci USA*. 2002;99(19): 12345-59. doi: 10.1073/pnas.192423399.
32. Omiya S, Hikoso S, Imanishi Y, Saito A, Yamaguchi O, Takeda T, et al. Downregulation of ferritin heavy chain increases labile iron pool, oxidative stress and cell death in cardiomyocytes. J Mol Cell Cardiol. 2009;46(1):59-66. doi: 10.1016/j.yjmcc.2008.09.714.
33. Drakesmith H, Nemeth E, Ganz T. Ironing out ferroportin. *Cell Metab*. 2015;22(5):777-87. doi: 10.1016/j.cmet.2015.09.006.
34. Chiabrando D, Fiorito V, Marro S, Silengo L, Altruda F, Tolosano E. Cell-specific regulation of ferroportin transcription following experimentally-induced acute anemia in mice. *Blood Cells Mol Dis*. 2013;50(1):25-30. doi: 10.1016/j.bcmd.2012.08.002.
35. Brewer CJ, Wood RI, Wood JC. mRNA regulation of cardiac iron transporters and ferritin subunits in a mouse model of iron overload. *Exp Hematol*. 2014;42(12):1059-67. doi: 10.1016/j.exphem.2014.09.002.
36. Delaby C, Pilard N, Hetet G, Driss F, Grandchamp B, Beaumont C, et al. A physiological model to study iron recycling in macrophages. *Exp Cell Res*. 2005; 310(1): 43-53. doi: 10.1016/j.yexcr.2005.07.002.
37. Knutson MD, Vafa MR, Haile DJ, Wessling-Resnick M. Iron loading and erythrophagocytosis increase ferroportin 1 (FPN1) expression in J774 macrophages. *Blood*. 2003; 102(12): 4191-7. doi: 10.1182/blood-2003-04-1250.
38. Delaby C, Pilard N, Puy H, Canonne-Hergaux F. Sequential regulation of ferroportin expression after erythrophagocytosis in murine macrophages: early mRNA induction by haem, followed by iron-dependent protein expression. *Biochem J*. 2008; 411(1): 123-31. doi: 10.1042/BJ20071474.
39. Brissot P, Ropert M, Le Lan C, Loreal O. Non-transferrin bound iron: a key role in iron overload and iron toxicity. *Biochim Biophys Acta*. 2012; 1820(3): 403-10. doi: 10.1016/j.bbagen.2011.07.014.
40. Breuer W, Hershko C, Cabantchik ZI. The importance of non-transferrin bound iron in disorders of iron metabolism. *Transfus Sci*. 2000; 23(3): 185-92. doi: 10.1016/s0955-3886(00)00087-4.
41. Gunshin H, Allerson CR, Polycarpou-Schwarz M, Rofts A, Rogers JT, Kishi F, et al. Iron-dependent regulation of the divalent metal iron transporter. *FEBS Lett*. 2001; 509(2): 309-16. doi: 10.1016/s0014-5793(01)03189-1.
42. Aydemir TB, Cousins RJ. The multiple faces of the metal transporter ZIP14 (SLC39A14). *J Nutr*. 2018; 148(2): 174-84. doi: 10.1093/jn/nxx041.
43. Nam H, Wang CY, Zhang L, Zhang W, Hojyo S, Fukada T, et al. ZIP14 and DMT1 in the liver, pancreas, and heart are differentially regulated by iron deficiency and overload: implications for tissue iron uptake in iron-related disorders. *Haematologica*. 2013; 98(7): 1049-57. doi: 10.3324/haematol.2012.072314.
44. Sulieman M, Asleh R, Cabantchik ZI, Breuer W, Aronson D, Suleiman A, et al. Serum chelatable redox-active iron is an independent predictor of mortality after myocardial infarction in individuals with diabetes. *Diabetes Care*. 2004; 27(11): 2730-2. doi: 10.2337/diacare.27.11.2730.
45. Prakash M, Upadhya S, Prabhu R. Serum non-transferrin bound iron in hemodialysis patients not receiving intravenous iron. *Clin Chim Acta*. 2005; 360(1-2): 194-8. doi: 10.1016/j.cccn.2005.04.024.

CHAPTER 3

GENE EXPRESSION CHANGES OCCURING WITH SYSTEMIC IRON OVERLOAD IN THE ARTICULAR CARTILAGE AND INFRAPATELLAR FAT PAD OF STRAIN 13 GUINEA PIGS[1]

3.1 Introduction.

Iron is a ubiquitous element that participates in numerous physiologic processes, including hemoglobin synthesis and oxidative phosphorylation. Unfortunately, excess levels can produce reactive oxygen species via the Fenton or Haber Weiss reactions (1-2). Despite this, there are no excretion mechanisms for iron beyond turnover of skin and enterocytes, and tissue iron accumulation occurs during aging (3-4). Indeed, progressive iron accrual has been linked to many age-associated chronic diseases, including type II diabetes, neurodegenerative disorders, atherosclerosis, and cancer (5-6). Additionally, iron overload within joint tissues has been implicated in arthropathies associated with hereditary hemochromatosis (7), rheumatoid arthritis (8-9), traumatic arthropathy, and hemophilic arthropathy (10). In these conditions, iron can accumulate from two sources: blood that enters the joint from either trauma or inflamed synovium and/or exchange from the non-heme iron pool (9,11). Several human studies have shown hemosiderin deposits in cartilage and synovium, as well as increased ferritin in the

[1] This article was published in Osteoarthritis and Cartilage, Volume 28, LH Burton, LB Radakovich, AJ Marolf, and KS Santangelo, Systemic Iron Overload Exacerbates Osteoarthritis in the Strain 13 Guinea Pig, Pages 1265-75, Copyright Elsevier (2020).

synovial fluid of affected joints (8-9). *In vivo* work has demonstrated that iron-overloaded synoviocytes release pro-inflammatory cytokines, including interleukin-1β (IL-1β), IL-6, and tumor necrosis factor (TNF), that stimulate catabolic activity in chondrocytes (10). Iron also has a direct effect on cartilage by inducing hydroxyl radical-driven chondrocyte apoptosis (10,12) and the breakdown of matrix components (13-14).

As age is the largest risk factor for primary/idiopathic OA (15), we theorize that iron accumulation may also be associated with the development of this disease. Interestingly, its role in the pathogenesis of OA has been explored in a handful of manuscripts. One study found that increased serum ferritin was correlated with more severe knee cartilage damage in individuals with primary OA; this finding was independent of age, sex, and BMI (16). Another manuscript demonstrated that synovial fluid iron concentrations were significantly higher in patients with OA than age-matched healthy subjects (17). Finally, iron deposition in synovium has been reported in individuals with OA (18). This evidence suggests that iron may play a role in both aging and knee OA and holds potential as a mechanistic connection between these coinciding conditions.

Because of this intriguing association, the current work was designed to demonstrate a direct relationship between excess cellular iron accumulation and OA in the absence of a genetic disorder. We hypothesized that administration of exogenous iron, resulting in moderate iron overload, would incite pathology in Strain 13 guinea pigs, a strain with decreased propensity for OA (19).

3.2 Materials and Methods.

3.2.1 Animals.

Procedures were approved by the Institutional Animal Care and Use Committee and performed in accordance with the NIH Guide for the Care and Use of Laboratory Animals. Group size was determined from a pilot study. Using a within group error of 0.5 and a detectible contrast of 1.0 (based on histologic assessment of OA) in a linear regression model considering treatment and sex, power associated with a Tukey's significant difference post-hoc analysis was calculated as 0.8 with a sample size of 4 per sex per treatment group. To ensure adequate power for all outcomes, 20 Strain 13 guinea pigs (11 males, 9 females) were purchased at 8 weeks of age from the US Army Medical Research Institute of Infectious Disease (Fort Detrick, MD). Animals were housed individually in solid bottom cages and provided standard guinea pig chow, hay cubes, and water *ad libitum*.

3.2.2 Iron Dextran Injections.

Injections were initiated when animals were 12 weeks of age and administered under isoflurane anesthesia. Ten guinea pigs (5 males, 5 females) were randomly assigned with respect to sex to the iron overload group; 10 animals (6 males, 4 females) were allocated to the control group. To induce a burden consistent with iron overload disorders, animals in the experimental group were administered 400 mg/kg of iron dextran solution (20) intraperitoneally once weekly for 4 weeks. Animals in the control group received 400 mg/kg of dextran solution. Body weights were recorded weekly.

3.2.3 Specimen Collection.

Termination occurred when animals were 16 weeks-of-age. Whole blood was collected via direct cardiac puncture under isoflurane anesthesia. Animals were then transferred to a CO_2 chamber for euthanasia.

Hind limbs were removed at the coxofemoral joints. The left limb was analyzed for OA-related structural changes previously reported by Radakovich 2018 (21). The right knee was dissected for gene expression analyses: the infrapatellar fat pad (IFP) was placed into All Tissue Protect reagent (Qiagen, Hilden, Germany); articular cartilage was isolated from the articular surface of the patella and the weight-bearing regions of the femoral condyles and tibial plateaus, and stored in RNAlater (Qiagen). Right femoral heads were placed into 10% neutral buffered formalin for 48 hours for iron quantification.

3.2.4 Iron Quantification by Atomic Absorption Spectroscopy (AAS).

Iron quantification was performed on samples of formalin-fixed liver tissue (Reported by Radakovich 2018) (21) and femoral head articular cartilage. Briefly, dried tissue weighed, ashed, sonicated in 3.6N nitric acid, and diluted 30-fold with deionized water (22). Diluted samples were analyzed using a Model 240 AA flame atomic absorption specrometer and SpectrAA software (Agilent Technologies, Santa Clara, California) (23). Iron levels were reported as parts per million (ppm) dry weight (dw) (24). The iron content of the IFP was also determined by enhanced iron staining and was previously reported (21).

3.2.5 Gene Expression Analysis Using NanoString Technology.

Total RNA was isolated from knee articular cartilage and IFPs using the RNeasy Lipid Tissue Mini Kit (Qiagen) and sent to University of Arizona Genetics Core (University of Arizona, Tucson, AZ). A custom set of guinea pig-specific probes were designed and manufactured by

NanoString Technologies (Seattle, WA) for the following genes: transferrin receptor (TFR), divalent metal transporter 1 (DMT1), zrt- irt- like protein 14 (ZIP14), cluster of differentiation protein 163 (CD163), ferritin heavy chain 1(FTH-1), ferroportin (FPN), collagen type II, aggrecan, IL-1β, TNF, IL-6, and transforming growth factor beta 1 (TGFβ1). Per Qubit and Fragment Analyzer quality control subsets, the optimal amount of total RNA (150-400 ng) was hybridized with the custom code-set in an overnight incubation (17 hours) at 65°C, followed by processing on the NanoString nCounter FLEX Analysis system. Results were reported as absolute transcript counts normalized to positive controls and two housekeeping genes, β-actin and eukaryotic translation elongation factor 1 alpha 1. Any potential sample input variance was corrected by use of housekeeping genes and application of a sample-specific correction factor to all target probes. Data analysis was conducted using nSolver™ software (NanoString Technologies).

3.2.6 Statistical Analyses.

Statistical analyses were performed with GraphPad Prism 8.3.1 (La Jolla, CA, USA). Data underwent normality and variance testing via the Shapiro-Wilk and F Test, respectively. Normally distributed data with similar variance were compared using parametric t tests†. Normally distributed data with significant differences in variance were compared using parametric t tests with Welch's correction$^{\diamond}$. Data with non-Gaussian distribution were compared using non-parametric Mann-Whitney tests$^{\times}$. Statistical tests used are noted in Figure Legends using superscripts. Statistical significance was set at $p \leq 0.05$.

3.3 Results.

3.3.1 Cartilage Iron Quantification.

The allocation of knee articular cartilage to transcript expression analyses prevented iron quantification from being conducted for this tissue. Femoral head articular cartilage was submitted for iron AAS to determine if differences were present in a diarthrodial joint environment. Relative to control animals, the concentration of iron was significantly higher within femoral cartilage from iron overloaded animals ($p = 0.0002$) (Figure 3.1).

3.3.2 Gene Expression Analysis.

3.3.2.1 Iron Trafficking and Storage Genes.

We were curious whether cellular iron metabolism in the cartilage and IFP was affected by systemic administration of iron dextran. Iron is imported into cells by select proteins, including TFR, DMT1, ZIP14, and CD163. Within the cartilage, iron overloaded animals had decreased mRNA expression for TFR ($p = 0.0007$) and DMT1 ($p = 0.0111$) while displaying increased transcript expression for the only known cellular iron export protein, FPN ($p = 0.0350$) (Figure 3.2 A-C). These effects were also observed within the IFPs of iron overloaded animals, with the exception that TFR expression did not change with iron overload in the IFP ($p = 0.7529$). Treatment with iron dextran did not significantly alter the gene expression of CD163 in the cartilage ($p = 0.1564$); however, a trend towards decreased CD163 expression was observed in the IFP ($p = 0.0524$) (Figure 3.2 D). Of note, there was no change in ZIP14 gene expression in either the cartilage or IFP with respect to treatment group ($p = 0.4470$ and $p = 0.9750$, respectively) (Figure 3.2 E).

Within the cell, iron can bind to the storage protein ferritin. Measuring the transcript expression of FTH-1 indicated that, relative to controls, iron overloaded animals had

significantly higher mRNA expression of ferritin within the cartilage ($p = 0.0082$) and IFP ($p < 0.0001$) (Figure 3.2 F).

3.3.2.2 Structural Components of Articular Cartilage.

The extracellular matrix (ECM) of articular cartilage is primarily composed of type II collagen and aggrecan (25). As OA is characterized by the loss of cartilage within affected joints, changes in the expression of these components can give insight to OA pathogenesis. Gene expression analysis revealed that iron overloaded animals had a lower expression of transcripts for type II collagen ($p = 0.0002$) and aggrecan ($p = 0.0038$) than control animals (Figure 3.3 A-B). There was no significant change in the expression of type II collagen ($p = 0.1431$) and aggrecan ($p = 0.1655$) within the IFP.

3.3.2.3 Cytokines.

Administration of iron dextran altered gene expression of the proinflammatory cytokines IL-1β, TNF, and IL-6, as well as the expression of TGFβ1. Relative to control animals, mean transcript expression of IL-1β was significantly higher in the cartilage ($p = 0.0015$) and IFPs ($p < 0.0001$) from iron overloaded animals (Figure 3.3 C). Similarly, iron overloaded animals exhibited increased gene expression of TNF in both the cartilage ($p = 0.0076$) and IFP ($p < 0.0001$) (Figure 3.3 D). Within the IFP, transcript counts for TGFβ1 were significantly higher for iron overloaded animals ($p < 0.0001$), and IL-6 demonstrated a trend towards increased expression relative to the control group ($p = 0.0524$) (Figure 3.3 E-F). Interestingly, treatment with iron dextran did not significantly alter the expression of IL-6 and TGFβ1 in cartilage.

3.4 Discussion.

The purpose of this work was to determine the gene expression changes within the knee joint of Strain 13 animals with administration of exogenous iron in order to provide a

mechanistic link for the findings reported by Radakovich in 2018 (21). Initial findings included that administration of exogenous iron significantly increased iron accrual within the serum, liver, and the IFP (21). The increase in tissue iron levels was accompanied by the development of both osteophytes (determined by microCT) and OA-associated cartilage lesions (determined by histologic evaluation of knee joints) in animals with a decreased propensity for OA (21).

In the present work, evaluation by AAS revealed that iron levels were also significantly higher within the femoral head articular cartilage of iron overloaded animals. Although articular cartilage is avascular, it is able to receive nutrients and other molecules by way of the synovial fluid present within the joint capsule. As synovial fluid is an ultrafiltrate from the blood supply, articular cartilage was likely exposed to systemic iron through the synovial fluid. Collectively, the increased concentration of iron within the knee IFP (21) and femoral head articular cartilage demonstrates that circulating iron does deposit and accumulate within tissues of diarthrodial joints and may contribute to the degradation that was noted in microCT and histologic evaluation of knee joints (21).

The increased development of OA-associated lesions in iron overloaded animals was supported by changes in tissue gene expression. In particular, cartilage degeneration in iron overloaded animals was accompanied by a relative decrease in the expression of transcripts for type II collagen and aggrecan. Previous studies have reported that chondrocyte exposure to iron *in vitro* decreased the synthesis of the ECM and increased the expression of matrix degrading enzymes (26-27). Cartilage lesions occurring with systemic iron overload were also associated with increased transcript counts of the proinflammatory cytokines IL-1β and TNF within both the cartilage and the IFP. Elevated protein levels of IL-1β and TNF have been widely observed in patients presenting with symptomatic knee OA and are considered to be key players in OA

pathogenesis (28). IL-1β reduces synthesis of type II collagen and aggrecan within articular cartilage and, along with TNF, induces the production of numerous other proinflammatory mediators, such as IL-6 (28). Joint tissues affected by OA have been demonstrated to express higher levels of IL-6 than non-OA joints (29), and the IFP has been shown to be a source of IL-6 production in OA-affected knees (30). In the current work, gene expression of IL-6 was relatively increased in the IFPs of iron overloaded animals. The presence of IL-6 protein regulates hepcidin, which in turn prompts the degradation of FPN and causes iron to accumulate within cells. The trend towards increased IL-6 mRNA observed within iron overloaded IFPs may have contributed to tissue iron accumulation and, therefore, the OA-associated changes to joint tissues. However, whether this increased IL-6 transcript number was driven by the iron overload or by OA remains to be determined.

Gene expression analysis suggest that both cartilage and IFPs are able to detect and respond to alterations in systemic iron status. Chondrocytes within iron overloaded cartilage exhibited decreased transcript expression for several proteins responsible for importing iron into the cell, while increasing the transcript expression for the iron export protein, FPN, and the storage protein, ferritin. These changes imply that cells within the cartilage were attempting to regain iron homeostasis, which is a well-documented response when iron stores are replete and/or overloaded (31-32). A similar trend was observed in the IFP, with the exception that TFR mRNA levels did not alter relative to iron status. Although the transcripts for TFR and DMT1 both contain at least one iron responsive element and, therefore, would be expected to be similarly regulated, DMT1 transports metals other than iron and may exhibit different expression in this tissue. The observation that ZIP14 mRNA levels did not change with cellular iron status

in either joint tissue evaluated is consistent with previously published findings (33-34) and suggests that ZIP14 expression is regulated post-translationally (34).

In conjunction with the results originally reported by Radakovich 2018 (21), this work establishes that exogenous iron overload is detrimental to knee joint health and, as such, indicates that systemic and/or local iron levels may be considered a factor in the development of OA. Notably, the expression of several genes were altered with systemic iron status. In the future, it may be worthwhile to determine whether a decrease in iron load prevents and/or delays OA lesions. Studies examining iron trafficking pathways within joint tissues are also needed to increase understanding of how this element contributes to development of primary OA in animals and humans.

3.5 Figures.

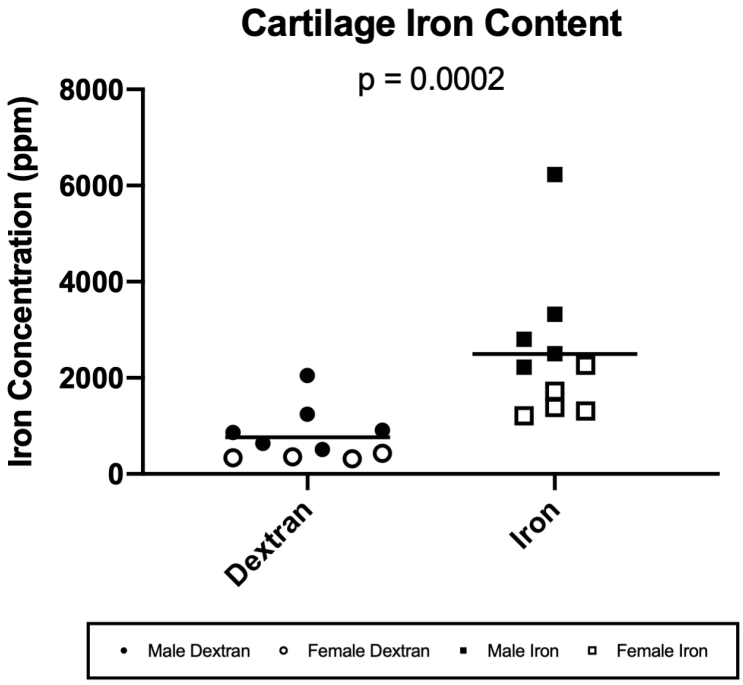

Figure 3.1. Cartilage iron quantification. Iron concentration of femoral head articular cartilage by AAS[×]. Mean concentration of iron within articular cartilage of iron overloaded animals was 2495.00 ppm. Mean concentration of iron within articular cartilage of dextran control animals was 765.40 ppm.

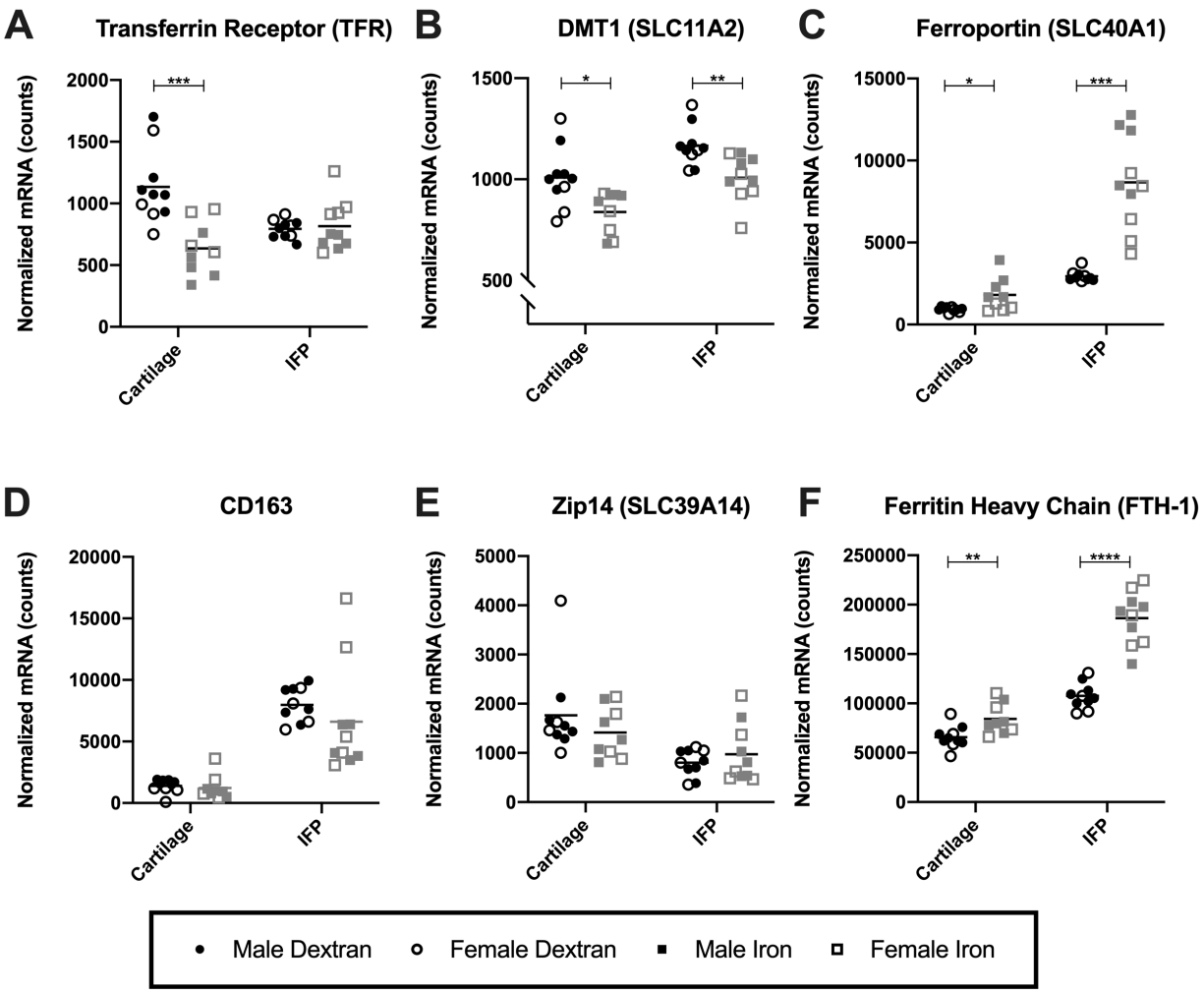

Figure 3.2. Normalized mRNA counts for iron trafficking genes in articular cartilage and the IFP. (A) TFR$^{+\Diamond}$ (B) DMT1^{+} (C) ZIP14$^{\times}$ (D) CD163$^{\times}$ (E) FPN$^{\times}$ and (F) FTH-1$^{+\Diamond}$.

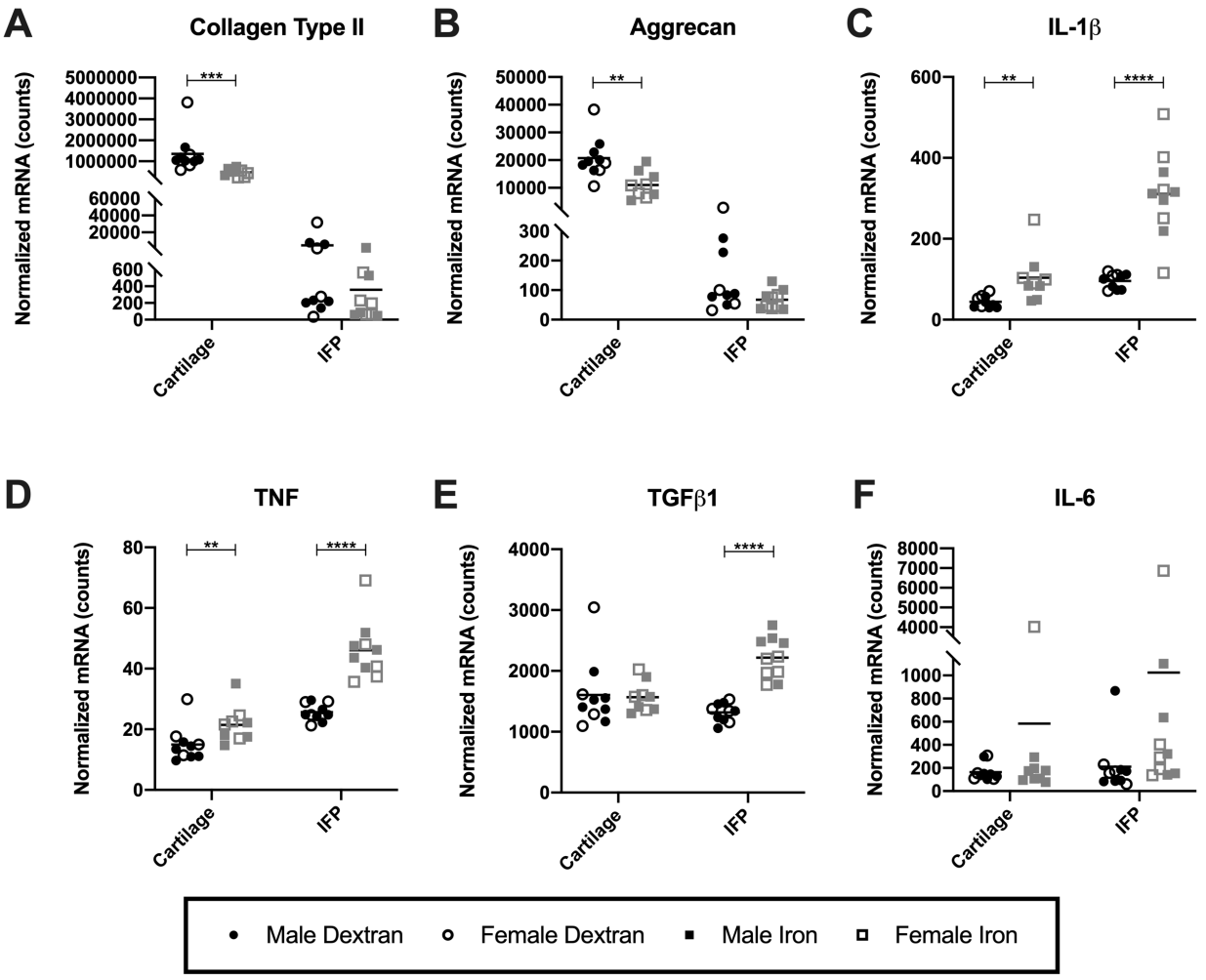

Figure 3.3. Normalized mRNA counts for select genes in articular cartilage and the IFP. (A) collagen type II$^{\times}$ (B) aggrecan$^{\dagger\times}$ (C) IL-1β$^{\times}$ (D) TNF$^{\times}$ (E) IL-6$^{\times}$ and (F) TGFß1$^{\times\diamond}$.

3.6 References.

1. Rigg T, Taylor W, Weiss J. The rate constant of the bimolecular reaction between hydrogen peroxide and ferrous ion. *Experientia*. 1954; 10(5): 202-03. doi: 10.1007/bf02159268.
2. Walling C. Fenton's reagent revisited. *Acc Chem Res*. 1975; 8(4): 125-31. doi:10.1021/ar50088a003.
3. Killilea DW, Wong SL, Cahaya HS, Atamna H, Ames BN. Iron accumulation during cellular senescence. *Ann N Y Acad Sci*. 2004; 1019(1): 365-7. doi: 10.1196/annals.1297.063.
4. Zacharski LR, Ornstein DL , Woloshin S , Schwartz LM. Association of age, sex, and race with body iron stores in adults: analysis of NHANES III data. *Am Heart J*. 2000; 140(1): 98-104. doi: 10.1067/mhj.2000.106646.
5. Xu J, Marzetti E, Seo AY, Kim JS, Prolla TA, Leeuwenburgh C. The emerging role of iron dyshomeostasis in the mitochondrial decay of aging. *Mech Ageing Dev*. 2010; 131(7-8): 487-93. doi:10.1016/j.mad.2010.04.007.
6. Liu J, Sun B, Yin H, Liu S. Hepcidin: a promising therapeutic target for iron disorders. *Med (United States)*. 2016; 95(14): e3150. doi:10.1097/MD.0000000000003150.
7. Camacho A, Simão M, Ea HK, Cohen-Solal M, Richette, P, Branco, J, et al. Iron overload in a murine model of hereditary hemochromatosis is associated with accelerated progression of osteoarthritis under mechanical stress. *Osteoarthr Cartil*. 2016; 24(3): 494-502. doi:10.1016/j.joca.2015.09.007.
8. Biemond P, Swaak AJ, van Eijk HG, Koster JF. Intraarticular ferritin-bound iron in rheumatoid arthritis. A factor that increases oxygen free radical-induced tissue destruction. *Arthritis Rheum*. 1986; 29(10): 1187-93. doi: 10.1002/art.1780291002.
9. Weinberg ED. The hazards of iron loading. *Metallomics*. 2010; 2(11): 732-40. doi:10.1039/c0mt00023j.
10. Nieuwenhuizen L, Schutgens RE, van Asbeck BS, Wenting MJ, van Veghel K, Roosendaal G, et al. Identification and expression of iron regulators in human synovium: evidence for upregulation in haemophilic arthropathy compared to rheumatoid arthritis, osteoarthritis, and healthy controls. *Haemophilia*. 2013; 19(4): e218-27. doi:10.1111/hae.12208.
11. Abbott DF, Gresham GA. Arthropathy in transfusional siderosis. *Br Med J*. 1972; 1(5797): 418-9. doi:10.1136/bmj.1.5797.418.
12. Hooiveld MJ, Roosendaal G, van den Berg HM, Bijlsma JW, Lafeber FP. Haemoglobin-derived iron-dependent hydroxyl radical formation in blood-induced joint damage: an in vitro study. *Rheumatology (Oxford)*. 2003; 42(6): 784-90. doi:10.1093/rheumatology/keg220.
13. Carroll GJ, Sharma G, Upadhyay A, Jazayeri JA. Ferritin concentrations in synovial fluid are higher in osteoarthritis patients with HFE gene mutations (C282Y or H63D). *Scand J Rheumatol*. 2010; 39(5): 413-20. doi:10.3109/03009741003677449.
14. Askari AD, Muir WA, Rosner IA, Moskowitz RW, McLaren GD, Braun WE. Arthritis of hemochromatosis. Clinical spectrum, relation to histocompatibility antigens, and effectiveness of early phlebotomy. *Am J Med*. 1983; 75(6): 957-65. doi: 10.1016/0002-9343(83)90875-6.
15. Anderson AS, Loeser RF. Why is osteoarthritis an age-related disease? *Best Pract Res Clin Rheumatol*. 2010; 24(1): 15. doi: 10.1016/j.berh.2009.08.006.
16. Nugzar O, Zandman-Goddard G, Oz H, Lakstein D, Feldbrin Z, Shargorodsky M. The role of ferritin and adiponectin as predictors of cartilage damage assessed by arthroscopy in patients with symtpmatic knee osteoarthritis. *Best Pract Res Clin Rheumatol*. 2018; 32(5): 662-8. doi:

10.1016/j.berh.2019.04.004.
17. Yazer M, Sarban S, Kocyigit A, Isikan UE. Synovial fluid and plasma selenium, copper, zinc, and iron concentrations in patients with rheumatoid arthritis and osteoarthritis. *Biol Trace Elem Res*. 2005; 106(2): 123-32. doi: 10.1385/BTER:106:2:123.
18. Ogilvie-Harris DJ, Fornasier VL. Synovial iron deposition in osteoarthritis and rheumatoid arthritis. *J Rheumatol*. 1980; 7(1): 30-6.
19. Kraus VB, Huebner JL, DeGroot J, Bendele A. The OARSI histopathology initiative - recommendations for histological assessments of osteoarthritis in the guinea pig. *Osteoarthritis Cartilage*. 2010; 18 Suppl 3(Suppl 3): S35-52. doi:10.1016/j.joca.2010.04.015.
20. Schwartz KA, Fisher J, Adams ET. Morphologic investigations of the guinea pig model of iron overload. *Toxicol Pathol*. 1993; 21(3): 311-20. doi: 10.1177/019262339302100307.
21. Radakovich LB. The roles of iron, the infrapatellar fat pad, and dietary factors in the Hartley guinea pig model of spontaneous osteoarthritis. *PhD Dissertation*. Fort Collins, Colorado: Colorado State University; 2018.
22. Helrich, K, eds; Association of Official Analytical Chemists. *Official Methods of Analysis of AOAC International*. 15th ed. Gaithersburg, MD, USA; AOAC International; 1990. Official method 968.08D.
23. Helrich, K, eds; Association of Official Analytical Chemists. *Official Methods of Analysis of AOAC International*. 15th ed. Gaithersburg, MD, USA; AOAC International; 1990. Official method 974.27A, B, E and F.
24. Helrich, K, eds; Association of Official Analytical Chemists. *Official Methods of Analysis of AOAC International*. 15th ed. Gaithersburg, MD, USA; AOAC International; 1990. Official method 985.40D.
25. Sophia Fox AJ, Bedi A, Rodeo SA. The basic science of articular cartilage: structure, composition, and function. *Sports Health*. 2009; 1(6): 461-8. doi: 10.1177/1941738109350438.
26. Simao M, Gavaia PJ, Camacho A, Porto G, Pinto IJ, Ea HK, et al. Intracellular iron uptake is favored in Hfe-KO mouse primary chondrocytes mimicking an osteoarthritis-related phenotype. *Biofactors*. 2019; 45(4): 583-97. doi: 10.1002/biof.1520.
27. Kirkpatrick CJ, Mohr W, Haferkamp O. Alterations in chondrocytes morphology, proliferation and binding. *Virchows Arch B Cell Pathol Incl Mol Pathol*. 1982; 38(3): 297-306. doi:10.1007/bf02892825.
28. Mabey T, Honsawek S. Cytokines as biochemical markers for knee osteoarthritis. *World J Orthop*. 2015; 6(1): 95-105. doi:10.5312/wjo.v6.i1.95.
29. Pearson MJ, Herndler-Brandstetter D, Tariq MA, Nicholson TA, Philp AM, Smith HL, et al. IL-6 secretion in osteoarthritis patients is mediated by chondrocyte-synovial fibroblast cross-talk and is enhanced by obesity. *Sci Rep*. 2017; 7(1): 3451. doi:10.1038/s41598-017-03759-w.
30. Ioan-Facsinay A, Kloppenburg M. An emerging player in knee osteoarthritis: the infrapatellar fat pad. *Arthritis Res Ther*. 2013; 15(6): 225. doi:10.1186/ar4422.
31. Anderson CP, Shen M, Eisenstein RS, Leibold EA. Mammalian iron metabolism and its control by iron regulatory proteins. *Biochim Biophys Acta*. 2012; 1823(9): 1468-83. doi: 10.1016/j.bbamcr.2012.05.010.
32. Hentze MW, Muckenthaler MU, Andrews NC. Balancing acts: molecular control of mammalian iron metabolism. *Cell*. 2004; 117(3): 285-97. doi: 10.1016/s0092-

8674(04)00343-5.
33. Sterling J, Guttha S, Song Y, Song D, Hadziahmetovic M, Dunalef JL. Iron importers zip8 and zip14 are expressed in retina and regulated by retinal iron levels. *Exp Eye Res*. 2017; 155: 15-23. doi: 10.1016/j.exer.2016.12.008.
34. Zhao N, Zang AS, Worthen C, Knutson MD, Enns CA. An iron-regulated and glycosylation-dependent proteasomal degradation pathway for the plasma membrane metal transporter zip14. *Proc Natl Acad Sci USA*. 2014; 111(25): 9175-80. doi:10.1073/pnas.1405355111.

CHAPTER 4

SYSTEMIC ADMINISTRATION OF A PHARMACOLOGIC IRON CHELATOR REDUCES CARTILAGE LESION DEVELOPMENT IN MALE DUNKIN-HARTLEY GUINEA PIGS

4.1 Introduction.

Iron is essential for numerous physiologic processes including oxygen transport, DNA synthesis, and ATP production. Mammals have developed complex systems to appropriately absorb, store, transport, and utilize this mineral, as unbound or partially-liganded iron can participate in redox chemistry (1-2). These reactions generate harmful reactive oxygen species (ROS) that can elicit or perpetuate inflammatory responses, damage DNA and cellular components, and promote cell death, which collectively encourage tissue damage (3-5). Thus, the risk for iron-mediated toxicity is not limited to overt excess and can also arise from conditions where intracellular iron becomes delocalized and/or inappropriately stored, causing the labile iron pool containing catalytically-active iron to expand (6-8). Despite this, mammals do not have a physiologically regulated mechanism for excreting iron and the majority of the iron absorbed is continuously recycled throughout the body (9). Indeed, iron progressively accumulates throughout the aging process (10-11) and has been linked to numerous aging-associated chronic diseases, including atherosclerosis (12), neurodegenerative disorders (13), cancer (14), and type II diabetes (15). Excess and/or improperly managed iron has also been implicated in several disorders with associated arthropathies, including hemophilic arthropathy (16), traumatic arthropathy, hereditary hemochromatosis (17), and rheumatoid arthritis (RA) (18). In these afflictions, iron-loaded human synoviocytes have been demonstrated to release

proinflammatory mediators which stimulate the catabolic activity of chondrocytes and contribute to joint degradation (19).

Although the role of iron has been explored in the arthropathies above, it has yet to be widely investigated in the context of primary/idiopathic osteoarthritis (OA). OA is a progressive joint disorder with the degradation and subsequent loss of articular cartilage as a central feature (20) accompanied by synovial hyperplasia, osteophyte formation and tissue remodeling, and narrowing of the joint space. These alterations cause pain and reduced mobility, resulting in increased susceptibility to developing comorbidities such as obesity, cardiovascular diseases, and depression (21). Healthy articular cartilage is maintained by a delicate balance between catabolic and anabolic actions; in OA, this homeostasis becomes disrupted and shifts in favor of catabolic events that degrade the cartilage extracellular matrix (ECM). OA-affected chondrocytes exhibit enhanced levels of ROS and oxidative stress (20,22), which may play a significant role in the progressive loss of the ECM (20,23). Additionally, as adult cartilage is unable to regenerate, the depletion of chondrocytes themselves due to ROS and other stressors has also been implicated in OA pathogenesis (20,24). While these findings are accepted, the underlying molecular mechanisms driving the development of OA remain loosely described.

There have been a handful of publications exploring the role of iron in primary OA. One human study reported that synovial fluid iron concentration was significantly higher in OA-affected patients relative to both healthy controls and individuals with RA (25). Another study found that serum ferritin levels were positively correlated with the severity of cartilage damage in people affected by OA; this finding was independent of age, sex, and BMI (26). Finally, enhanced iron deposition in the synovium has been reported in patients with OA (27). These

studies suggest that iron may be a contributing factor in knee OA and may provide mechanistic insight to the development of the disorder.

As advancing age is the leading risk factor for developing primary OA (28), we theorize that age-related iron accumulation in joint tissues may contribute to the development of the disorder. Recently, we determined that administering excess iron systemically exacerbated the development of OA-like lesions in the knee joints of disease-resistant Strain 13 guinea pigs (29).

To build on this finding, we designed a study to assess the effects of systemic iron reduction on the development of primary knee OA in an animal model of the disorder: the Dunkin-Hartley guinea pig. This well-described model develops bilateral, age-related knee OA with a predictable progression that closely mimics the pathology observed in humans (30-31). As in humans, these spontaneous lesions tend to develop first within the medial compartment of the knee, with the tibia being more severely affected before the femur (31). Histopathologic evidence of knee OA can be detected after 2 months-of-age, with severe, late-stage OA occurring between 15-18 months-of-age (31).

For this work, systemic iron reduction was achieved by administration of the pharmacologic iron chelator deferoxamine (DFO). DFO has a high affinity for binding iron relative to other transition metals and has been used to treat acute iron toxicity and iron overload conditions since the 1960's. Based on our previous findings (29), we hypothesized that systemic administration of DFO would decrease the development of OA-like lesions in the knees of Dunkin-Hartley guinea pigs.

4.2 Materials and Methods.

4.2.1 Animals.

All procedures were approved by the Institutional Animal Care and Use Committee and performed in accordance with the NIH Guide for the Care and Use of Laboratory Animals. Group size was determined from a pilot study with the primary outcome being the histologic assessment of OA. Using a within group error of 0.5 with a detectable difference between means of 1.0, power associated with an alpha of 0.5 (two sided) was calculated as 0.9 with a sample size of 6 animals per group. To ensure adequate power for all study outcomes, a total of 16, 8-week-old male Dunkin-Hartley guinea pigs were purchased from Charles River Laboratories (Wilmington, MA). Guinea pigs were individually housed in solid bottom cages with appropriate bedding and were monitored daily by a veterinarian. Iron chelation therapy was supplied to reduce, but not deplete, systemic iron levels and encourage iron mobilization out of storage in tissues. As such, animals were allowed unlimited access to standard guinea pig chow that was replete in iron; hay cubes and water were also provided *ad libitum*.

4.2.2 Deferoxamine (DFO) Injections.

Injections were initiated at 12-weeks-of-age. Eight guinea pigs were randomly assigned by cage card number to the DFO group, with the remainder in the control group. Using the lowest dose and dosing frequency utilized in humans with chronic iron overload (32), allometric scaling was conducted to determine the equivalent dose for use in the guinea pig (33). Animals within the DFO group received 46 mg/kg of DFO (Fresenius Kabi, Lake Zurich, IL) injected subcutaneously twice daily for 5 consecutive days, followed by 2 days without receiving any treatment. Control animals received an equivalent dose of lactated ringers solution (Pfizer, Lake Forest, IL) subcutaneously at the same frequency. Injections were given for 18 weeks. Body

weights were recorded prior to starting treatments, as well as weekly throughout the study. One animal in the control group was lost prior to study termination due to the presence of underlying pathologies unrelated to the study at hand. This animal was excluded from all analyses; n=7 animals were evaluated for the control group.

4.2.3 Specimen Collection.

The study was terminated when animals were 30-weeks-of-age, with the final treatment occurring the night prior. Animals were placed under isoflurane anesthesia to collect whole blood via direct cardiac puncture. Urine was saved following involuntary voiding during the initial anesthetic transition. After fluids were collected, animals were transferred to a CO_2 chamber for euthanasia. Serum was separated and, along with urine, submitted for iron quantification using the Roche Cobas 6000 (Basel, Switzerland). Complete blood count (CBC) and serum biochemistry profiles were also determined. The liver from each animal was collected into 10% (v/v) neutral buffered formalin (NBF) for 48 hours for iron quantification.

Hind limbs were removed at the coxofemoral joints. The left limb was placed into 10% NBF for 48 hours and subsequently transferred to a solution of 12.5% (w/v) ethylenediaminetetracetic acid (pH 7.00) for decalcification and histologic evaluation. The right hind limb was dissected to expose the knee joint and cartilage was collected from the articular surface of the patella and the weight-bearing regions of the femoral condyles and tibial plateaus. Cartilage was stored in RNAlater (Qiagen, Hilden, Germany) for gene expression analysis. The length of the right tibia was measured with calipers. Articular cartilage was isolated from the right femoral head and stored in 10% NBF for 48 hours for iron quantification.

4.2.4 Iron Quantification by Atomic Absorption Spectroscopy (AAS).

Iron quantification was performed on samples of NBF-fixed liver tissue and femoral head articular cartilage, as previously described (29). The coxofemoral joint was selected as knee articular cartilage was reserved for gene expression analysis. Briefly, dried tissue was weighed, ashed, sonicated in nitric acid, and diluted 30-fold with deionized water (34). Diluted samples were analyzed using a Model 240 AA flame atomic absorption spectrometer and SpectrAA software (Agilent Technologies, Santa Clara, CA) (35). Iron levels were reported as parts per million (ppm) dry weight (36).

4.2.5 Histologic Evaluation of Knee Joints.

Following decalcification, knee joints were divided through the central plane into sagittal sections of the medial and lateral joint compartments and embedded in paraffin wax. Five-micron segments were stained with toluidine blue, and medial and lateral femoral condyles and tibias were scored in a blinded fashion by two assessors (LHB and KSS) using the Osteoarthritis Research Society International (OARSI) guidelines (31). One slide from the medial and lateral compartment of each knee joint was evaluated, for a total of 2 slides per animal. Values from the 4 anatomic locations were summed to obtain a whole joint knee OA score.

4.2.6 Gene Expression Analysis of Knee Articular Cartilage.

As previously described (29), total RNA was isolated from knee articular cartilage using the RNeasy Lipid Tissue Mini Kit (Qiagen) and was sent to the University of Arizona Genetics Core (University of Arizona, Tucson, AZ) for analysis. A custom set of guinea pig-specific probes were designed and manufactured by NanoString Technologies (Seattle, WA) for the following genes: B-cell lymphoma 2 (BCL-2), BCL-2-associated death promoter (BAD), BCL-2-associated x protein (BAX), BCL-2 homologous antagonist killer (BAK), caspase-3, caspase-

8, caspase-9, aggrecan (ACAN), type II collagen (COL2A1), matrixmetalloproteinase-2 (MMP-2), MMP-9, MMP-13, tissue inhibitor of matrixmetalloproteinases-2 (TIMP-2), transferrin receptor 1 (TFR1), divalent metal transporter 1 (SLC11A2/DMT1), ZRT/IRT-like protein 14 (SLC39A14/ZIP14), ferroportin (SLC40A1/FPN), and ferritin heavy chain (FTH). Based on initial RNA quantification (Invitrogen Qubit 2.0 Fluorometer and RNA High Sensitivity Assay Kit, Thermo Fisher Scientific, Waltham, MA) and fragment analysis quality control subsets (Fragment Analyzer Automated CE System and High Sensitivity RNA Assay Kit, Agilent Technologies), the optimal amount of total RNA (150-400 ng) was hybridized with the custom codeset in an overnight incubation at 65ºC, followed by processing on the NanoString nCounter® FLEX Analysis System (NanoString Technologies). Results are reported as absolute transcript counts normalized to 2 housekeeping genes, β-actin and eukaryotic elongation factor 1α1. Any potential sample input variance was normalized by use of housekeeping genes and application of a sample-specific correction factor to all target probes. Data analysis was conducted using nSolver™ software (NanoString Technologies).

4.2.7 Overhead Enclosure Monitoring.

Animal movement was monitored using ANY-maze behavioral tracking software (Stoelting Co., Wood Dale, IL). To conduct overhead enclosure monitoring, guinea pigs were placed into an open top apparatus containing a habitat hut, with a camera positioned above the enclosure. The activity of animals was recorded during 10-minute sessions occurring once per month throughout the study. Baseline parameters were collected at the one-month time point to allow guinea pigs to acclimate to the system. Results are presented as the difference in activity levels from the first month to the final month of treatment.

4.2.8 Statistical Analyses.

Statistical analyses were performed with GraphPad Prism 8.4.2 (La Jolla, CA). Rationale for the exclusion of an entire animal from the study were determined *a priori* and included the presence of any pathologies and/or the inability to complete the study for any reason. Prior to conducting analyses, the authors determined that individual points would be excluded from data sets if: a sample did not pass quality control parameters set for an experimental method, the integrity of a sample was compromised, or an appropriate sample was unable to be obtained for analysis. Urine and cartilage iron quantification are incomplete data sets due to the inability to acquire adequate urine at euthanasia and absence of available tissue, respectively. Authors were not blinded to group allocation during data analysis. The distribution and variance of data sets were determined with the Shapiro-Wilk and F-Test, respectively. Normally distributed data with similar variance were compared using parametric t-tests$^{\blacklozenge}$. Normally distributed data with significant differences in variance were compared using parametric t-tests with Welch's correction$^{\lozenge}$. Data with non-Gaussian distribution was compared using non-parametric Mann-Whitney U-test$^{\times}$. Statistical tests are noted in figure legends using designated superscripts. For data analyzed by parametric t-tests, black lines on graphs represent mean values. Black lines on graphs represent median values for data analyzed by Mann-Whitney U-tests. Statistical significance was set at $P \leq 0.05$.

4.3 Results.

4.3.1 General Description of Animals.

Animals receiving iron chelation therapy appeared clinically healthy; no changes in cage behavior were observed at any point during the study. At the time of termination, mean total body weight was 1116.00 grams (g) in control animals and 1084.00 g in DFO-treated animals

(95% confidence interval (CI): -155.10-90.04 g; p=0.58; data not shown). Mean tibia length was similar between animals in the control group (49.06 millimeters, mm) and in animals receiving DFO (49.59 mm), indicating that iron chelation therapy did not alter the skeletal growth of these animals (95% CI: -1.28-2.33 mm; p=0.53; data not shown). CBC profiles showed minimal evidence of clinically-relevant iron deficiency or anemia and suggests that that DFO-treated animals had sufficient iron to maintain physiologic processes (data not shown).

4.3.2 Tissue Iron Quantification.

Administration of DFO allowed for iron to be chelated and eliminated via the urine. Relative to the control group, animals receiving iron chelation therapy had increased urinary iron levels (p=0.04; Figure 4.1 A). Consistent with increased iron mobilization, DFO-treated animals had significantly higher serum iron concentration than control animals (p=0.0009; Figure 4.1 B). Overall, iron elimination was also reflected in tissue iron quantification. Iron AAS revealed that animals receiving DFO had significantly lower iron concentration in both the liver (p=0.02; Figure 4.1 C) and femoral head articular cartilage (p=0.0006; Figure 4.1 D).

4.3.3 Histologic Scoring of Knee Joints.

Histologic evaluation of knee joints (31) demonstrated significantly lower total joint OA scores, and therefore decreased OA development, in DFO-treated animals (p=0.0001; Figure 4.2 A). Reduced OA in DFO animals was maintained when medial and lateral compartments were evaluated separately (p=0.0002 and p=0.0012, respectively; Figure 4.3 A-B). Representative photomicrographs depicting articular cartilage in the medial compartment are provided in Figures 4.2 B-C. The representative image from a control animal shows a disrupted tibial surface with fissures and proteoglycan loss in the superficial zone and chondrocyte hypocellularity distributed throughout ECM (Figure 4.2 B). Conversely, the DFO-treated animal had cartilage

surface with mild irregularities, uniform proteoglycan content, and slight chondrocyte hypercellularity (Figure 4.2 C). Figure 4.3 provides the four main parameters that contributed to the whole joint OA score. Relative to the control group, animals receiving DFO had significantly lower values for articular cartilage structure ($p=0.0007$), proteoglycan content ($p=0.003$), and cellularity ($p<0.0001$) (Figure 4.3 C-E). There was no notable difference in the tidemark integrity between groups (>0.9999; Figure 4.3 F). Histologic evidence of osteophytes was not documented in any animals evaluated.

4.3.4 Gene Expression Analysis of Knee Articular Cartilage.

4.3.4.1 Cell Death-Related Genes.

Several genes associated with cell death were differentially expressed in animals treated with DFO. Relative to control animals, gene transcript counts for the proapoptotic genes BAD ($p=0.0004$), BAX ($p=0.008$), and BAK ($p=0.04$) were significantly reduced in DFO-treated animals (Figure 4.4 A-C). Additionally, expression of the antiapoptotic gene BCL-2 was significantly higher in the DFO group ($p<0.0001$; Figure 4.4 D). Animals treated with DFO displayed significantly decreased mRNA expression of the apoptosis initiator caspase-9 ($p=0.002$) and effector caspase-3 ($p=0.007$) (Figure 4.4 E-F). Of note, there was not a substantial difference in caspase-8 transcripts between groups (95% CI: -8.13-16.88 normalized mRNA counts; $p=0.4$; data not shown).

4.3.4.2 Genes Related to Articular Cartilage Structure.

Type II collagen and aggrecan are two of the most abundant molecules within the cartilage ECM (37) and contribute to cartilage structure and proteoglycan content, respectively. Compared to the control group, animals treated with DFO had significantly lower transcript counts of COL2A1 ($p=0.0003$) and ACAN ($p=0.002$) (Figure 4.5 A-B). Likewise, administration

of the iron chelator resulted in decreased expression of several genes for MMPs that degrade the ECM of articular cartilage, including MMP-2 ($p<0.0001$), MMP-9 ($p=0.02$), and MMP-13 ($p=0.02$) (Figure 4.5 C-E). Finally, treatment with DFO resulted in a significant increase in gene expression for the MMP inhibitor, TIMP-2 ($p=0.03$; Figure 4.5 F).

4.3.4.3 Overhead Enclosure Monitoring.

Overhead enclosure monitoring revealed that, relative to the first month of the study, control animals moved a mean distance of 5.71 meters (m) less during the final monitored activity session, while the DFO group maintained their mean distance traveled ($p=0.05$; Figure 4.6 A). Likewise, control animals moved an average of 9.7 millimeters/second (mm/s) slower by study termination, while DFO-treated animals sustained the mean speed of travel initially recorded ($p=0.05$; Figure 4.6 B).

4.4 Discussion.

In the present work, we demonstrated that systemic iron reduction decreases the development of OA-associated cartilage lesions in the knee joints of male Hartley guinea pigs. To our knowledge, this is the first published study reporting the effects of extraarticular pharmacologic iron chelation on primary knee OA in a spontaneous/idiopathic animal model. The results indicate that lowering iron levels by administration of DFO is beneficial to knee joint articular cartilage and may suggest that systemic and/or local iron concentrations be considered as a factor in primary OA development.

Treatment with DFO was successful at decreasing tissue iron content both systemically (measured within the liver) and in a diarthrodial joint environment (femoral head articular cartilage). The enhanced urine iron concentration with DFO treatment reflects the major mechanism of iron elimination by this compound (38) and thus provides an explanation for

reduced tissue iron within these animals. Although iron levels were reduced in the DFO group, animals were still regularly receiving iron through the standard, iron-replete diet, and CBC data indicated these animals contained sufficient iron for normal physiologic processes. An interesting finding from this study was the increased serum iron concentration in chelated animals, despite an overall decrease in iron within the organs investigated. A potential explanation for increased serum iron with treatment is that DFO encouraged iron to be mobilized out of tissues into systemic rotation; this hypothesis is supported by the altered expression of several iron transport genes within knee articular cartilage. Correspondingly, transcript counts for the iron import genes TFR1, DMT1, and ZIP14 were decreased, suggesting reduced iron uptake by chondrocytes (Figure 4.7 A-C). Additionally, higher expression of the iron export gene FPN was observed in this same tissue, further supporting increased iron removal from these cells (Figure 4.7 D). Additional iron-related genes are presented in Figure 4.7.

Relative to control animals, iron chelation therapy reduced the development and/or severity of OA-associated cartilage lesions within the knee joint. Analysis of the individual OARSI score components revealed that variations in chondrocyte cellularity was the largest contributor to the histologic differences present between groups. Within the medial compartment, all control animals exhibited tibial hypocellularity; this was only observed in 2 of the 8 DFO animals evaluated. The beneficial retention of chondrocyte density within the DFO group was supported by alterations in gene expression of knee articular cartilage. In particular, iron chelated animals displayed decreased expression of several genes associated with promoting the intrinsic pathway of apoptosis, while simultaneously showing a significant increase in the antiapoptotic gene BCL-2. Indeed, iron has been shown to induce chondrocyte apoptosis by mediating the production of hydroxyl radicals (19), resulting in accelerated degradation of the

ECM (19,39). It is interesting that caspase-8, which is required to progress apoptosis triggered by external stimuli, did not have significant changes in gene expression with iron chelation treatment. When considered with the reduced transcript expression of BAX, BAK, and caspase-3, the relative consistency in caspase-8 supports that the intrinsic pathway of apoptosis was modulated in chondrocytes from treated animals more than the extrinsic pathway. However, additional work is required to determine the mechanisms by which iron promotes chondrocyte apoptosis and the type(s) of cell death observed in OA.

While most studies investigating ROS have largely focused on the direct damage to DNA and mitochondria, lysosomes have also emerged as playing a vital role in the early phases of cellular damage from oxidative stress and are involved in the apoptotic process (40-41). Pertaining to arthropathies, a study reported that the large amounts of iron sequestered in RA-affected human synoviocytes was often concentrated within lysosomes, and that this was associated with extensive cytoplasmic damage (42). Lysosomes can contain large amounts of redox-active iron from the autophagic degradation of cellular molecules as well as those endocytosed from extracellular sources (4,40,43). This labile iron can participate in redox chemistry, with the damaging radical products causing membrane permeabilization that releases lysosomal contents into the cytosol, initiating proapoptotic signaling (43-46). Additionally, iron recycled from the regular digestion of metalloproteins is released from lysosomes in the redox-active form and may serve as a major source of intracellular labile iron that can further contribute to cellular damage (41,43). Of relevance to the current study, DFO has been demonstrated to enter cells via fluid-phase endocytosis and is subsequently transported to the lysosomes (45-46), where it binds the redox-active iron present. By chelating lysosomal iron, DFO decreases the formation of damaging radicals and indirectly reduces the concentration of labile iron in the

cytosol (43). Accordingly, DFO can protect against hydrogen peroxide-mediated DNA damage by binding the free lysosomal iron that is critical in this process (40,46). As such, DFO may have contributed to chondrocyte preservation by chelating unstable iron within lysosomes, resulting in the rapid reduction of tissue iron levels that, in turn, protected against destruction of the ECM. In support of this, transcript counts for type II collagen and aggrecan were significantly reduced in DFO-treated animals, suggesting that less matrix synthesis was required to replace degraded molecules.

The preservation of knee articular cartilage may have also been influenced by decreased gene expression of several matrix degrading proteinases. Augmented enzymatic digestion of proteoglycans and collagens is a major mechanism of ECM degradation in OA (47) and represents one of several catabolic events inappropriately upregulated in the disorder. Within the DFO group, there were significantly lower transcript counts of MMP-2, -9, and -13; this was accompanied by an increased expression of the MMP inhibitor TIMP-2. Indeed, enhanced expression of these MMPs has been documented in OA-affected human chondrocytes (47-48). The altered expression of MMPs and TIMP-2 hint that reduced tissue iron from DFO treatment may have helped restore the imbalanced expression of these enzymes occurring in OA pathogenesis.

While the activity of control animals declined by study termination, 8-month-old animals with reduced systemic iron exhibited mobility similar to that measured at 3-months-of-age. This finding is of interest as a main consequence of knee OA is reduced movement (49), leading to an increased risk of developing comorbidities (21) and ultimately impacting an individual's quality of life. Conversely, physical movement has been demonstrated to reduce pain and increase bodily function by up to 40% in individuals already affected by arthritis (50), and therefore may

help combat both the deleterious effects of OA itself and the development of other chronic disorders. Regardless of the rationale, maintaining physical activity throughout aging is undeniably beneficial, as it allows for the maintenance of strength that helps prevent functional decline and lowers susceptibility to morbidity and mortality (51). At present, it is not clear whether systemic DFO had ramifications beyond preserving the knee joint cartilage that contributed to conserved animal motion. As such, there is the distinct possibility that the activity level observed with treatment may have also been influenced by the effects of DFO outside of the joint, cumulatively resulting in these animals performing better overall.

There are confines to this work worthy of discussion. Although DFO has been primarily used for its iron chelating properties, there has been evidence that the parent compound can also act as a radical scavenger through interaction with hydroxyl radicals, superoxide radicals, and peroxy-radicals (52-53). Given this, it is unclear whether the results observed in this study were due to iron removal by DFO alone and/or through another direct mechanism of the pharmacologic agent itself. Future work should focus on whether the effects observed in this study were from a reduction in ROS or through other processes influenced by reduced iron levels. Next, the authors recognize that changes in gene expression do not necessarily correlate to protein abundance and/or activity; indeed, the limited availability of guinea pig antibody-based reagents remains an unfortunate hurdle. While we were unable to provide corresponding protein data in the present study, it is noteworthy that the expression of the genes provided was consistent with what was observed during histologic analysis of knee joints. The authors aim to establish immunostaining protocols for select genes presented in this work (BAD, BAX, BCL-2, caspase-3, and iron-related genes), as well as related proteins for elucidating mechanisms of chondrocyte cell death (such as phosphorylated p53), as reagents become available. It is possible

that, at the ages investigated in this work, iron dysregulation contributing to disease development preceded oxidative stress documented in OA pathogenesis (20, 22-24). Indeed, iron dyshomeostasis preceding oxidative stress has been documented in chronic aging-associated disorders (54-56) as well as within general aging and senescence models (57-58). At 8-months-of-age (30-weeks-of-age), the Dunkin-Hartley guinea pig have developed moderate OA, with late stage/severe OA occurring around 15-months-of-age (28). Similar to the aforementioned diseases, it is possible that iron homeostasis is dysregulated and involved in OA development, but does not reach the point of inflicting/contributing to oxidative stress until later, more severe stages of OA. In addition, while the results from this study are promising, the pursuit of more localized and/or clinically feasible iron chelators would enhance the translatability of this research for the treatment of OA. Finally, to elucidate the role that sex may play in this work, the authors have recently finished a study to examine the relationship between systemic iron levels and OA development in females.

4.5 Figures.

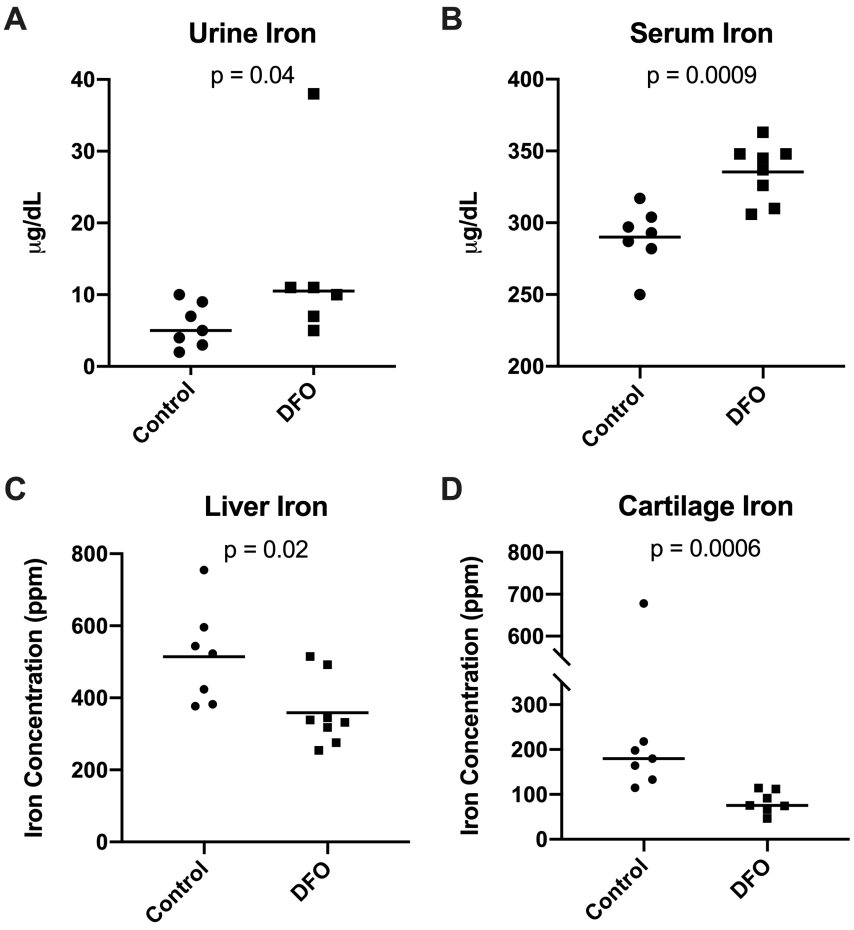

Figure 4.1. Tissue iron quantification. (A) Median urine iron× concentration was 5.00 micrograms/deciliter (µg/dL) in the control group and 10.50 µg/dL in the DFO group. (B) Mean serum iron concentration♦ was 290.00 µg/dL in the control group and 335.40 µg/dL in the DFO group. (C) Mean liver iron concentration♦ was 514.40 ppm in the control group and 358.90 in the DFO group. (D) Median femoral head cartilage iron concentration× was 180.00 ppm in the control group and 75.80 ppm in the DFO group.

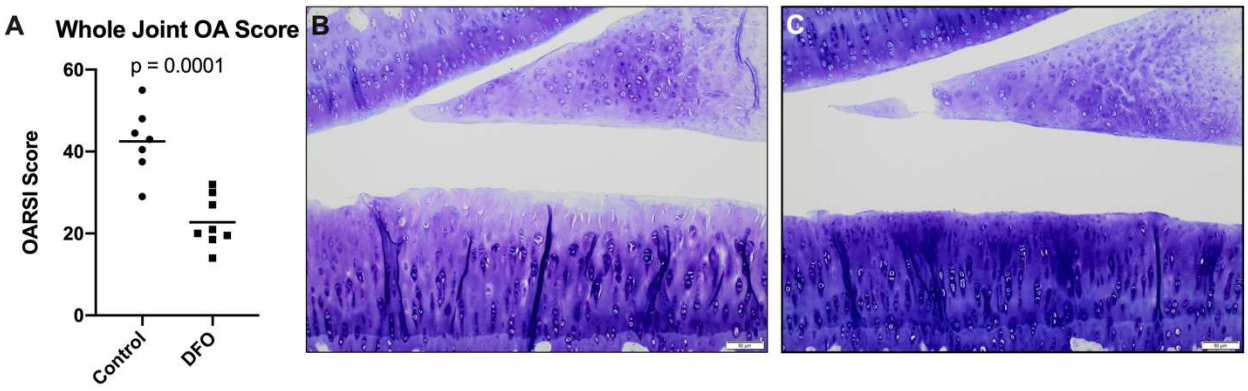

Figure 4.2. Histologic evaluation of knee joints. (A) Mean whole joint OA score♦ was 42.50 in the control group and 22.75 in the DFO group. (B) 10X representative histologic image of a control animal knee joint. (C) 10X representative histologic image of a knee joint from an animal treated with DFO.

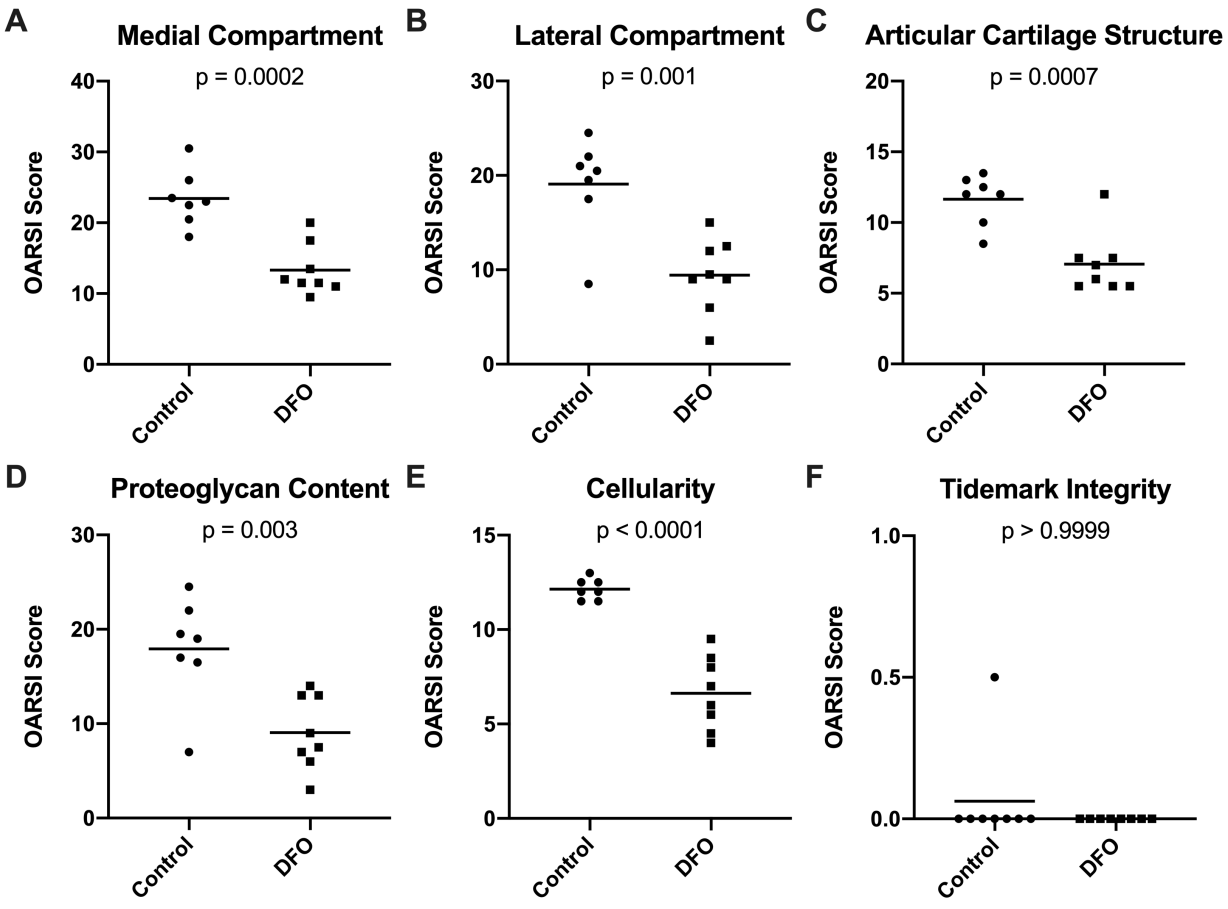

Figure 4.3. Contributions to histologic whole joint OA score. (A) Mean OARSI score in the medial compartment♦ was 23.43 in the control group and 13.31 in the DFO group. (B) Mean OARSI score in the lateral compartment♦ was 19.07 in the control group and 9.44 in the DFO group. (C) Mean whole joint score for articular cartilage structure♦ was 11.64 in the control group and 7.06 in the DFO group. (D) Mean whole joint score for proteoglycan content♦ was 17.93 in the control group and 9.06 in the DFO group. (E) Mean whole joint score for chondrocyte cellularity◊ was 12.14 in the control group and 6.63 in the DFO group. (F) Median whole joint score for tidemark integrity× was 0.00 in both the control and DFO group.

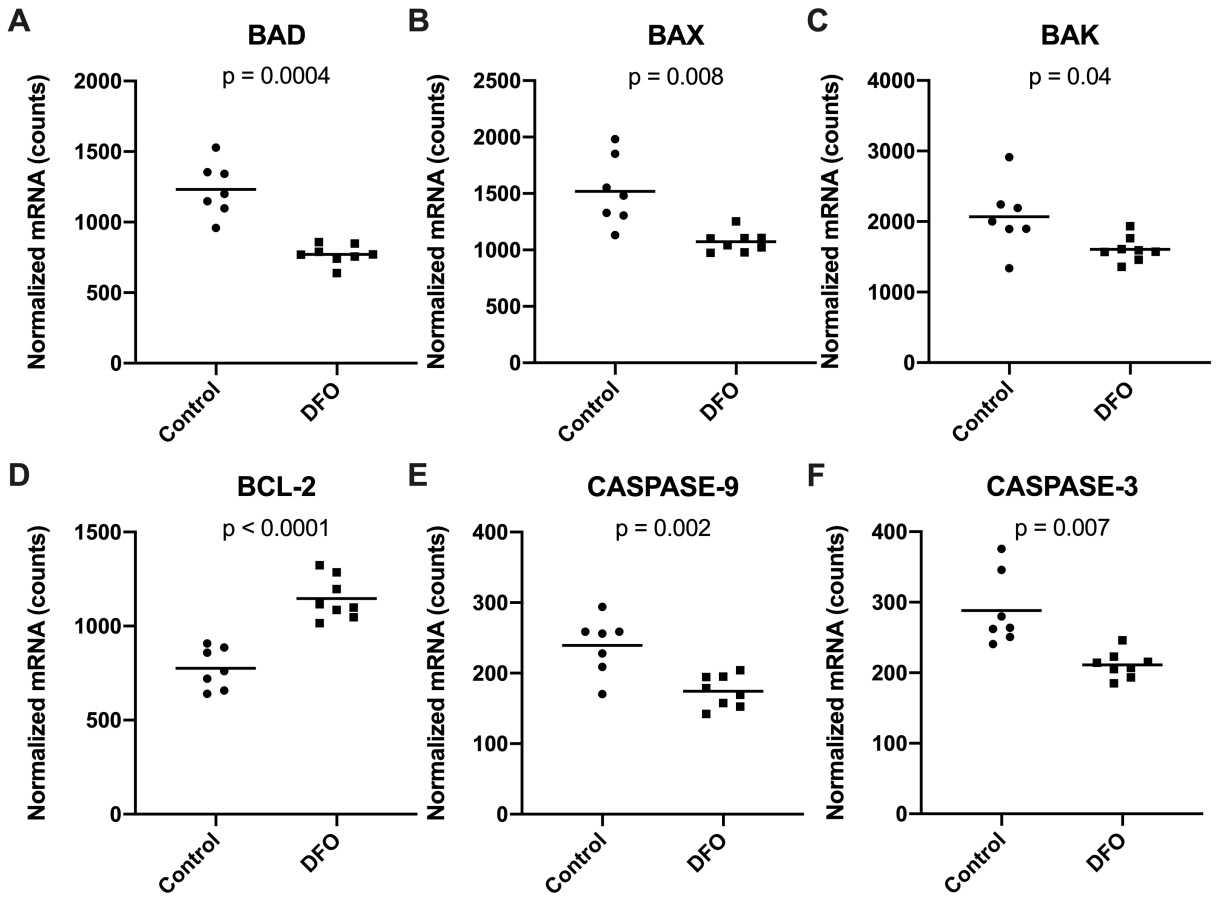

Figure 4.4. Normalized mRNA counts for cell death genes. (A) Mean transcript counts of BAD◊ were 1233.00 in the control group and 771.80 in the DFO group. (B) Mean transcript counts of BAX◊ were 1519.00 in the control group and 1073.00 in the DFO group. (C) Mean transcript counts of BAK◊ were 2068.00 in the control group and 1608.00 in the DFO group. (D) Mean transcript counts of BCL-2♦ were 775.90 in the control group and 1146.00 in the DFO group. (E) Mean transcript counts of caspase-9♦ were 239.20 in the control group and 174.20 in the DFO group. (F) Mean transcript counts of caspase-3◊ were 288.40 in the control group and 211.10 in the DFO group.

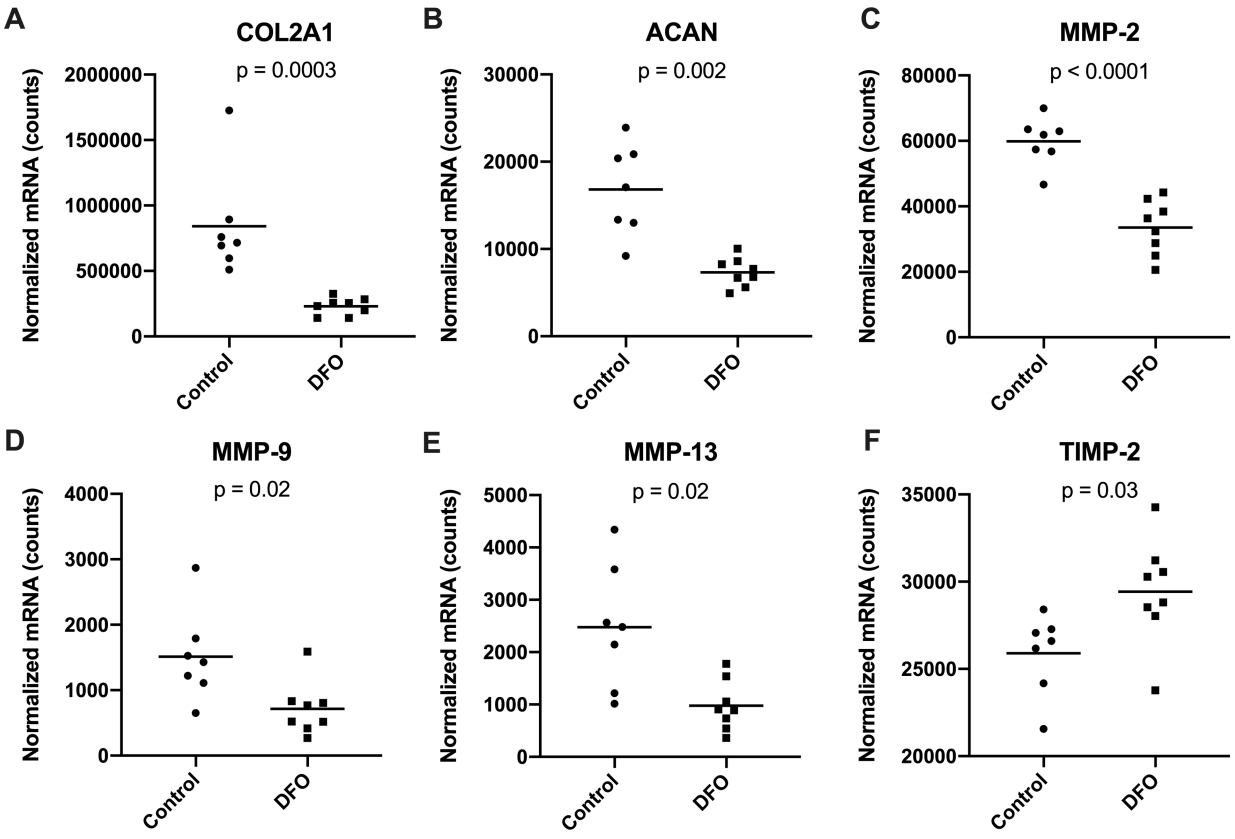

Figure 4.5. Normalized mRNA counts for genes related to the structure of knee articular cartilage. (A) Median transcript counts for type II collagen (COL2A1) × were 715415.00 in the control group and 156550.00 in the DFO group. (B) Mean transcript counts for aggrecan (ACAN) ◊ were 16828.00 in the control group and 7331 in the DFO group. (C) Mean transcript counts for MMP-2♦ were 59889.00 in the control group and 33501.00 in the DFO group. (D) Mean transcript counts for MMP-9♦ were 1514.00 in the control group and 715.20 in the DFO group. (E) Mean transcript counts for MMP-13◊ were 2478.00 in the control group and 976.50 in the DFO group. (F) Mean transcript counts for TIMP-2♦ were 25897.00 in the control group and 29433.00 in the DFO group.

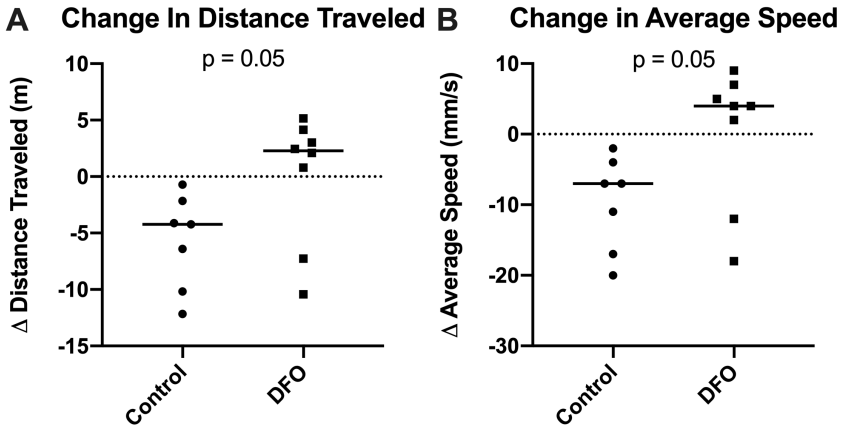

Figure 4.6. Movement parameters from overhead enclosure monitoring. (A) Change in distance traveled[×]. During the final monitoring session, control animals were traveling a median distance of 4.22 m less than what was recorded in the first monitoring session. Conversely, DFO-treated animals traveled a median distance of 2.28 m more in the final monitoring session relative to the first activity session. (B) Change in the average speed of travel[×]. During the final monitoring session, control animals were moving a median speed[×] of 7.00 mm/s slower than values recorded in the first session. DFO treated animals moved at a median speed of 4.00 mm/s faster than what was recorded in the first activity session.

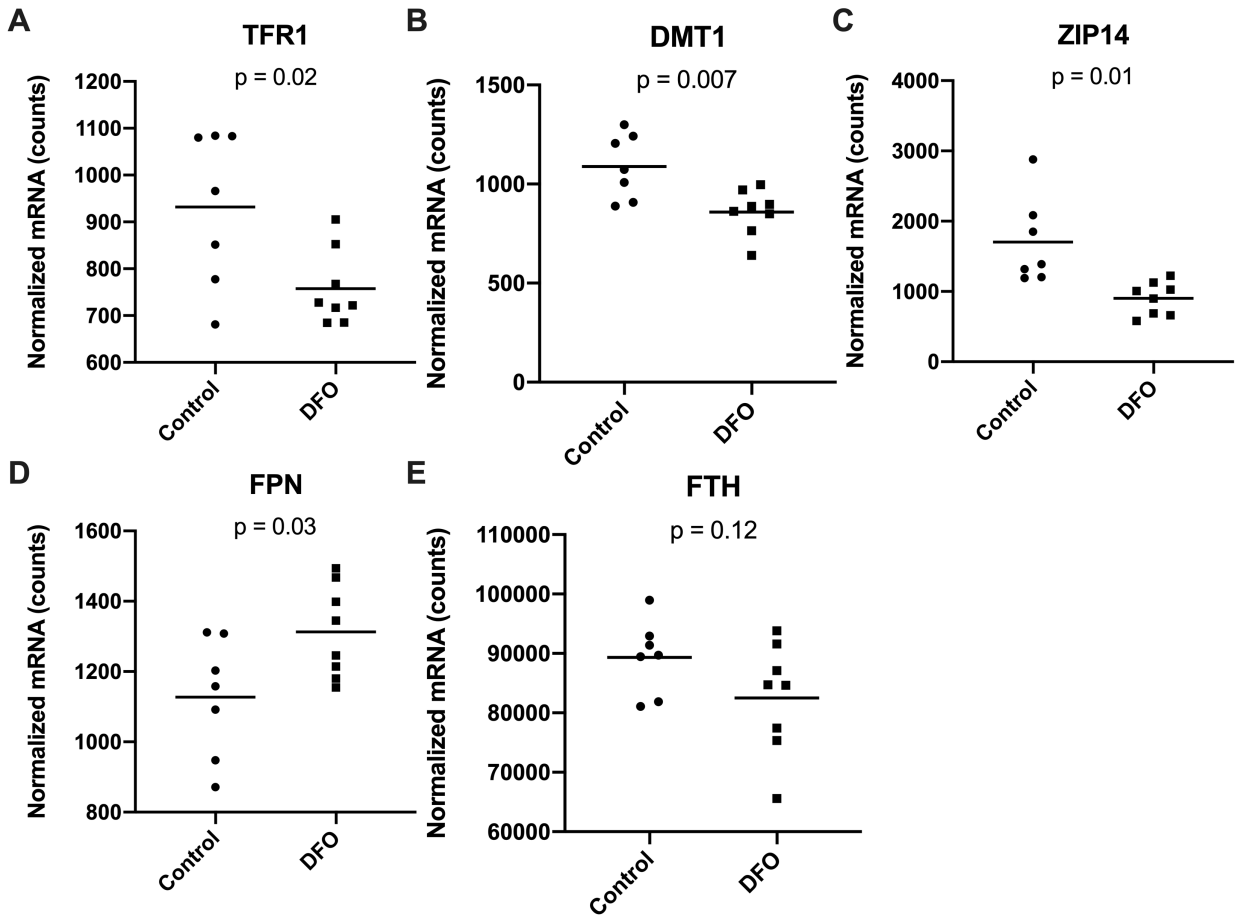

Figure 4.7. Normalized mRNA counts for genes related to iron metabolism (supplemental). (A) Mean transcript counts for TFR1♦ were 932.10 in the control group and 757.70 in the DFO group. (B) Mean transcript counts for DMT1♦ were 1089.00 in the control group and 858.90 in the DFO group. (C) Mean transcript counts for ZIP14◊ were 1703.00 in the control group and 901.60 in the DFO group. (D) Mean transcript counts for FPN♦ were 1127.00 in the control group and 1313.00 in the DFO group. (E) Mean transcript counts for FTH♦ were 89350.00 in the control group and 82526.00 in the DFO group.

4.6 References.

1. Winterbourn CC. Toxicity of iron and hydrogen peroxide: the Fenton reaction. *Toxicol Lett*. 1995; 82-83:969-74. doi: 10.1016/0378-4274(95)03532-x.
2. Koppenol WH, Hider RH. Iron and redox cycling. Do's and don'ts. *Free Radic Biol Med*. 2019; 133: 3-10. doi: 10.1016/j.freeradbiomed.2018.09.022.
3. Voest EE, Vreugdenhil G, Marx JJ. Iron-chelating agents in non-iron overload conditions. *Ann Intern Med.* 1994; 120(6): 490-9. doi: 10.7326/0003-4819-120-6-199403150-00008.
4. Dixon SJ, Stockwell BR. The role of iron and reactive oxygen species in cell death. *Nat Chem Biol*. 2014; 10(1): 9-17. doi: 10.1038/nchembio.1416.
5. Raven EP, Lu PH, Tishler TA, Heydari P, Bartzokis G. Increased iron levels and decreased tissue integrity in hippocampus of Alzheimer's disease detected in vivo with magnetic resonance imaging. *J Alzheimers Dis*. 2013; 37(1): 127-36. doi: 10.3233/JAD-130209.
6. Xu J, Marzetti E, Seo AY, Kim JS, Prolla TA, Leeuwenburgh C. The emerging role of iron dyshomeostasis in the mitochondrial decay of aging. *Mech Ageing Dev*. 2010; 131(7-8): 487-93. doi: 10.1016/j.mad.2010.04.007.
7. Paesano R, Natalizi T, Berlutti F, Valenti P. Body iron delocalization: the serious drawback in iron disorders in both developing and developed countries. *Pathog Glob Health*. 2012; 106(4): 200-16. doi: 10.1179/2047773212Y.0000000043.
8. Wessling-Resnick M. Iron homeostasis and the inflammatory response. *Annu Rev Nutr*. 2010; 30: 105-22. doi: 10.1146/annurev.nutr.012809.104804.
9. Silva B, Faustino P. An overview of molecular basis of iron metabolism regulation and the associated pathologies. *Biochim Biophys Acta*. 2015; 1852(7): 1347-59. doi: 10.1016/j.bbadis.2015.03.011.
10. Cook CI, Yu BP. Iron accumulation in aging: modulation by dietary restriction. *Mech Ageing Dev*. 1998; 102(1): 1-13. doi: 10.1016/s0047-6374(98)00005-0.
11. Zacharski LR, Ornstein DL, Woloshin S, Schwartz LM. Association of age, sex, and race with body iron stores in adults: analysis of NHANES III data. *Am Heart J*. 2000; 140(1): 98-104. doi: 10.1067/mhj.2000.106646.
12. Stadler N, Lindner RA, Davies MJ. Direct detection and quantification of transition metal ions in human atherosclerotic plaques: evidence for the presence of elevated levels of iron and copper. *Arterioscler Thromb Vasc Biol*. 2004; 24(5): 949-54. doi: 10.1161/01.ATV.0000124892.90999.cb.
13. Smith MA, Harris PL, Sayre LM, Perry G. Iron accumulation in Alzheimer disease is a source of redox-generated free radicals. *Proc Natl Acad Sci*. 1997; 94(18): 9866-8. doi: 10.1073/pnas.94.18.9866.
14. Stevens RG, Graubard BI, Micozzi MS, Neriishi K, Blumberg BS. Moderate elevation of body iron level and increased risk of cancer occurrence and death. *Int J Cancer*. 1994; 56(3): 364-9. doi: 10.1002/ijc.2910560312.
15. Ford ES, Cogswell ME. Diabetes and serum ferritin concentration among U.S. adults. *Diabetes Care*. 1999; 22(12): 1978-83. doi: 10.2337/diacare.22.12.1978.
16. Roosendaal G, Vianen ME, Venting MJ, van Rinsum AC, van den Berg HM, Lafeber FP. Iron deposits and catabolic properties of synovial tissue from patients with haemophilia. *J Bone Joint Surg Br*. 1998; 80(3): 540-5. doi: 10.1302/0301-620x.80b3.7807.

17. Richette P, Ottaviani S, Vicaut E, Bardin T. Musculoskeletal complications of hereditary hemochromatosis: a case-control study. *J Rheumatol*. 2010; 37(10): 2145-50. doi: 10.3899/jrheum.100234.
18. Biemond P, Swaak AJ, van Eijk HG, Koster JF. Intraarticular ferritin-bound iron in rheumatoid arthritis. A factor that increases oxygen free radical-induced tissue destruction. *Arthritis Rheum*. 1986; 29(10): 1187-93. doi: 10.1002/art.1780291002.
19. Nieuwenhuizen L, Schutgens REG, van Asbeck BS, Wenting MJ, van Veghel K, Roosendaal G, et al. Identification and expression of iron regulators in human synovium: evidence for upregulation in haemophilic arthropathy compared to rheumatoid arthritis, osteoarthritis, and healthy controls. *Haemophilia*. 2013; 19(4): e218-27. doi: 10.1111/hae.12208.
20. Henrotin Y, Kurz B, Aigner T. Oxygen and reactive oxygen species in cartilage degradation: friends or foes? *Osteoarthritis Cartilage*. 2005; 13(8): 643-54. doi: 10.1016/j.joca.2005.04.002.
21. Hunter DJ, Neogi T, Hochberg MC. Quality of osteoarthritis management and the need for reform in the US. *Arthritis Care Res*. 2011; 63(1): 31-8. doi: 10.1002/acr.20278.
22. Altindag O, Erel O, Aksoy N, Selek S, Celik H, Karaoglanoglu. Increased oxidative stress and its relation with collagen metabolism in knee osteoarthritis. *Rheumatol Int*. 2007; 27(4): 339-44. doi: 10.1007/s00296-006-0247-8.
23. Tiku ML, Shah R, Allison GT. Evidence linking chondrocyte lipid peroxidation to cartilage matrix protein degradation. Possible role in cartilage aging and the pathogenesis of osteoarthritis. *J Biol Chem*. 2000; 275(26): 20069-76. doi: 10.1074/jbc.M907604199.
24. Carlo MD Jr, Loeser RF. Increased oxidative stress with aging reduces chondrocyte survival: correlation with intracellular glutathione levels. *Arthritis Rheum*. 2003; 48(12): 3419-30. doi: 10.1002/art.11338.
25. Yazer M, Sarban S, Kocyigit A, Isikan UE. Synovial fluid and plasma selenium, copper, zinc, and iron concentrations in patients with rheumatoid arthritis and osteoarthritis. *Biol Trace Elem Res*. 2005;106(2): 123-32. doi: 10.1385/BTER:106:2:123.
26. Nugzar O, Zandman-Goddard G, Oz H, Lakstein D, Feldbrin Z, Shargorodsky M. The role of ferritin and adiponectin as predictors of cartilage damage assessed by arthroscopy in patients with symptomatic knee osteoarthritis. *Best Pract Rest Clin Rheumatol*. 2018; 32(5): 662-8. doi: 10.1016/j.berh.2019.04.004.
27. Ogilvie-Harris DJ, Fornasier VL. Synovial iron deposition in osteoarthritis and rheumatoid arthritis. *J Rheumatol*. 1980; 7(1): 30-6. https://pubmed.ncbi.nlm.nih.gov/7354467/.
28. Martin JA, Buckwalter JA. Aging, articular cartilage chondrocyte senescence and osteoarthritis. *Biogerontology*. 2002; 3(5): 257-64. doi: 10.1023/a:1020185404126.
29. Burton LH, Radakovich LB, Marolf AJ, Santangelo KS. Systemic iron overload exacerbates osteoarthritis in the strain 13 guinea pig. *Osteoarthritis Cartilage*. 2020; 28(9): 1265-75. doi: 10.1016/j.joca.2020.06.005.
30. Tessier JJ, Bowyer J, Brownrigg NJ, Peers IS, Westwood FR, Waterton JC, et al. Characterisation of the guinea pig model of osteoarthritis by in vivo three-dimensional magnetic resonance imaging. *Osteoarthritis Cartilage*. 2003; 11(12): 845-53. doi: 10.1016/s1063-4584(03)00162-6.
31. Kraus VB, Huebner JL, DeGroot J, Bendele A. The OARSI histopathology initiative—recommendations for histological assessments of osteoarthritis in the guinea pig. *Osteoarthritis Cartilage*. 2010; 18 Suppl 3(Suppl 3): S35-52. doi: 10.1016/j.joca.2010.04.015.

32. Ehlers KH, Giardina PJ, Lesser ML, Engle MA, Hilgartner MW. Prolonged survival in patients with beta-thalassemia major treated with deferoxamine. *J Pediatr*. 1991; 118(4 Pt 1): 540-5. doi: 10.1016/s0022-3476(05)83374-8.
33. Nair AB, Jacob S. A simple practice guide for dose conversion between animals and human. *J Basic Clin Pharm*. 2016; 7(2): 27-31. doi: 10.4103/0976-0105.177703.
34. Helrich, K, eds; Association of Official Analytical Chemists. *Official Methods of Analysis of AOAC International*. 15th ed. Gaithersburg, MD, USA; AOAC International; 1990. Official method 968.08D.
35. Helrich, K, eds; Association of Official Analytical Chemists. *Official Methods of Analysis of AOAC International*. 15th ed. Gaithersburg, MD, USA; AOAC International; 1990. Official method 974.27A, B, E and F.
36. Helrich, K, eds; Association of Official Analytical Chemists. *Official Methods of Analysis of AOAC International*. 15th ed. Gaithersburg, MD, USA; AOAC International; 1990. Official method 985.40D.
37. Fox AJS, Bedi A, Rodeo SA. The basic science of articular cartilage: structure, composition, and function. *Sports Health*. 2009; 1(6): 461-8. doi: 10.1177/1941738109350438.
38. Gerhardsson L, Kazantzis G. Diagnosis and treatment of metal poisoning: general aspects. In: Nordberg GF, Fowler BA, Nordberg M, eds. Handbook on the toxicology of metals. Amsterdam: Academic Press; 2015. p. 487-505. doi: 10.1016/B978-0-444-59453-2.00023-8.
39. Madhock R, Bennet D, Sturrock RD, Forbes CD. Mechanisms of joint damage in an experimental model of hemophilic arthritis. *Arthritis Rheum*. 1988; 31(9): 1148-55. doi: 10.1002/art.1780310910.
40. Kurz T, Gustafsson B, Brunk UT. Intralysosomal iron chelation protects against oxidative stress-induced cellular damage. *FEBS J*. 2006; 273(13): 3106-17. doi: 10.1111/j.1742-4658.2006.05321.x.
41. Li Y, Chen M, Xu Y, Yu X, Xiong T, Du M, et al. Iron-mediated lysosomal membrane permeabilization in ethanol-induced hepatic oxidative damage and apoptosis: protective effects of Quercetin. *Oxid Med Cell Longev*. 2016; 2016: 4147610. doi: 10.1155/2016/4147610.
42. Morris CJ, Blake DR, Wainwright AC, Steven MM. Relationship between iron deposits and tissue damage in the synovium: an ultrastructural study. *Ann Rheum Dis*. 1986; 45(1): 21-6. doi: 10.1136/ard.45.1.21.
43. Yu Z, Persson HL, Eaton JW, Brunk UT. Intralysosomal iron: a major determinant of oxidant-induced cell death. *Free Radic Biol Med*. 2003; 34(10): 1243-52. doi: 10.1016/s0891-5849(03)00109-6.
44. Hellquist HB, Svensson I, Brunk UT. Oxidant-induced apoptosis: a consequence of lethal lysosomal leak? *Redox Rep*. 1997; 3(1): 65-70. doi: 10.1080/13510002.1997.11747092.
45. Antunes F, Cadenas E, UT Brunk. Apoptosis induced by exposure to a low steady-state concentration of H2O2 is a consequence of lysosomal rupture. *Biochem J*. 2001; 356(Pt 2): 549-55. doi: 10.1042/0264-6021:3560549.
46. Doulias PT, Christoforidis S, Brunk UT, Galaris D. Endosomal and lysosomal effects of desferroxamine: protection of HeLa cells from hydrogen peroxide-induced DNA damage and induction of cell-cycle arrest. *Free Radic Biol Med*. 2003; 35(7): 719-28. doi: 10.1016/s0891-5849(03)00396-4.

47. Lipari L, Gerbino A. Expression of gelatinases (MMP-2, MMP-9) in human articular cartilage. *Int J Immunopathol Pharmacol*. 2013;26(3):817-23. doi: 10.1177/039463201302600331.
48. Bau B, Gebhard PM, Haag J, Knorr T, Bartnik E, Aigner T. Relative messenger RNA expression profiling of collagenases and aggrecanases in human articular chondrocytes in vivo and in vitro. *Arthritis Rheum*. 2002;46(10):2648-57. doi: 10.1002/art.10531.
49. Litwic A, Edwards MH, Dennison EM, Cooper C. Epidemiology and burden of osteoarthritis. *Br Med Bull*. 2013;105:185-99. doi: 10.1093/bmb/lds038.
50. Barbour KE, Helmick CG, Boring M, Brady TJ. Vital signs: prevalence of doctor-diagnosed arthritis and arthritis-attributable activity limitation—United States, 2013-2015. *MMWR Morb Mortal Wkly Rep*. 2017;66(9):246-253. doi: 10.15585/mmwr.mm6609e1.
51. World Health Organization. Health in older age. In: World report on ageing and health. Geneva: World Health Organization; 2015. p. 43-74.
52. Halliwell B. Protection against tissue damage in vivo by desferrioxamine: what is its mechanism of action? *Free Radic Biol Med*. 1989;7(6):645-51. doi: 10.1016/0891-5849(89)90145-7.
53. Zhu BZ, Har-El R, Kitrossky N, Chevion M. New modes of action of desferrioxamine: scavenging of semiquinone radical and stimulation of hydrolysis of tetrachlorohydroquinone. *Free Radic Biol Med*. 1998;24(2):390-9. doi: 10.1016/s0891-5849(97)00220-7.
54. Ashraf A, Jeandriens J, Parkes HG, So PW. Iron dyshomeostasis, lipid peroxidation and perturbed expression of cystine/glutamate antiporter in Alzheimer's disease: Evidence of ferroptosis. *Redox Biol*. 2020; 32: 101494. doi: 10.1016/j.redox.2020.101494.
55. Myhre O, Ultkilen H, Duale N, Brunborg G, Hofer T. Metal dyshomeostasis and inflammation in Alzheimer's and Parkinson's diseases: possible impact of environmental exposures. *Oxid Med Cell Longev*. 2013; 2013: 726954. doi: 10.1155/2013/726954.
56. Hung SH, DeRuisseau LR, Kavazis AN, DeRuisseau KC. Plantaris muscle of aged rats demonstrates iron accumulation and altered expression of iron regulated proteins. *Exp Physiol*. 2008; 93(3): 407-14. doi: 10.1113/expphysiol.2007.039453.
57. James SA, Roberts BR, Hare DJ, de Jonge MD, Birchall IE, Jenkins NL, et al. Direct in vivo imaging of ferrous iron dyshomeostasis in ageing Caenorhabditis elegans. *Chem Sci*. 2015; 6(5): 2952-62. doi: 10.1039/c5sc00233h.
58. Seo AY, Xu J, Servais S, Hofer T, Marzetti E, Wohlgemuth SE, et al. Mitochondrial iron accumulation with age and functional consequences. *Aging Cell*. 2008; 7(5): 706-16. doi: 10.1111/j.1474-9726.2008.00418.x.

CHAPTER 5

GENE EXPRESSION CHANGES OCCURING WITH SYSTEMIC IRON DEFICIENCY IN THE KNEE ARTICULAR CARTILAGE OF MALE DUNKIN-HARTLEY GUINEA PIGS

5.1 Introduction.

We recently established that systemic iron reduction via pharmacologic iron chelation was beneficial for decreasing the presence and/or severity of OA-associated cartilage lesions in the disease-prone Dunkin-Hartley guinea pig. However, use of the iron chelator deferoxamine (DFO) has the potential of inducing off-target effects unrelated to tissue iron levels (1-2). As such, the authors wanted to investigate whether an alternative method for achieving systemic iron reduction would produce similar results obtained in males treated with DFO.

For this proof-of-principle study, systemic iron reduction was achieved in treatment animals with a diet completely deficient in iron. This iron deficient diet was nutritionally comparable to the control guinea pig chow, with the exception that iron was absent from the treatment diet. Structural assessments of OA were previously reported in Radakovich 2018 (3), but the iron concentration and gene expression of knee articular cartilage was not evaluated at that time. Accordingly, the purpose of this work was to analyze the changes in transcript expression occurring with treatment in study animals.

5.2 Materials and Methods.

5.2.1 Animals.

All procedures were approved by the university's Institutional Animal Care and Use Committee and were performed in accordance with the NIH Guide for the Care and Use of

Laboratory Animals. Group size was determined from a pilot study with the histologic assessment of OA as the primary outcome. Using a within group error of 0.5 with a detectable difference between means of 1.0, power associated with an alpha of 0.5 (two sided) was calculated as 0.9 with a sample size of 6 animals per group. Twelve male Dunkin-Hartley guinea pigs were purchased from Charles River Laboratories (Wilmington, MA) at 8-weeks-of-age and maintained at Colorado State University's Laboratory Animal Resources housing facilities. Animals were housed individually in solid bottom cages and monitored daily by a veterinarian. Guinea pigs were given food and water *ad libitum*, as described below.

5.2.2 Iron Deficient and Control Diets.

As stated in Radakovich 2018 (3), 6 animals were randomly placed on either an iron deficient diet or an iron sufficient (control) diet; randomization was achieved via initial cage assignment, with alternating cage card numbers to assign animals to groups. Guinea pigs were transitioned from a regular chow diet (Teklad Global Guinea Pig Diet #2040, Madison, WI) to either the iron deficient or iron sufficient (control) diet over 2 weeks by mixing the diets (3). They were fully switched to the experimental diets at 12-weeks-of-age (3). These diets were specially formulated from Harlan Teklad and were identical in composition with the exception of iron content (3). The iron sufficient (control) diet contained 0.735 g/kg of ferric citrate added as the source of iron (3). Conversely, the iron deficient diet was formulated without the addition of ferric citrate, and the background levels of iron were limited to 25 parts per million (ppm) or less (3). Animals were fed these diets for 19 weeks, and body weights were recorded weekly throughout the study (3). Fleece material was used to prevent consumption of bedding, a common behavior of guinea pigs, as all available bedding options contained high levels of iron (data not shown) (3).

5.2.3 Specimen Collection.

The study was terminated when animals were 31-weeks-of-age. Animals were placed under isoflurane anesthesia and whole blood was collected with 20-gauge butterfly catheter via direct cardiac puncture. Following fluid collection, anesthetized animals were immediately transferred to a carbon dioxide chamber for euthanasia.

Hind limbs were removed at the coxofemoral joint, and femur length was measured using calipers. The left limb was analyzed for OA-related structural changes previously reported by Radakovich 2018 (3). The right limb was dissected to expose the knee joint and cartilage was collected from the weight-bearing regions of the femoral condyles and tibial plateaus. Cartilage was stored in RNAlater (Qiagen, Hilden, Germany) for gene expression analysis. Patellar cartilage was isolated from the right knee, fixed in 10% NBF for 48 hours, and submitted for iron quantification.

5.2.4 Tissue Iron Quantification by Atomic Absorption Spectroscopy (AAS).

Iron quantification was performed on sections of formalin-fixed liver tissue (reported by Radakovich 2018) (3) and patellar cartilage, as previously described (4) using a Model 240 AA flame atomic absorption spectrometer and SpectrAA software (Agilent Technologies, Santa Clara, CA) (5-7). Iron levels were reported in ppm dry weight (7).

5.2.5 Gene Expression Analysis of Knee Articular Cartilage.

RNA initially collected from articular cartilage at animal harvest degraded in storage and was deemed unsuitable for analysis. As such, total RNA was isolated from the remaining articular cartilage in the formalin-fixed paraffin-embedded (FFPE) knee joint previously used for histologic evaluation. This was performed using the High Pure FFPET RNA Isolation Kit (Roche, Basel, Switzerland) with modifications to the standard protocol. First, 10-micrometer

thick sections were deparaffinized with 1.00 mL of xylene (Fisher Scientific, Waltham, MA) and centrifuged for 2 minutes at maximum speed. The supernatant was discarded and the pellet was rehydrated per the kit instructions. The proteins were degraded by combining 280.00 µL of tissue lysis buffer with 80.00 µL Proteinase K under incubation for 30 minutes at 85°C, with a subsequent incubation for 30 minutes at 30°C. RNA was isolated by adding 350.00 µL of RNA binding buffer to the sample and transferring the suspension to the supplied purification column. The column was washed twice with RNA binding buffer and DNase treatment was performed. The column was again washed 2 additional times. The resulting RNA was eluted in 30.00 µL of elution buffer, according to the manufacturer's instructions. RNA concentration was assessed using the NanoDrop 2000 (ThermoFisher Scientific, Waltham, MA) and was sent to University of Arizona Genetics Core (University of Arizona, Tucson, AZ) for analysis.

A custom set of guinea pig-specific probes were designed and manufactured by NanoString Technologies (Seattle, WA) for the following genes: transferrin receptor 1(TFR1), divalent metal transporter 1 (DMT1), zrt- irt- like protein 14 (ZIP14), ferritin heavy chain (FTH), ferroportin (FPN), collagen type II (COL2A1), aggrecan (ACAN), Matrix Metalloproteinase-2 (MMP-2), MMP-9, MMP-13, B-cell lymphoma 2 (BCL-2), BCL-2-associated death promoter (BAD), BCL-2-associated x protein (BAX), BCL-2 homologous antagonist killer (BAK), caspase-3, caspase-8, and caspase-9. Per Qubit and Fragment Analyzer quality control subsets, the optimal amount of total RNA (800 ng) was hybridized with the custom code-set in an overnight incubation (17 hours) at 65°C, followed by processing on the NanoString nCounter FLEX Analysis system. Results were reported as absolute transcript counts normalized to positive controls and two housekeeping genes, β-actin and eukaryotic translation elongation factor 1 alpha 1. Any potential sample input variance was corrected by use of housekeeping

genes and application of a sample-specific correction factor to all target probes. Data analysis was conducted using nSolver™ software (NanoString Technologies).

5.2.6 Statistical Analyses.

Statistical analyses were performed with GraphPad Prism 8.4.2 (La Jolla, CA). The distribution and variance of data sets were determined with the Shapiro-Wilk and F-Test, respectively. Normally distributed data with similar variance were compared using parametric t-tests♦. Normally distributed data with significant differences in variance were compared using parametric t-tests with Welch's correction◊. Data with non-Gaussian distribution was compared using non-parametric Mann-Whitney U-test×. Statistical tests are noted in figure legends using designated superscripts. For data analyzed by parametric t-tests, black lines on graphs represent mean values. Black lines on graphs represent median values for data analyzed by Mann-Whitney U-tests. Statistical significance was set at $P \leq 0.05$.

5.3 Results.

5.3.1 Cartilage Iron Concentration.

Patellar articular cartilage was submitted for iron quantification by AAS. Animals receiving the iron deficient diet had significantly lower cartilage iron concentration than control animals ($p = 0.03$; Figure 5.1).

5.3.2 Gene Expression Analysis of Knee Articular Cartilage.

5.3.2.1 Iron Trafficking and Storage Genes.

We were curious whether genes related to cellular iron metabolism would be altered in animals receiving the iron deficient diet. Relative to the control group, iron deficient guinea pigs had significantly higher gene expression of the iron importer TFR1 within knee articular cartilage ($p = 0.03$; Figure 5.2 A). Similarly, treated animals had significantly higher transcript

counts of the gene coding for the cellular iron exporter, FPN ($p = 0.009$; Figure 5.2 D). The mRNA expression of DMT1 ($p = 0.3$; Figure 5.2 B), ZIP14 ($p = 0.3$; Figure 5.2 C), and FTH ($p > 0.9999$; Figure 5.2 E) did not significantly change with dietary treatment.

5.3.2.2 Genes Related to Articular Cartilage Structure.

Aggrecan and type II collagen are major constituents of the extracellular matrix (ECM) of articular cartilage. Gene expression analysis revealed that expression of COL2A1 ($p = 0.7$; Figure 5.3 A) and ACAN ($p = 0.3$; Figure 5.3 B) were not significantly altered with the iron deficient diet. Additionally, there was no change in the expression of several matrix degrading enzymes, including MMP-2 ($p = 0.99$; Figure 5.3 C), MMP-9 ($p = 0.9$; Figure 5.3 D), and MMP-13 ($p = 0.3$; Figure 5.3 E).

5.4 Discussion.

The purpose of this work was to determine gene expression changes in knee articular cartilage occurring with dietary iron deficiency in the OA-susceptible Hartley guinea pig. Initial results reported by Radakovich 2018 confirmed that treated animals had lower systemic iron levels, as evidenced by the significant decrease in liver and serum iron concentration (3). Relative to controls, guinea pigs receiving the iron deficient diet had a significant decrease in the development of OA-associated cartilage lesions, suggesting that decreased iron was beneficial to knee joint health in disease-prone animals (3).

Animals receiving the iron deficient diet had a significantly lower concentration of iron within cartilage from the patella, demonstrating that systemic treatment reduced iron levels within the knee joint. The reduction in local tissue iron levels may have contributed to the structural changes reported by Radakovich 2018 (3).

To further investigate the reduced development of cartilage lesions with systemic iron deficiency, we conducted gene expression analysis of knee articular cartilage. Surprisingly, there were few notable changes in transcript expression to report. Relative to the control group, gene expression of TFR1 was significantly lower in the cartilage of treated animals. The mRNA for TFR1 contains 5 iron responsive elements within the 3' untranslated region (UTR) (8), making the gene expression of this transporter highly sensitive to fluctuations in iron levels within the environment. When cellular iron stores are reduced, the interaction of IREs with iron regulatory proteins (IRPs) slows the degradation of TFR1 mRNA (8-9). The enhanced stability of TFR1 transcripts ultimately augments the corresponding protein expression, allowing for more iron to be imported in an attempt to correct the cellular iron deficiency. Therefore, the increased gene expression of TFR1 reflects the decrease in cartilage iron observed in this study.

Transcript expression of FPN was also significantly increased in the cartilage of iron deficient animals. The product of the FPN gene is the only known cellular iron export protein, ferroportin. Though FPN also contains a singular IRE region in the 5' UTR, IRP-mediated regulation of FPN largely occurs at the post-translational level (8). In iron deficient conditions, IRE-IRP binding results in decreased translation of the FPN protein in order to prevent iron export and keep iron within cells (10). However, post-transcriptional regulation of FPN has also been documented with modified iron levels in a cell-dependent manner (11-13). Increased gene expression of FPN was also observed in the cartilage of males treated with DFO and was attributed to enhanced iron mobilization occurring with iron chelation treatment (chapter 4). As these findings were maintained with dietary iron reduction, it is possible that decreased systemic iron may influence chondrocytes to export whatever cellular iron is present, presumably for use in other vital organs. These changes suggest that FPN may be a key player in chondrocyte iron

homeostasis, particularly when iron levels are reduced, and future work should continue to examine the relationship between systemic iron levels and FPN expression within this cell type.

Histologic evaluation of OA revealed that the structure and proteoglycan content of the knee articular cartilage were the largest contributors to improved whole joint scores (data not shown). The decreased development of cartilage lesions was not supported by gene expression analysis, as there were no significant changes in the expression of matrix degrading enzymes, ACAN, or COL2A1. Consequently, the structural benefits reported by Radakovich 2018 (3) may be from the direct influence of iron on the ECM. Indeed, reactive oxygen species (ROS), such as the hydroxyl radical produced from the iron-mediated Fenton reaction (14-15), can directly damage proteoglycans and collagens present within the articular cartilage ECM (16-17). Future work should focus on the direct effect of excess iron on the articular cartilage ECM. Of note, histologic evaluation of knee joints did not indicate any differences in chondrocyte cellularity, nor the expression of cell death-related genes, between treatment groups (data not shown).

Overall, the cartilage structural changes observed in this work were similar to the results obtained in male Hartley guinea pigs receiving DFO (chapter 4). The approach for tissue iron reduction differed between the 2 studies, with one method being a commercial pharmacologic agent and the other a dietary intervention. Unfortunately, the original tissue reserved for gene expression analysis degraded in storage, and the samples ultimately analyzed in this study were preserved by a different method. As such, a direct comparison of transcript expression could not be conducted between studies. Future work should continue to investigate the effects of iron homeostasis on articular cartilage, as well as cellular pathways influenced by various modifications to iron status.

5.5 Figures.

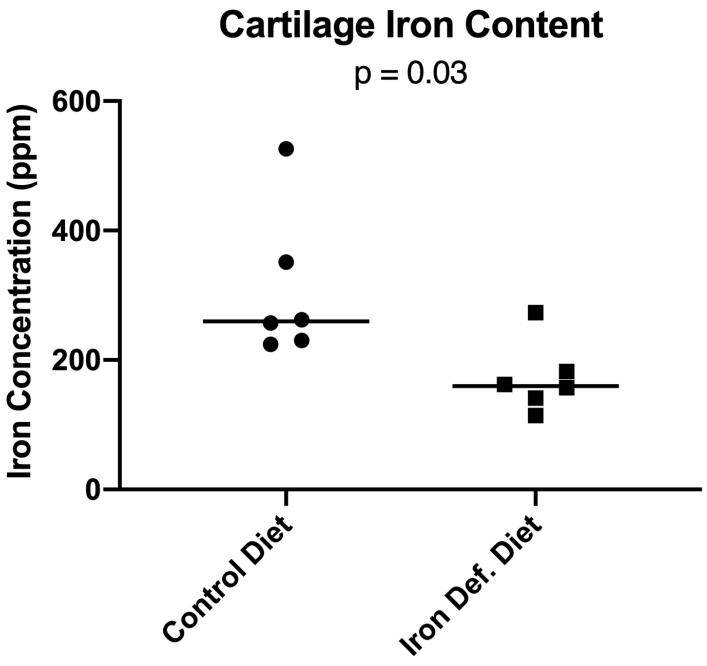

Figure 5.1. Cartilage iron quantification. Iron concentration of patellar cartilage by AAS×. Mean concentration of iron within knee cartilage was 308.30 ppm in control animals and 171.50 ppm in animals receiving the iron deficient diet.

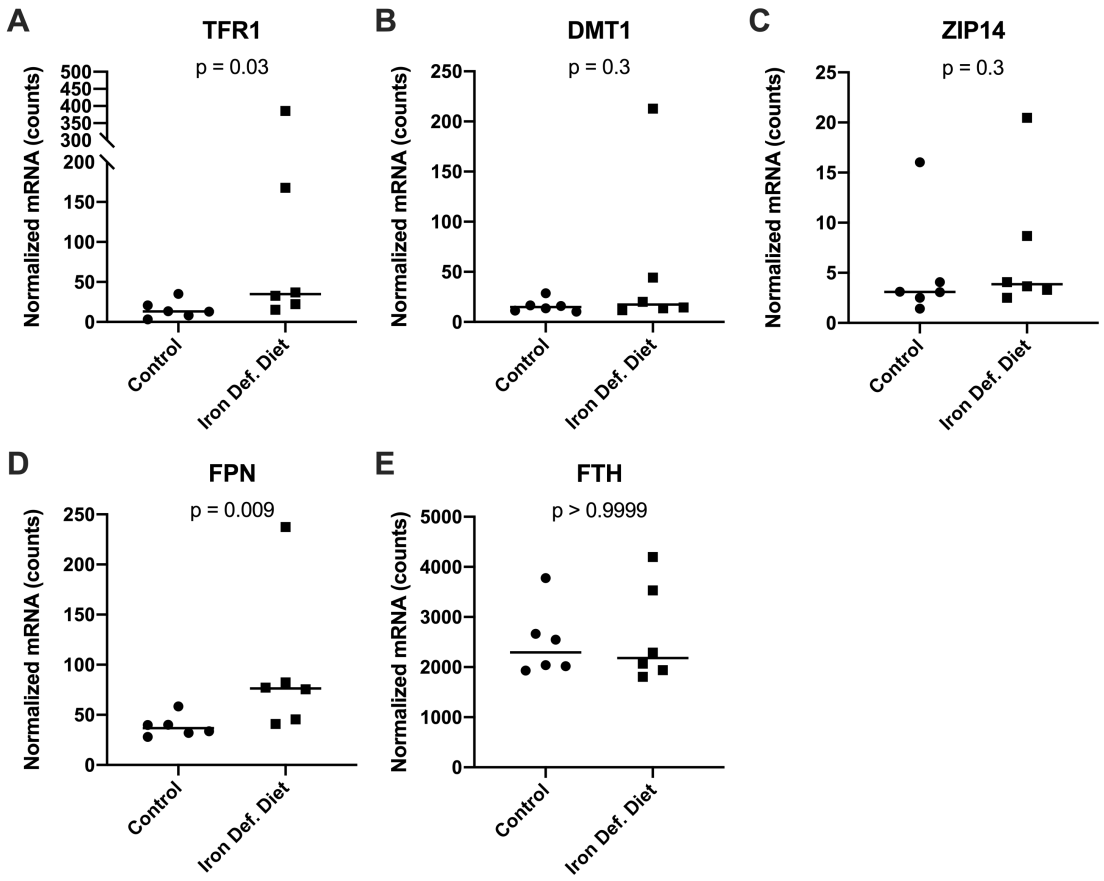

Figure 5.2. Normalized mRNA counts for genes related to iron metabolism. (A) Median transcript counts for TFR1$^{\times}$ were 13.20 in the control group and 110.20 in the iron deficient diet group. (B) Median transcript counts for DMT1$^{\times}$ were 14.80 in the control group and 17.34 in the iron deficient diet group. (C) Median transcript counts for ZIP14$^{\times}$ were 3.09 in the control group and 3.86 in the iron deficient diet group. (D) Median transcript counts for FPN$^{\times}$ were 36.86 in the control group and 76.42 in the iron deficient diet group. (E) Median transcript counts for FTH$^{\times}$ were 2294.00 in the control group and 2640.00 in the iron deficient diet group.

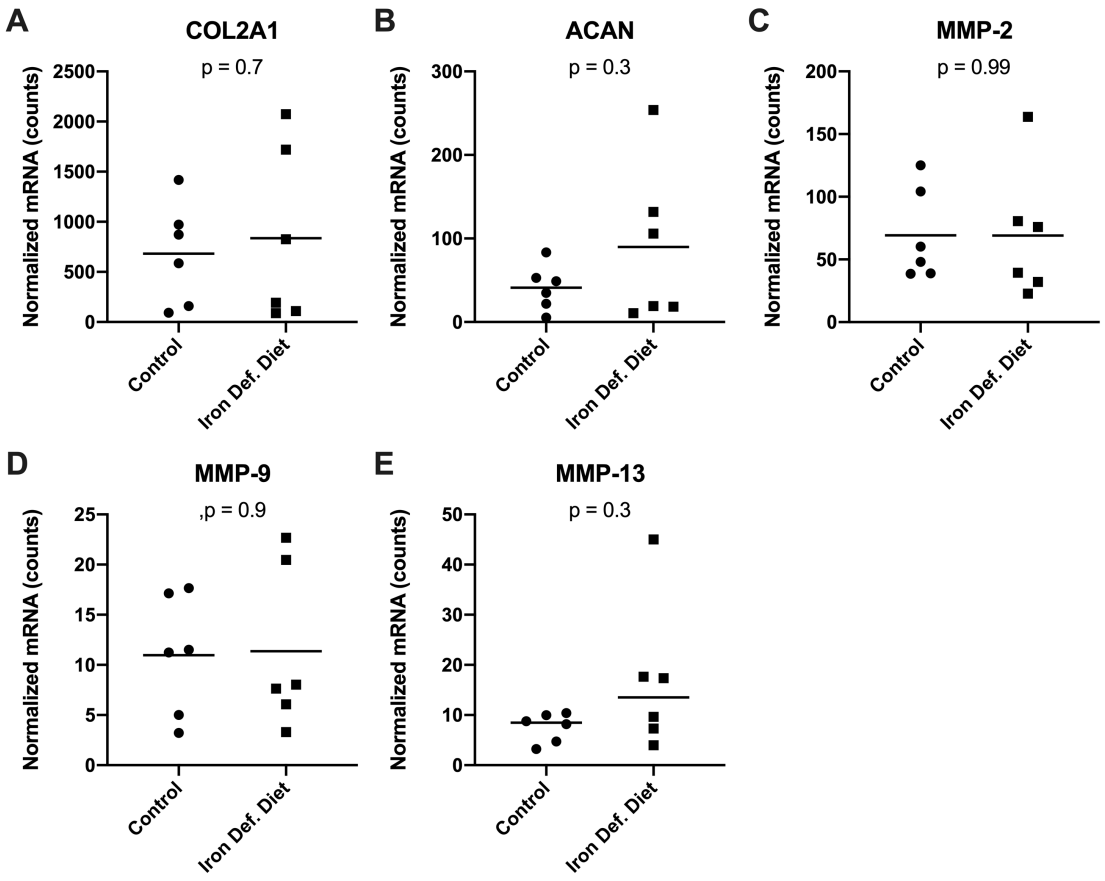

Figure 5.3. Normalized mRNA counts for genes related to the structure of knee articular cartilage. (A) Mean transcript counts for COL2A1⬧ were 683.20 in the control group and 835.60 in the iron deficient diet group. (B) Median transcript counts for ACAN◊ were 41.19 in the control group and 89.87 in the iron deficient diet group. (C) Mean transcript counts for MMP-2⬧ were 69.18 in the control group and 69.08 in the iron deficient diet group. (D) Mean transcript counts for MMP-9⬧ were 10.96 in the control group and 11.36 in the iron deficient diet group. (E) Median transcript counts for MMP-13× were 8.48 in the control group and 13.50 in the iron deficient diet group.

5.6 References.

1. Halliwell B. Protection against tissue damage in vivo by desferrioxamine: what is its mechanism of action? *Free Radic Biol Med*. 1989;7(6):645-51. doi: 10.1016/0891-5849(89)90145-7.
2. Zhu BZ, Har-El R, Kitrossky N, Chevion M. New modes of action of desferrioxamine: scavenging of semiquinone radical and stimulation of hydrolysis of tetrachlorohydroquinone. *Free Radic Biol Med*. 1998;24(2):390-9. doi: 10.1016/s0891-5849(97)00220-7.
3. Radakovich LB. The roles of iron, the infrapatellar fat pad, and dietary factors in the Hartley guinea pig model of spontaneous osteoarthritis. *PhD Dissertation*. Fort Collins, Colorado: Colorado State University; 2018.
4. Burton LH, Radakovich LB, Marolf AJ, Santangelo KS. Systemic iron overload exacerbates osteoarthritis in the strain 13 guinea pig. *Osteoarthritis Cartilage*. 2020; 28(9): 1265-75. doi: 10.1016/j.joca.2020.06.005.
5. Helrich, K, eds; Association of Official Analytical Chemists. *Official Methods of Analysis of AOAC International*. 15th ed. Gaithersburg, MD, USA; AOAC International; 1990. Official method 968.08D.
6. Helrich, K, eds; Association of Official Analytical Chemists. *Official Methods of Analysis of AOAC International*. 15th ed. Gaithersburg, MD, USA; AOAC International; 1990. Official method 974.27A, B, E and F.
7. Helrich, K, eds; Association of Official Analytical Chemists. *Official Methods of Analysis of AOAC International*. 15th ed. Gaithersburg, MD, USA; AOAC International; 1990. Official method 985.40D.
8. Wilkinson N, Pantopoulos K. The IRP/IRE system in vivo: insights from mouse models. *Front Pharmacol*. 2014;5:176. doi: 10.3389/fphar.2014.00176.
9. Cairo G, Recalcati S. Iron-regulatory proteins: molecular biology and pathophysiological implications. *Expert Rev Mol Med*. 2007; 9(33): 1-13. doi: 10.1017/S1462399407000531.
10. Hentze MW, Muckenthaler MU, Galy B, Camaschella C. Two to tango: regulation of mammalian iron metabolism. *Cell*. 2010; 142(1): 24-38. doi: 10.1016/j.cell.2010.06.028.
11. Chiabrando D, Fiorito V, Marro S, Silengo L, Altruda F, Tolosano E. Cell-specific regulation of ferroportin transcription following experimentally-induced acute anemia in mice. *Blood Cells Mol Dis*. 2013;50(1):25-30. doi: 10.1016/j.bcmd.2012.08.002.
12. Delaby C, Pilard N, Hetet G, Driss F, Grandchamp B, Beaumont C, et al. A physiological model to study iron recycling in macrophages. *Exp Cell Res*. 2005; 310(1): 43-53. doi: 10.1016/j.yexcr.2005.07.002.
13. Knutson MD, Vafa MR, Haile DJ, Wessling-Resnick M. Iron loading and erythrophagocytosis increase ferroportin 1 (FPN1) expression in J774 macrophages. *Blood*. 2003; 102(12): 4191-7. doi: 10.1182/blood-2003-04-1250.
14. Winterbourn CC. Toxicity of iron and hydrogen peroxide: the Fenton reaction. *Toxicol Lett*. 1995; 82-83:969-74. doi: 10.1016/0378-4274(95)03532-x.
15. Koppenol WH, Hider RH. Iron and redox cycling. Do's and don'ts. *Free Radic Biol Med*. 2019; 133: 3-10. doi: 10.1016/j.freeradbiomed.2018.09.022.
16. Henrotin YE, Bruckner P, Pukol JPL. The role of reactive oxygen species in the homeostasis and degradation of cartilage. *Osteoarthritis Cartilage*. 2003; 11(10): 747-55. doi: 10.1016/s1063-4584(03)00150-x.

17. Henrotin Y, Kurz B, Aigner T. Oxygen and reactive oxygen species in cartilage degradation: friends or foes? *Osteoarthritis Cartilage*. 2005; 13(8): 643-54. doi: 10.1016/j.joca.2005.04.002.

CHAPTER 6

SEX DIFFERENCES AND ASSOCIATED TISSUE RESPONSES WITH DEFEROXAMINE TREATMENT IN FEMALE VERSUS MALE DUNKIN-HARTLEY GUINEA PIGS

6.1 Introduction.

Iron is an essential element for sustaining life, allowing for physiologic processes such as oxygen transport, mitochondrial respiration, and the synthesis of nucleic acids. However, iron also has the potential to be toxic, as excess or unbound iron can participate in redox reactions that generate reactive oxygen species (ROS) and free radicals (1-2). These unstable molecules react with biological molecules, including proteins, lipids, and DNA, ultimately causing tissue damage (3-5). Despite this, mammals do not have a regulated mechanism for excreting iron, and all iron absorbed is continuously recycled throughout the body (6). Iron has been demonstrated to accumulate throughout the aging process (7-8) and has been linked to several aging-associated chronic disorders, including retinal degeneration (9), atherosclerosis (10), type II diabetes (11), neurodegenerative disorders (12-13), and cancer (14). Excess or improperly managed iron has also been implicated in disorders with associated arthropathies, including hemophilic arthropathy (15), hereditary hemochromatosis (16), traumatic arthropathy, and rheumatoid arthritis (RA) (17). Despite this, the role of iron has not been widely investigated within the context of osteoarthritis (OA).

OA is the most prevalent joint disorder and is among the top 5 causes of adult disability worldwide (18). While the factors driving the development of idiopathic OA remain poorly understood, advancing age has been identified as the largest risk factor (19). Notably, women

have been documented to have more severe knee OA than men, particularly when over the age of 55 (20). This finding suggests that biological sex, or sex-related factors, may play a role in the pathogenesis of knee OA. Women have more dramatic changes in hormones as well as physiologic processes throughout lifetime due to reproductive factors (21). However, the impact of sex differences is unlikely to be limited to hormone-related disorders and may have widespread physiologic effects within the body. Indeed, sex differences have also been documented for aging-related iron accumulation. A study conducted in aged retinas found that female humans had higher iron content within retinas than males at all age groups investigated (22). A second study demonstrated that serum ferritin levels began drastically increasing when women reached the ages of 45-49 and continued to increase through ages 60-64 (23), again suggesting that females exhibit aging-related iron accumulation, particularly around the age that knee OA becomes more severe (20). Relevant to chronic disorders, a study conducted in over 30,000 apparently healthy women found that higher iron stores were associated with an increased risk of type II diabetes independent of known diabetes risk factors (24).

Unfortunately, the inclusion of females within biomedical research has been historically limited, and much of our understanding for the pathophysiology of disorders has been determined in male physiology to date. It is not surprising that, of the 10 prescription pharmaceutical drugs withdrawn from market between 1997-2000, 8 of these drugs were removed due to posing significantly greater health risks to women than men (25). Given this, it is important to include both males and females when investigating disorders in order to elucidate the presence of sex differences, particularly beyond those related to hormones.

We recently demonstrated that systemic iron reduction decreased the development of cartilage lesions within male Dunkin-Hartley guinea pigs, an animal model of idiopathic OA. In

this work, systemic iron reduction was achieved by administration of the pharmacologic iron chelator deferoxamine (DFO). The purpose of this study was to determine if administration of DFO to females of the same age, at the same dose and frequency, would yield similar results achieved in males. We hypothesized that treatment with DFO would be successful in reducing iron levels in female animals, and that animals treated with DFO would have decreased severity of OA. We anticipated that the tissue changes in the joint environment occurring with DFO treatment would likely vary with respect to sex.

6.2 Materials and Methods.

6.2.1 Animals.

All procedures were approved by the Institutional Animal Care and Use Committee and performed in accordance with the NIH Guide for the Care and Use of Laboratory Animals. Group size was determined from a pilot study with the histologic assessment of OA as the primary outcome. Using a within group error of 0.5 and a detectable difference between means of 1.0, power associated with an alpha of 0.5 was calculated as 0.9 with a sample size of 6 animals per group. To ensure adequate power for all study outcomes, a total of 16, 8-week-old female Dunkin-Hartley guinea pigs were purchased from Charles River Laboratories (Wilmington, MA). Guinea pigs were individually housed in solid bottom cages and monitored daily by a veterinarian. In this work, DFO was administered to reduce, but not completely deplete, systemic iron levels. As such, animals were allowed unlimited access to standard guinea pig chow replete in iron; hay cubes and water were also provided *ad libitum*.

6.2.2 Deferoxamine (DFO) Injections.

Injections began when animals were 12-weeks-of-age. Eight guinea pigs were randomly assigned by cage card number to receive DFO, while the remaining 8 animals were placed in the

control group. Allometric scaling (26) was conducted to convert the lowest dose and dosing frequency utilized in humans with chronic iron overload (27) to the equivalent dose in the guinea pig. Animals within the DFO group received 46 mg/kg of DFO (Fresenius Kabi, Lake Zurich, IL) injected subcutaneously twice daily for 5 consecutive days, followed by 2 days without receiving any treatment. Control animals received an equivalent dose of lactated ringer's solution (Pfizer, Lake Forest, IL) subcutaneously at the same frequency. Injections were given for a total duration of 19 weeks. Body weights were recorded prior to initiating treatment as well as weekly throughout the study.

6.2.3 Specimen Collection.

The study was terminated when animals were 31-weeks-of-age, with the final treatments administered the night prior. Animals were placed under isoflurane anesthesia, and whole blood was collected via direct cardiac puncture with a 20-gauge butterfly needle. Urine was collected following involuntary voiding during the initial transition to anesthesia. Serum was separated from the whole blood and, along with the urine, submitted for iron quantification using the Roche Cobas 6000 (Basel, Switzerland). Complete blood count (CBC) and serum biochemistry profiles were also determined. A portion of liver was collected from each animal and placed into 10% neutral buffered formalin (NBF) for 48 hours for iron quantification.

Hind limbs were removed at the coxofemoral joint. The left limb was placed into 10% NBF for 48 hours and then transferred to a 12.5% solution of ethylenediaminetetraacetic acid (pH 7.00) for decalcification and histologic evaluation. The right hind limb was dissected to expose the knee joint and articular cartilage was collected from the articular surface of the patella as well as the weight-bearing regions of the femoral condyles and tibial plateaus. Cartilage was stored in RNAlater (Qiagen, Hilden, Germany) at -80ºC until RNA could be isolated for gene

expression analysis. Articular cartilage was collected from the right femoral head and frozen at -80ºC, followed by storage in 10% NBF for 48 hours for iron quantification.

6.2.4 Tissue Iron Quantification by Atomic Absorption Spectroscopy (AAS).

Gene expression analysis on knee joint cartilage prevented use of this tissue for iron quantification. As such, iron quantification was performed on sections of NBF-fixed liver tissue and femoral head articular cartilage with methods previously described (28). Briefly, dried samples were weighed, ashed, sonicated in nitric acid, and diluted 30-fold with deionized water (29). Diluted samples were analyzed using a Model 240 AA flame atomic absorption spectrometer and SpectraAA software (Agilent Technologies, Santa Clara, CA) (30). Iron levels were reported as parts per million (ppm) dry weight (31).

6.2.5 Histologic Evaluation of Knee Joints.

Following decalcification, knee joints were divided into sagittal sections through the mid-plane and embedded in paraffin wax. 5-micron sections were stained with toluidine blue, and medial and lateral femurs and tibias were scored in a blinded fashion by two assessors using the Osteoarthritis Research Society International (OARSI) guidelines (32). One slide from the medial and lateral compartment were analyzed, for a total of two slides assessed per animal. Values from the four anatomic locations were summed to obtain the whole joint OA score.

6.2.6 Gene Expression Analysis of Knee Articular Cartilage.

As previously described (28), total RNA was isolated from knee articular cartilage using the RNeasy Lipid Tissue Mini Kit (Qiagen) and was sent to the University of Arizona Genetics Core (University of Arizona, Tucson, AZ) for analysis. A custom set of guinea pig-specific probes were designed and manufactured by NanoString Technologies (Seattle, WA) for the following genes: aggrecan (ACAN), type II collagen (COL2A1), C-C Motif Chemokine Ligand

2 (CCL2), cluster of differentiation protein 163 (CD163), ferritin heavy chain (FTH), interleukin-1ß (IL-1ß), mitogen-activated protein kinase 1 (MAPK/ERK2), matrix metalloproteinase-2 (MMP-2), MMP-3, MMP-9, MMP-13, transferrin receptor 1 (TFR1), tumor necrosis factor (TNF), rela/p65, nucleardivalent metal transporter 1 (SLC11A2/DMT1), ZRT/IRT-like protein 14 (SLC39A14/ZIP14), and ferroportin (SLC40A1/FPN). Based on initial RNA quantification (Invitrogen Qubit 2.0 Fluorometer and RNA High Sensitivity Assay Kit, Thermo Fisher Scientific, Waltham, MA) and fragment analysis quality control subsets (Fragment Analyzer Automated CE System and High Sensitivity RNA Assay Kit, Agilent Technologies), the optimal amount of total RNA (150-400 ng) was hybridized with the custom codeset in an overnight incubation at 65ºC, followed by processing on the NanoString nCounter® FLEX Analysis System (NanoString Technologies). Results are reported as absolute transcript counts normalized to two housekeeping genes, β-actin (ACTB) and eukaryotic elongation factor 1α1 (EEF1A1). Any potential sample input variance was normalized by use of housekeeping genes and application of a sample-specific correction factor to all target probes. Data analysis was conducted using nSolver™ software (NanoString Technologies).

6.2.7 Overhead Enclosure Monitoring.

Animal movement was documented throughout the study using ANY-maze behaviorial tracking software Stoelting Co., Wood Dale, IL). To conduct overhead enclosure monitoring, guinea pigs were placed into an open top apparatus with a camera permanently positioned above the pen. The activity of animals was recorded during 10-minute sessions occurring once per month for the duration of the study. Baseline parameters were collected at the one-month time point to allow guinea pigs to acclimate to the system.

6.2.8 Statistical Analyses.

Statistical analyses were performed with GraphPad Prism 8.4.2 (La Jolla, CA). Rationale for the exclusion of an entire animal from the study were determined *a priori* and included the presence of any pathologies and/or the inability to complete the study for any reason. Prior to conducting analyses, the authors determined that individual points would be excluded from data sets if: a sample did not pass quality control parameters set for an experimental method, the integrity of a sample was compromised, or an appropriate sample was unable to be obtained for analysis. One animal in the DFO group did not involuntarily void urine during anesthetic transition; two animals from the control group did not have appropriate knee tissue sections for histologic evaluation; and two cartilage samples from the DFO group were degraded during storage and were unsuitable for gene expression analysis. Therefore, urine iron, OARSI histologic evaluation of knee joints, and gene expression analysis of knee articular cartilage are incomplete data sets. For comparisons between 2 groups, the distribution and variance of data sets were determined with the Shapiro-Wilk and F-Test, respectively. Normally distributed data with similar variance were compared using parametric t-tests$^{\blacklozenge}$. Normally distributed data with significant differences in variance were compared using parametric t-tests with Welch's correction$^{\lozenge}$. Data with non-Gaussian distribution was compared using non-parametric Mann-Whitney U-test$^{\times}$. Statistical tests are noted in figure legends using designated superscripts. For data analyzed by parametric t-tests, black lines on graphs represent mean values. Black lines on graphs represent median values for data analyzed by Mann-Whitney U-tests. Overhead enclosure monitoring data was compared by two-way analysis of variance (ANOVA) with Sidak multiple comparisons test. Statistical significance was set at $P \leq 0.05$.

6.3 Results.

6.3.1 General Description of Animals.

Throughout the study, animals appeared to be clinically healthy and no changes in cage activity were noted. At the time of study termination, the mean body weight was 969.20 g in the control group and 942.70 g in the DFO group ($p = 0.4$; data not shown). Likewise, mean femur length was similar between the control group (43.81 mm) and DFO-treated animals (44.29 mm), indicating that treatment with DFO did not significantly alter the skeletal growth of these animals ($p = 0.3$; data not shown). CBC profiles did not show any evidence of iron deficiency or anemia occurring with treatment and suggest that animals receiving DFO had sufficient iron to maintain physiologic processes (data not shown).

6.3.2 Tissue Iron Quantification.

Treatment with DFO allows for chelated iron to be eliminated in the urine. Relative to the control group, animals receiving iron chelation treatment had a significantly higher urinary iron concentration ($p = 0.01$; Figure 6.1 A); this statistical significance was maintained when excluding two highest values in the DFO group ($p = 0.05$; data not shown). Despite increased iron excretion with DFO treatment, there was no significant difference in the concentration of iron within the serum ($p = 0.6$; Figure 6.1 B), liver ($p = 0.9$; Figure 6.1 C), or femoral head articular cartilage ($p = 0.8$; Figure 6.1 D) between groups.

6.3.3 Histologic Scoring of Knee Joints.

Histologic evaluation of knee joints revealed a trend towards lower whole joint OA scores, and thus decreased development of OA-associated cartilage lesions, in animals treated with DFO ($p = 0.08$; Figure 6.2 A). When medial and lateral joint compartments were considered separately, differences were more pronounced in the medial compartment ($p = 0.2$; Figure 6.3 A)

than the lateral compartment (p = 0.4; Figure 6.3 B). Representative photomicrographs are provided in Figure 6.2 B-C. The representative image from a control animal depicts a disrupted tibial surface with fissures and proteoglycan loss extending into the mid-zone of the cartilage and diffuse chondrocyte hypocellularity in the same area; regions of hypocellularity were also observed in the deep zone (Figure 6.2 B). A portion of the duplicated tidemark is visible near the scale bar. Conversely, the representative photo from a DFO-treated animal demonstrates a tibia with an irregular cartilage surface with several fissures accompanied by proteoglycan loss in extending into the mid-zone, with chondrocyte hypocellularity in the same area (Figure 6.2 C).

The published OARSI guideline has four parameters that, when considered together, assess the severity of OA-related lesions in the articular cartilage and comprise the whole joint OA score. Relative to the control group, animals treated with DFO exhibited a significant decrease in the scores for tidemark integrity (p = 0.01; Figure 6.3 F). Animals receiving iron chelation therapy also had slightly lower scores for the articular cartilage structure (p = 0.1; Figure 6.3 C) and chondrocyte cellularity (p = 0.1; Figure 6.3 E). Of note, there was no significant difference in the proteoglycan content of knee articular cartilage between groups (p = 0.6; Figure 6.3 D).

6.3.4 Gene Expression Analysis of Knee Articular Cartilage.

6.3.4.1 Genes Related to Iron Transport and Storage.

We wanted to determine the effect that systemic iron chelation had on iron-related genes within chondrocytes. Iron bound to transferrin is imported into cells by TFR1, while non-transferrin bound iron (NTBI) can be transported by both DMT1 and ZIP14. Relative to control animals, treatment with DFO did not cause variations in cartilage gene expression for TFR1 (p = 0.9; Figure 6.4 A). Animals in the DFO group did have slightly lower transcript counts for both

DMT1 (p = 0.1; Figure 6.4 B) and ZIP14 (p = 0.1; Figure 6.4 C) when compared to controls, but these differences were not significant. Additionally, there was no significant difference in gene expression for the only known cellular iron exporter FPN (p = 0.3; Figure 6.4 E).

Within the cell, iron that is not immediately required for use is stored in the protein ferritin. Measuring the transcript counts for the FTH revealed no significant differences between treatment groups (p = 0.7; Figure 6.4 D).

6.3.4.2 Genes Related to Articular Cartilage Structure.

Aggrecan and type II collagen are among the most abundant molecules comprising the extracellular matrix (ECM) of articular cartilage (33). As OA is primarily characterized by the progressive loss of articular cartilage within an affected joint, changes in the expression of these molecules can give insight to disease development. Relative to controls, animals within the DFO group had no change in the gene expression of COL2A1 (p = 0.4; Figure 6.5 A) and a trend towards increased expression of ACAN (p = 0.08; Figure 6.5 B). MMPs are catabolic enzymes that degrade the ECM of cartilage. Administration of DFO caused a marked trend towards decreased gene expression of MMP-3 (p = 0.06; Figure 6.5 C).

CD163 is a marker commonly expressed by phagocytotic cells that clear debris from tissues. Animals treated with DFO had significantly lower mRNA expression of CD163 within knee articular cartilage (p = 0.02; Figure 6.5 D). Additionally, females within the DFO group had significantly lower transcript expression for the inflammatory chemokine CCL2 (p = 0.03; Figure 6.5 E) and slightly decreased gene expression for the enzyme ERK2 (p = 0.09; Figure 6.5 F).

6.3.5 Overhead Enclosure Monitoring.

Overhead enclosure monitoring revealed no significant differences between treatment groups for total distance traveled (Figure 6.6 A) or average speed of travel (Figure 6.6 B) at any point in the study.

6.4 Discussion.

This is the second half of a two-part study with DFO in the OA-prone Dunkin-Hartley guinea pig. Previous work demonstrated reduced tissue iron levels and significantly decreased development of OA-associated cartilage lesions in the knee joint of males treated with DFO; unfortunately, these findings were not present to the same extent in female Hartley guinea pigs at the same ages. The results from this study suggest that iron metabolism and homeostasis may differ between males and females, as well as the factors contributing to OA pathogenesis in each sex.

Urine iron concentration was increased in females treated with DFO, reflecting the major route of iron elimination by this compound (34) and indicating that iron chelation and subsequent removal was occurring in treated females. However, despite enhanced urine iron excretion, iron chelated females did not have a notable change in iron concentration systemically (within the serum and the liver) or locally within a diarthrodial joint environment (femoral head articular cartilage). This is in contrast to males treated with DFO, which experienced a significant decrease in iron concentration within the serum, liver, and femoral head articular cartilage (Figure 4.1 B-D).

Iron metabolism and homeostasis has been reported to differ between male and female mammals (35-37), and clinical reports suggest sex may influence observed differences for the progression of iron-related disorders (37-38), although the mechanisms driving these differences

have yet to be clearly established. Human females have traditionally been cited as having lower body iron stores than males due to the physiologic loss of blood from menstruation (39); this has often been used to explain sex differences in adult iron metabolism. In the present work, untreated females had comparable iron concentrations to untreated males both in the liver ($p = 0.9$; data not shown) and circulating in the serum ($p = 0.2$; data not shown), despite being of reproductive age. Therefore, innate differences in tissue iron concentration cannot account for the iron levels maintained in iron chelated females but altered in DFO-treated males. The claims of females exhibiting lower iron status due to menstruation are almost completely based on serum iron measurements (23,40-41), which may only represent a small fraction of the total iron burden in the body (42-43). As such, effects of sex on the tissue distribution of iron have yet to be widely established (44).

Sex differences in iron metabolism have also been documented in adolescent humans with similar dietary iron intake (45-46), further supporting that there are inherent biological differences in iron metabolism attributed to factors other than menstrual bleeding. In particular, there has been evidence that female mammals exhibit enhanced dietary iron absorption relative to males (46-47). One study suggested that this increased iron absorption is the result of a hepcidin-mediated feedback loop in response to reduced tissue iron stores (23). Indeed, serum hepcidin expression has been negatively correlated with dietary iron absorption in adult, healthy females (48). However, rather than being regulated by tissue iron concentrations, hepcidin expression has been widely correlated with serum ferritin levels (40,49), which has repeatedly been demonstrated as a poor indicator of total iron status (42). On average, males have been demonstrated to have higher serum ferritin (44-45,50-51) and serum hepcidin levels (40,50) than females and, as such, may account for sex differences in dietary iron absorption and the differing

results for males and females in the present work. Unfortunately, the mechanisms driving the sex differences in serum ferritin expression currently remain unknown.

The ability for females to effectively replace DFO-chelated iron was also reflected in the gene expression analysis of knee cartilage tissue. Treatment with DFO did not significantly change in the transcript expression of any iron-related genes investigated, including the major cellular iron importer TFR1 and the storage molecule FTH. Both TFR1 and FTH-1 transcripts contain an iron responsive element (IRE) that allow their expression to be modulated by cellular iron levels to maintain homeostasis (52). In reduced iron states, IRE-binding of TFR1 delays mRNA degradation, thereby prolonging its expression to encourage iron transport into cells (52-53). In the present work, this mechanism did not appear to be altered between treatment groups in knee articular cartilage, further supporting that tissue iron levels were maintained by females treated with DFO. Though IRE-regulation of FTH primarily occurs at the translational level, transcriptional regulation has also been documented in response to iron levels and other factors such as oxidative stress (53-54).

Despite comparable cartilage iron levels between groups, whole joint histologic OA scores were moderately, but not statistically, reduced in females treated with DFO. A potential explanation for this finding may be that DFO beneficially mobilized iron out of body stores (55-56), despite not changing the overall tissue iron concentration. Preventing long-term storage of iron may provide physiologic benefit that warrants further investigation. The difference in OA severity was largely driven by the decreased prevalence of duplicated tidemarks in treated animals, which was observed in at least one area of the joint for all control animals. The tidemark is the boundary between the articular cartilage tissue and the underlying calcified cartilage present closer to the bone. When the calcified cartilage layer advances into the articular

cartilage, the location of the tidemark advances as well, creating an additional (or duplicated) band. Articular cartilage mineralization with tidemark replication is a key feature of OA pathology/progression (57) and is associated with enhanced joint degeneration. To date, tidemark variations have not been widely noted in the Dunkin-Hartley model of OA, though this may be influenced by the primary use of males in OA publications historically (32). Indeed, human females exhibit more pronounced thickening of calcified cartilage with age than males (58). As such, articular cartilage mineralization and related tidemark replication may be a more relevant/prominent feature in female pathogenesis and should be considered when evaluating OA in this sex.

Serum levels of CCL2 have been found to be significantly associated with radiographic knee OA in human patients (59), and chondrocytes exposed to this chemokine have been demonstrated to upregulate the production of catabolic markers, such as MMP-3, via activation of ERK (60). In the present work, systemic iron chelation reduced the gene expression of CCL2 within knee articular cartilage, which was accompanied by a notable trend towards decreased transcript counts of both MMP-3 and MAPK/ERK2. Outside of the joint environment, CCL2 protein expression recruits macrophages to sites of inflammation or tissue damage (61-62). Macrophages are not present in articular cartilage; instead, chondrocytes themselves have adapted the role of macrophages to clear debris in the ECM (63). Of note, laboratory models have demonstrated that OA-affected chondrocytes express significantly more CD163 mRNA than controls (63). In this study, transcript expression of CD163 was significantly reduced in the cartilage of animals treated with DFO. When these results are considered together, it is possible that the significant reduction in CCL2 mRNA contributed to ECM preservation by moderately decreasing the expression of MMP-3; this trend may have become more pronounced had the

study continued longer and/or the dose of DFO was modified for females. Enhanced maintenance of the ECM was reflected by decreased gene expression of the phagocytosis marker CD163 by chondrocytes. However, it is important to note that there was no significant change in cartilage gene expression for several relevant proinflammatory mediators (IL-1ß, TNF, p65) or other catabolic enzymes (MMP-2, MMP-9, MMP-13) occurring with treatment (data not shown). Thus, the relationship between DFO and matrix integrity without reduced iron levels is unclear and the mechanisms influenced by treatment warrants further investigation.

Collectively, the results from this study suggest that there may be sex differences present for both iron metabolism and OA and indicate there may be value in considering sex as a treatment factor in clinical settings. Despite utilizing an identical dose of DFO via the same route of administration and dosing frequency, tissue iron levels were not altered in females as they were in males; this may be attributed to enhanced dietary iron absorption by females. Consequently, there were fewer differences in OA development and relevant gene expression for females treated with DFO. An interesting result from this work was the trend towards decreased OA development in DFO despite maintained iron levels. DFO itself has been discovered to act as a free radical scavenger (64-65) and may have additional off-target effects that are not currently known. As such, the effects observed in this study may have occurred through unknown effects of DFO unrelated to iron chelation and subsequent removal. Of note, though there was no evidence of altered ROS production (data not shown), we hypothesize that oxidant-induced tissue damage is not detectable until later ages/more advanced stages of OA development in the Hartley guinea pig.

There are additional limitations to note for the present work. Due to differences in preservation methods between studies, cartilage iron concentrations could not be directly

compared between males and females. Additionally, the authors recognize that gene expression does not necessarily correlate to protein abundance and/or activity. The limited availability of guinea pig reagents/antibodies substantially restricts the ability to investigate protein expression. The authors are working to develop immunostaining protocols to investigate protein levels resulting from the gene expression differences presented above.

6.5 Figures.

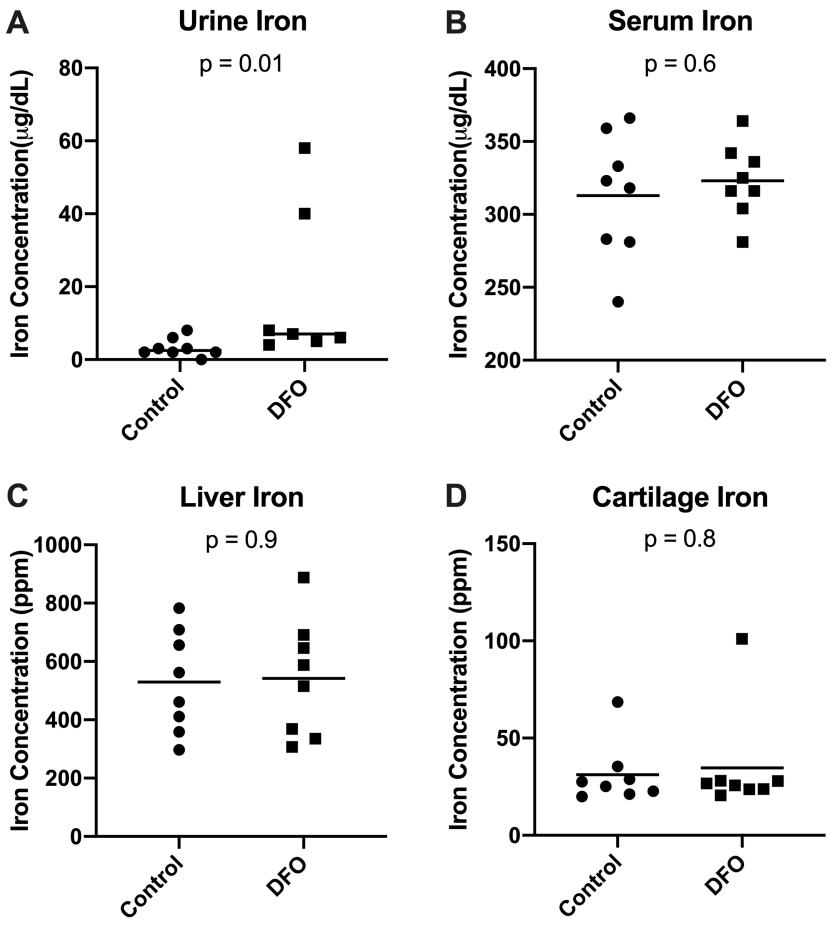

Figure 6.1. Tissue iron quantification. (A) Median urine iron× concentration was 2.50 micrograms/deciliter (μg/dL) in the control group and 7.00 μg/dL in the DFO group. (B) Mean serum iron concentration♦ was 312.90 μg/dL in the control group and 323.00 μg/dL in the DFO group. (C) Mean liver iron concentration♦ was 529.80 ppm in the control group and 542.40 in the DFO group. (D) Mean femoral head cartilage iron concentration♦ was 31.18 ppm in the control group and 34.68 ppm in the DFO group.

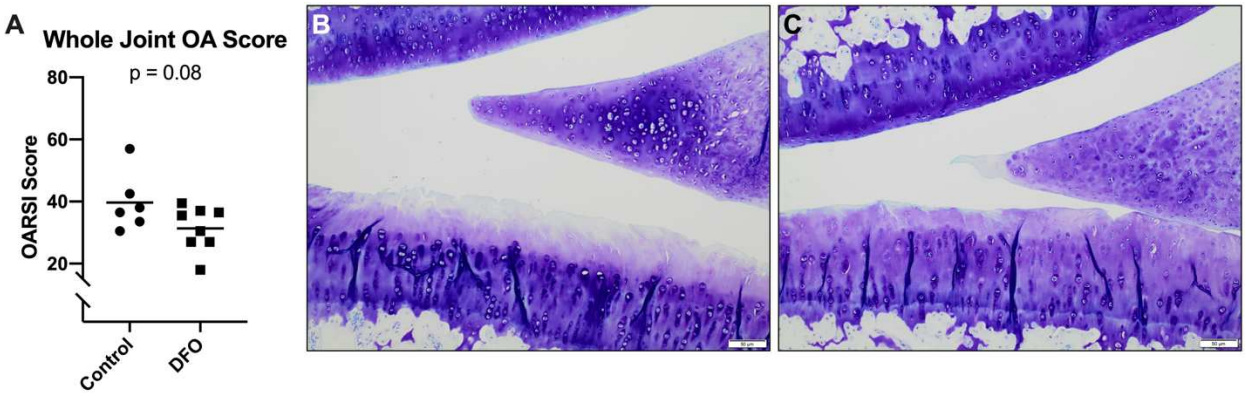

Figure 6.2. Histologic evaluation of knee joints. (A) Mean whole joint OA score♦ was 39.67 in the control group and 31.38 in the DFO group. (B) 10X representative histologic image of a control animal knee joint. (C) 10X representative histologic image of a knee joint from an animal treated with DFO.

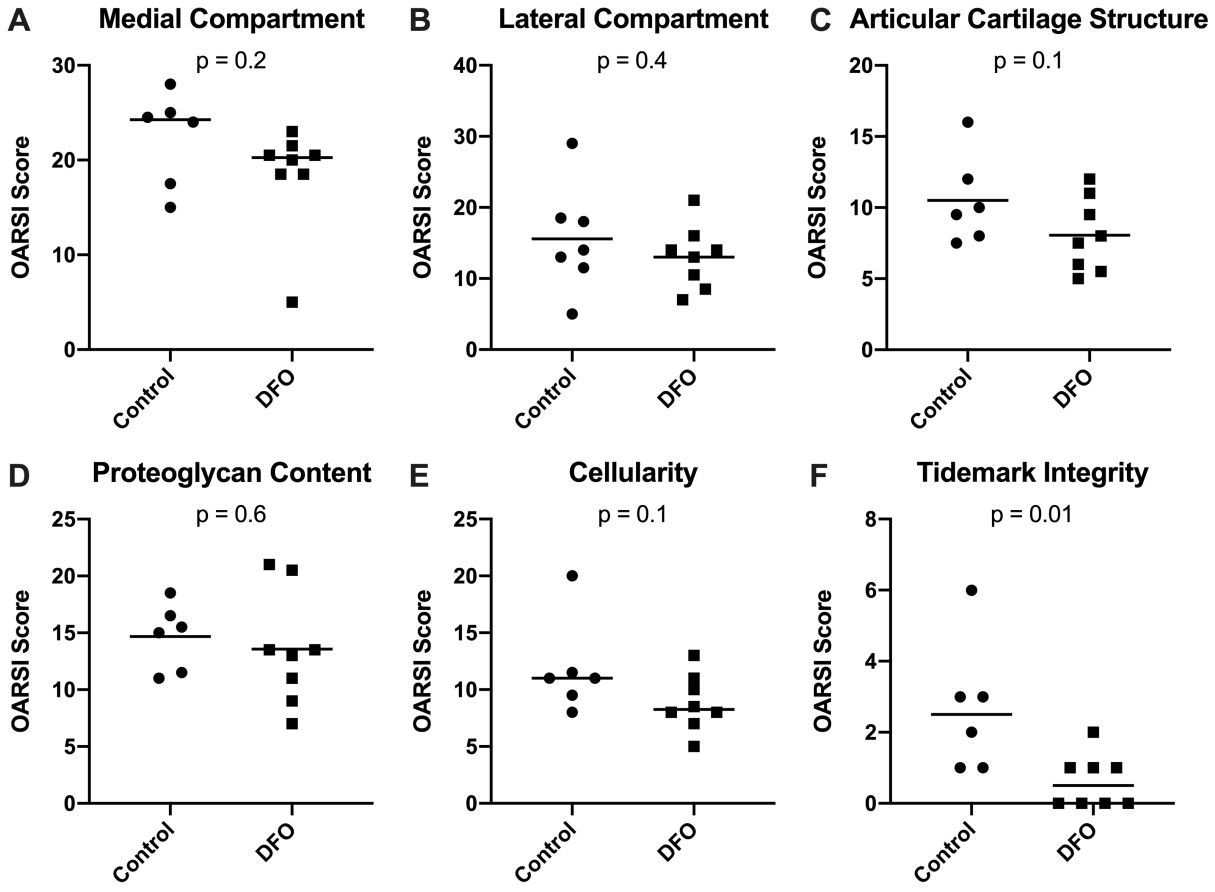

Figure 6.3. Contributions to histologic whole joint OA score. (A) Median OARSI score in the medial compartment× was 24.25 in the control group and 20.25 in the DFO group. (B) Mean OARSI score in the lateral compartment♦ was 15.57 in the control group and 13.00 in the DFO group. (C) Mean whole joint score for articular cartilage structure♦ was 10.50 in the control group and 8.06 in the DFO group. (D) Mean whole joint score for proteoglycan content♦ was 14.67 in the control group and 13.56 in the DFO group. (E) Median whole joint score for chondrocyte cellularity× was 9.13 in the control group and 7.25 in the DFO group. (F) Median whole joint score for tidemark integrity× was 2.50 in the control group and 0.50 in the DFO group.

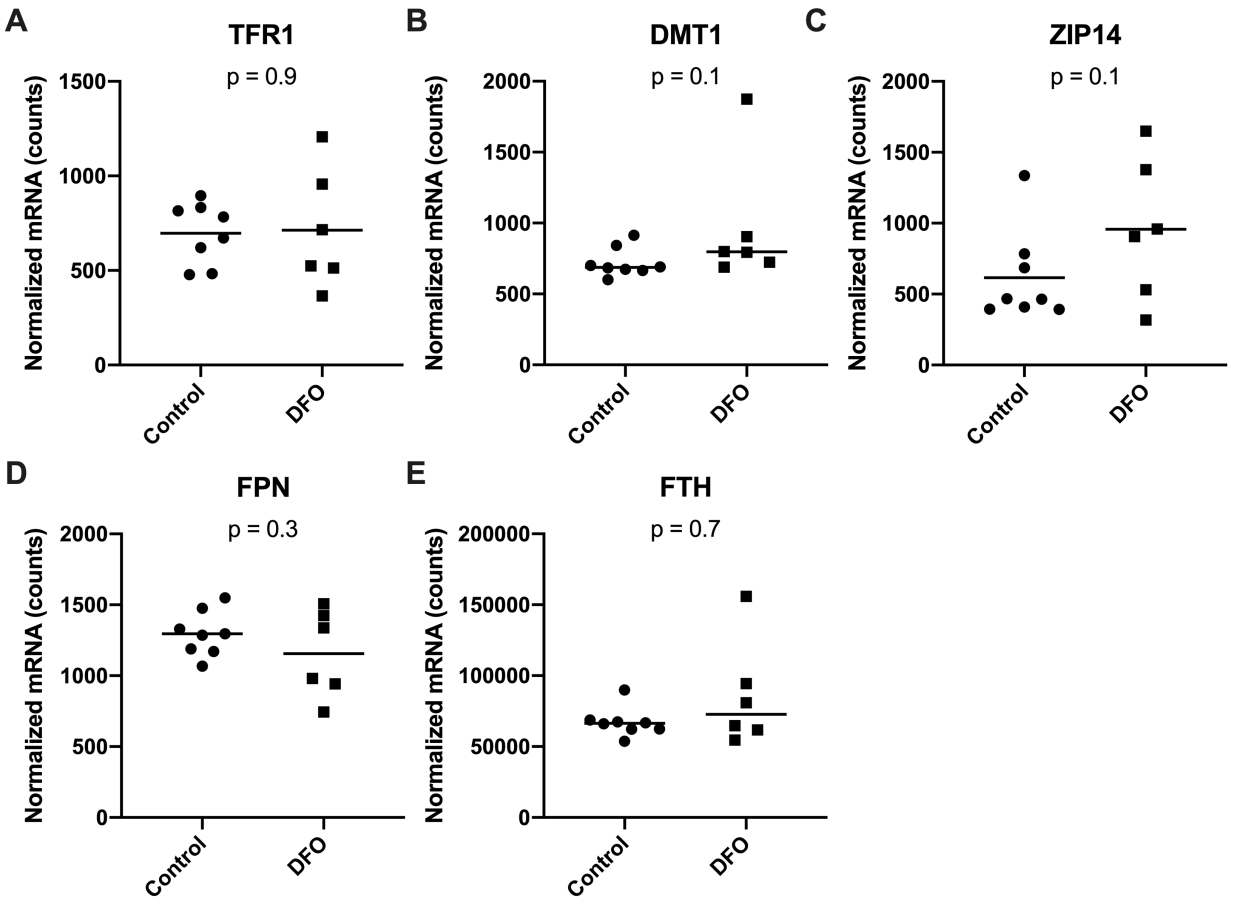

Figure 6.4. Normalized mRNA counts for genes related to iron metabolism. (A) Mean transcript counts for TFR1♦ were 697.50 in the control group and 713.70 in the DFO group. (B) Median transcript counts for DMT1× were 721.50 in the control group and 964.20 in the DFO group. (C) Mean transcript counts for ZIP14♦ were 616.60 in the control group and 956.80 in the DFO group. (D) Mean transcript counts for FPN♦ were 1296.00 in the control group and 1156.00 in the DFO group. (E) Median transcript counts for FTH× were 66456.00 in the control group and 72807.00 in the DFO group.

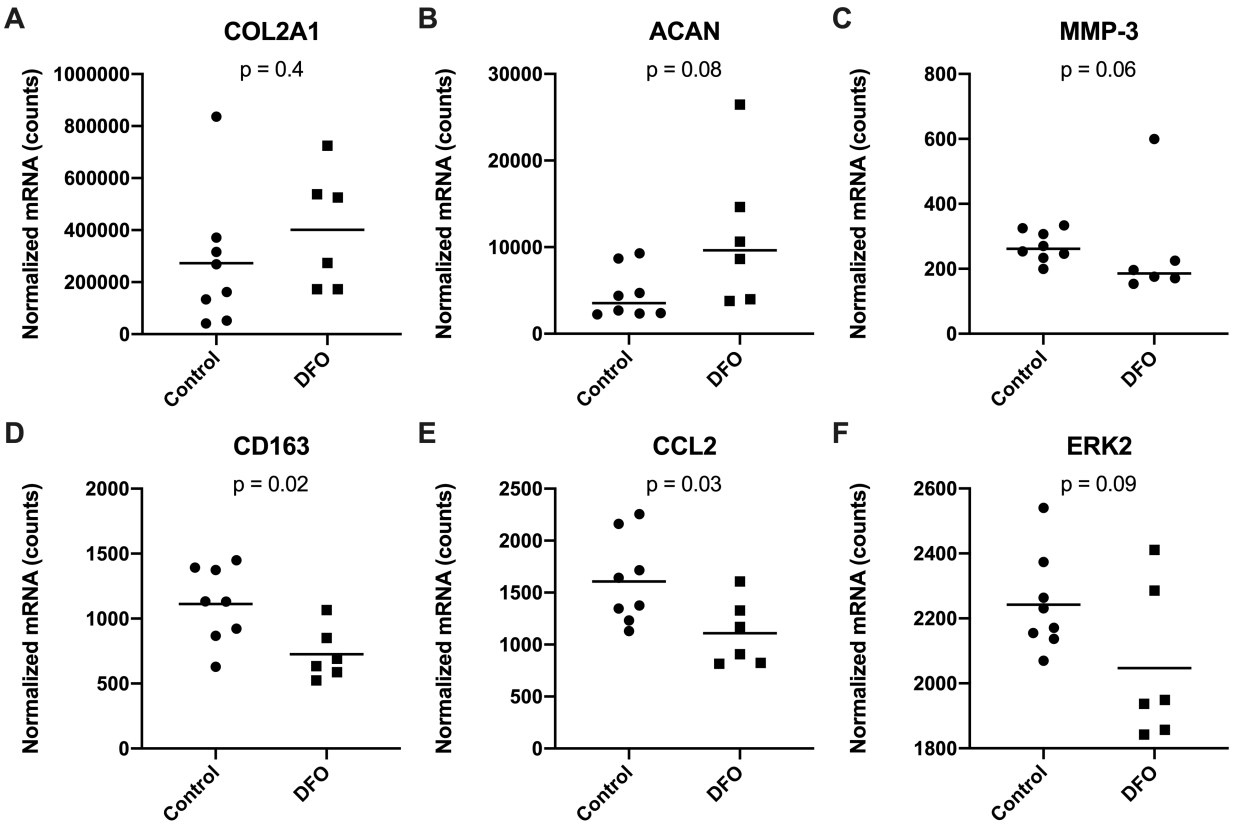

Figure 6.5. Normalized mRNA counts for genes related to the structure of knee articular cartilage. (A) Mean transcript counts for type II collagen (COL2A1) ♦ were 272693.00 in the control group and 401264.00 in the DFO group. (B) Median transcript counts for aggrecan (ACAN) × were 3529.00 in the control group and 9634.00 in the DFO group. (C) Median transcript counts for MMP-3× were 261.90 in the control group and 185.70 in the DFO group. (D) Mean transcript counts for CD163♦ were 1112.00 in the control group and 715.60 in the DFO group. (E) Mean transcript counts for CCL2♦ were 1608.00 in the control group and 1109.00 in the DFO group. (F) Mean transcript counts for ERK2♦ were 2243.00 in the control group and 2047.00 in the DFO group.

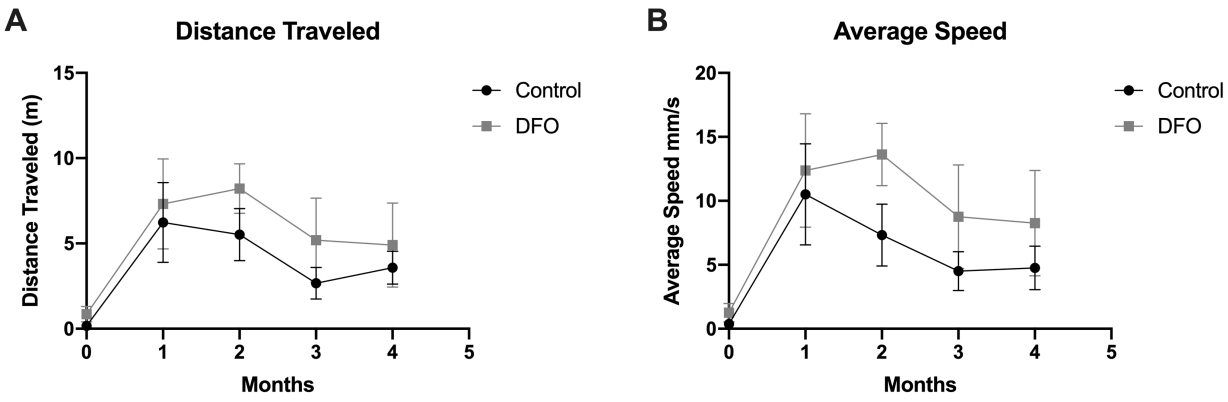

Figure 6.6. Movement parameters from overhead enclosure monitoring. (A) Distance traveled (m) by the animals during enclosure monitoring sessions throughout the study. (B) Average speed of travel during enclosure monitoring sessions throughout the study.

6.6 References.

1. Winterbourn CC. Toxicity of iron and hydrogen peroxide: the Fenton reaction. *Toxicol Lett*. 1995; 82-83:969-74. doi: 10.1016/0378-4274(95)03532-x.
2. Koppenol WH, Hider RH. Iron and redox cycling. Do's and don'ts. *Free Radic Biol Med*. 2019; 133: 3-10. doi: 10.1016/j.freeradbiomed.2018.09.022.
3. Voest EE, Vreugdenhil G, Marx JJ. Iron-chelating agents in non-iron overload conditions. *Ann Intern Med.* 1994; 120(6): 490-9. doi: 10.7326/0003-4819-120-6-199403150-00008.
4. Dixon SJ, Stockwell BR. The role of iron and reactive oxygen species in cell death. *Nat Chem Biol*. 2014; 10(1): 9-17. doi: 10.1038/nchembio.1416.
5. Raven EP, Lu PH, Tishler TA, Heydari P, Bartzokis G. Increased iron levels and decreased tissue integrity in hippocampus of Alzheimer's disease detected in vivo with magnetic resonance imaging. *J Alzheimers Dis*. 2013; 37(1): 127-36. doi: 10.3233/JAD-130209.
6. Silva B, Faustino P. An overview of molecular basis of iron metabolism regulation and the associated pathologies. *Biochim Biophys Acta*. 2015; 1852(7): 1347-59. doi: 10.1016/j.bbadis.2015.03.011.
7. Cook CI, Yu BP. Iron accumulation in aging: modulation by dietary restriction. *Mech Ageing Dev*. 1998; 102(1): 1-13. doi: 10.1016/s0047-6374(98)00005-0.
8. Zacharski LR, Ornstein DL, Woloshin S, Schwartz LM. Association of age, sex, and race with body iron stores in adults: analysis of NHANES III data. *Am Heart J*. 2000; 140(1): 98-104. doi: 10.1067/mhj.2000.106646.
9. He X, Hahn P, Lacovelli J, Wong R, King C, Bhisitkul R, et al. Iron homeostasis and toxicity in retinal degeneration. *Prog Retin Eye Res*. 2007; 26(6): 649-73. doi: 10.1016/j.preteyeres.2007.07.004.
10. Stadler N, Lindner RA, Davies MJ. Direct detection and quantification of transition metal ions in human atherosclerotic plaques: evidence for the presence of elevated levels of iron and copper. *Arterioscler Thromb Vasc Biol*. 2004; 24(5): 949-54. doi: 10.1161/01.ATV.0000124892.90999.cb.
11. Ford ES, Cogswell ME. Diabetes and serum ferritin concentration among U.S. adults. *Diabetes Care*. 1999; 22(12): 1978-83. doi: 10.2337/diacare.22.12.1978.
12. Smith MA, Harris PL, Sayre LM, Perry G. Iron accumulation in Alzheimer disease is a source of redox-generated free radicals. *Proc Natl Acad Sci*. 1997; 94(18): 9866-8. doi: 10.1073/pnas.94.18.9866.
13. Ashraf A, Jeandriens J, Parkes HG, So PW. Iron dyshomeostasis, lipid peroxidation and perturbed expression of cystine/glutamate antiporter in Alzheimer's disease: Evidence of ferroptosis. *Redox Biol*. 2020; 32: 101494. doi: 10.1016/j.redox.2020.101494.
14. Stevens RG, Graubard BI, Micozzi MS, Neriishi K, Blumberg BS. Moderate elevation of body iron level and increased risk of cancer occurrence and death. *Int J Cancer*. 1994; 56(3): 364-9. doi: 10.1002/ijc.2910560312.
15. Roosendaal G, Vianen ME, Venting MJ, van Rinsum AC, van den Berg HM, Lafeber FP. Iron deposits and catabolic properties of synovial tissue from patients with haemophilia. *J Bone Joint Surg Br*. 1998; 80(3): 540-5. doi: 10.1302/0301-620x.80b3.7807.
16. Richette P, Ottaviani S, Vicaut E, Bardin T. Musculoskeletal complications of hereditary hemochromatosis: a case-control study. *J Rheumatol*. 2010; 37(10): 2145-50. doi: 10.3899/jrheum.100234.

17. Biemond P, Swaak AJ, van Eijk HG, Koster JF. Intraarticular ferritin-bound iron in rheumatoid arthritis. A factor that increases oxygen free radical-induced tissue destruction. *Arthritis Rheum*. 1986; 29(10): 1187-93. doi: 10.1002/art.1780291002.
18. Pereira D, Peleteiro B, Araujo J, Branco J, Santos RA, Ramos E. The effect of osteoarthritis definition on prevalence and incidence estimates: a systematic review. *Osteoarthritis Cartilage*. 2011;19(11): 1270-85. doi: 10.1016/j.joca.2011.08.009.
19. Felson DT. The epidemiology of knee osteoarthritis: Results from the Framingham osteoarthritis study. *Semin Arthritis Rheum*. 1990;20(3):42-50. doi:10.1016/0049-0172(90)90046-I.
20. Srikanth VK, Fryer JL, Zhai G, Winzenberg TM, Hosmer D, Jones G. A meta-analysis of sex differences prevalence, incidence and severity of osteoarthritis. *Osteoarthritis Cartilage*. 2005; 13(9): 769-81. doi: 10.1016/j.joca.2005.04.014.
21. Kautzky-Willer A, Harreiter J, Pacini G. Sex and gender differences in risk, pathophysiology and complications of type 2 diabetes mellitus. *Endocr Rev*. 2016; 37(3): 278-316. doi: 10.1210/er.2015-1137.
22. Hahn P, Ying GS, Beard J, Dunaief JL. Iron levels in human retina: sex difference and increase with age. *Neuroreport*. 2006; 17(17): 1803-6. doi: 10.1097/WNR.0b013e3280107776.
23. Whitfield JB, Treloar S, Zhu G, Powell LW, Martin NG. Relative importance of female-specific and non-female-specific effects on variation in iron stores between women. *Br J Haematol*. 2003; 120(5): 860-6. doi: 10.1046/j.1365-2141.2003.04224.x.
24. Jiang R, Manson JE, Meigs JB, Ma J, Rifai N, Hu FB. Body iron stores in relation to risk of type 2 diabetes in apparently healthy women. *JAMA*. 2004; 291(6): 711-17. doi: 10.1001/jama.291.6.711.
25. Heinrich J; US General Accountability Office. Drug safety: most drugs withdrawn in recent years had greater health risks for women. Publication No. GAO-01-286R. Washington: US General Accountability Office; 2001. https://www.gao.gov/assets/gao-01-286r.pdf.
26. Nair AB, Jacob S. A simple practice guide for dose conversion between animals and human. *J Basic Clin Pharm*. 2016; 7(2): 27-31. doi: 10.4103/0976-0105.177703.
27. Ehlers KH, Giardina PJ, Lesser ML, Engle MA, Hilgartner MW. Prolonged survival in patients with beta-thalassemia major treated with deferoxamine. *J Pediatr*. 1991; 118(4 Pt 1): 540-5. doi: 10.1016/s0022-3476(05)83374-8.
28. Burton LH, Radakovich LB, Marolf AJ, Santangelo KS. Systemic iron overload exacerbates osteoarthritis in the strain 13 guinea pig. *Osteoarthritis Cartilage*. 2020; 28(9): 1265-75. doi: 10.1016/j.joca.2020.06.005.
29. Helrich, K, eds; Association of Official Analytical Chemists. *Official Methods of Analysis of AOAC International*. 15th ed. Gaithersburg, MD, USA; AOAC International; 1990. Official method 968.08D.
30. Helrich, K, eds; Association of Official Analytical Chemists. *Official Methods of Analysis of AOAC International*. 15th ed. Gaithersburg, MD, USA; AOAC International; 1990. Official method 974.27A, B, E and F.
31. Helrich, K, eds; Association of Official Analytical Chemists. *Official Methods of Analysis of AOAC International*. 15th ed. Gaithersburg, MD, USA; AOAC International; 1990. Official method 985.40D.
32. Kraus VB, Huebner JL, DeGroot J, Bendele A. The OARSI histopathology initiative—recommendations for histological assessments of osteoarthritis in the guinea pig.

Osteoarthritis Cartilage. 2010; 18 Suppl 3(Suppl 3): S35-52. doi: 10.1016/j.joca.2010.04.015.
33. Fox AJS, Bedi A, Rodeo SA. The basic science of articular cartilage: structure, composition, and function. *Sports Health*. 2009; 1(6): 461-8. doi: 10.1177/1941738109350438.
34. Gerhardsson L, Kazantzis G. Diagnosis and treatment of metal poisoning: general aspects. In: Nordberg GF, Fowler BA, Nordberg M, eds. Handbook on the toxicology of metals. Amsterdam: Academic Press; 2015. p. 487-505. doi: 10.1016/B978-0-444-59453-2.00023-8.
35. Widdowson EM, McCance RA. Sexual differences in the storage and metabolism of iron. *Biochem J*. 1948; 42(4): 577-8. doi: 10.1042/bj0420577.
36. Grubic Kezele T, Curko-Cofek B. Age-related changes and sex-related differences in brain iron metabolism. *Nutrients*. 2020; 12(9): 2601. doi: 10.3390/nu12092601.
37. Harrison-Findik DD. Gender-related variations in iron metabolism and liver diseases. *World J Hepatol*. 2010; 2(8): 302-10. doi: 10.4254/wjh.v2.i8.302.
38. Dekker LH, Nicolaou M, van der A DL, Busschers WB, Brewster LM, Snijder MB, et al. Sex differences in the association between serum ferritin and fasting glucose in type 2 diabetes among south Asian Surinamese, African Surinamese, and ethnic Dutch: the population-based SUNSET study. *Diabetes Care*. 2013; 36(4): 965-71. doi: 10.2337/dc12-1243.
39. Heath AL, Skeaff CM, Williams S, Gibson RS. The role of blood loss and diet in the aetiology of milk iron deficiency in premenopausal adult New Zealand women. *Public Health Nutr*. 2001; 4(2): 197-206. doi: 10.1079/phn200054.
40. Ganz T, Olbina G, Girelli D, Nemeth E, Westerman M. Immunoassay for human serum hepcidin. *Blood*. 2008; 112(10): 4292-7. doi: 10.1182/blood-2008-02-139915.
41. Jian J, Pelle E, Huang X. Iron and menopause: does increased iron affect the health of postmenopausal women?. *Antioxid Redox Signal*. 2009; 11(12): 2939-43. doi: 10.1089/ars.2009.2576.
42. Cohen LA, Gutierrez L, Weiss A, Leichtmann-Bardoogo Y, Zhang DL, Crooks DR, et al. Serum ferritin is derived primarily from macrophages through a nonclassical secretory pathway. *Blood*. 2010; 116(9): 1574-84. doi: 10.1182/blood-2009-11-253815.
43. Pfeiffer CM, Looker AC. Laboratory methodologies for indicators of iron status: strengths, limitations, and analytical challenges. *Am J Clin Nutr*. 2017; 106(Suppl 6): 1606S-14S. doi: 10.3945/ajcn.117.155887.
44. Kong WN, Niu QM, Ge L, Zhang N, Yan SF, Chen WB, et al. Sex differences in iron status and hepcidin expression in rats. *Biol Trace Elem Res*. 2014; 160(2): 258-67. doi: 10.1007/s12011-014-0051-3.
45. Bergstrom E, Hernell O, Lonnerdal B, Persson LA. Sex differences in iron stores of adolescents: what is normal?. *J Pediatr Gastroenterol Nutr*. 1995; 20(2): 215-24. doi: 10.1097/00005176-199502000-00013.
46. Wood JC, Drulis JM, Nelson SE, Janghorbani M, Fomon SJ. Gender-related differences in iron absorption by preadolescent children. *Pediatr Res*. 1991; 29(5): 435-9. doi: 10.1203/00006450-199105010-00005.
47. Jacobs A. Sex differences in iron absorption. *Proc Nutr Soc*. 1976; 35(2): 159-62. doi: 10.1079/pns19760028.
48. Young MF, Glahn RP, Ariza-Nieto M, Inglis J, Olbina G, Westerman M. Serum hepcidin is significantly associated with iron absorption from food and supplemental sources in healthy young women. *Am J Clin Nutr*. 2009; 89(2): 533-8. doi: 10.3945/ajcn.2008.26589.

49. Hadley KB, Johnson LK, Hunt JR. Iron absorption by healthy women is not associated with either serum or urinary prohepcidin. *Am J Clin Nutr*. 2006; 84(1): 150-5. doi: 10.1093/ajcn/84.1.150.
50. Galesloot TE, Vermeulen SH, Geurts-Moespot AJ, Klaver SM, Kroot JJ, van Tienoven D, et al. Serum hepcidin: reference ranges and biochemical correlates in the general population. *Blood*. 2011; 117(25): e218-25. doi: 10.1182/blood-2011-02-337907.
51. Samuelson G, Lonnerdal B, Kempe B, Elverby JE, Bratteby LE. A follow-up study of serum ferritin and transferrin receptor concentrations in Swedish adolescents at age 17 age 15. *Acta Paediatr*. 2000; 89(10): 1162-8. doi: 10.1080/080352500750027501.
52. Wilkinson N, Pantopoulos K. The IRP/IRE system in vivo: insights from mouse models. *Front Pharmacol*. 2014;5:176. doi: 10.3389/fphar.2014.00176.
53. Torti FM, Torti SV. Regulation of ferritin genes and protein. *Blood*. 2002; 99(10): 3505-16. doi: 10.1182/blood.v99.10.3505.
54. Munro HN. Iron regulation of ferritin gene expression. *J Cell Biochem*. 1990; 44(2): 107-15. doi: 10.1002/jcb.240440205.
55. Shiloh H, Lancu TC, Bauminger ER, Link G, Pinson A, Hershko C. Deferoxamine-induced iron mobilization and redistribution of myocardial iron in cultured rat heart cells: studies of the chelatable iron pool by electron microscopy and Mossbauer spectroscopy. *J Lab Clin Med*. 1992; 119(4): 428-36.
56. Mostert LJ, de Jong G, Koster JF, van Eijk HG. Iron mobilization from isolated hepatocytes. *Int J Biochem*. 1986; 18(11): 1061-4. doi: 10.1016/0020-711x(86)90254-5.
57. Fuerst M, Bertrand J, Lammers L, Dreier R, Echtermeyer F, Nitschke Y, et al. Calcification of articular cartilage in human osteoarthritis. *Arthritis Rheum*. 2009; 60(9): 2694-703. doi: 10.1002/art.24774.
58. Nielsen AW, Klose-Jensen R, Hartley LB, Boel LWT, Thomsen JS, Keller KK, et al. Age-related histological changes in calcified cartilage and subchondral bone in femoral heads from healthy humans. *Bone*. 2019; 129: 115037. doi: 10.1016/j.bone.2019.115037.
59. Longobardi L, Jordan JM, Shi XA, Renner JB, Schwartz TA, Nelson AE. Associations between the chemokine biomarker CCL2 and knee osteoarthritis outcomes: the Johnston County Osteoarthritis Project. *Osteoarthritis Cartilage*. 2018; 26(9): 1257-1261. doi: 10.1016/j.joca.2018.04.012.
60. Willcockson H, Ozkan H, Chubinskaya S, Loeser RF, Longobardi L. CCL2 induces chondrocyte MMP expression through ERK and p38 signaling pathways. *Osteoarthr Cartil Open*. 2021; 3(1): 100136. doi: 10.1016/j.ocarto.2020.100136.
61. Xu Z, Li J, Yang H, Jiang L, Zhou X, Huang Y, et al. Association of CCL2 gene variants with osteoarthritis. *Arch Med Res*. 2019; 50(3): 86-90. doi: 10.1016/j.arcmed.2019.05.014.
62. Guo Q, Liu Z, Wang M, Guo S, Cong H, Liu L. Analysis on the expression and value of CCL2 and CCL3 in patients with osteoarthritis. *Exp Mol Pathol*. 2021; 118: 104576. doi: 10.1016/j.yexmp.2020.104576.
63. Jiao K, Zhang J, Zhang M, Wei Y, Wu Y, Qiu ZY, et al. The identification of CD163 expression phagocytic chondrocytes in joint cartilage and its novel scavenger role in cartilage degeneration. *PLoS One*. 2013; 8(1): e53312. doi: 10.1371/journal.pone.0053312.
64. Halliwell B. Protection against tissue damage in vivo by desferrioxamine: what is its mechanism of action? *Free Radic Biol Med*. 1989;7(6):645-51. doi: 10.1016/0891-5849(89)90145-7.

65. Zhu BZ, Har-El R, Kitrossky N, Chevion M. New modes of action of desferrioxamine: scavenging of semiquinone radical and stimulation of hydrolysis of tetrachlorohydroquinone. *Free Radic Biol Med*. 1998;24(2):390-9. doi: 10.1016/s0891-5849(97)00220-7.